1994

Study of directionally solidified eutectics with emphasis on oscillatory instabilities

Brenda Wolfe Diesslin
Iowa State University

INFORMATION TO USERS

This manuscript has been reproduced from the microfilm master. UMI films the text directly from the original or copy submitted. Thus, some thesis and dissertation copies are in typewriter face, while others may be from any type of computer printer.

The quality of this reproduction is dependent upon the quality of the copy submitted. Broken or indistinct print, colored or poor quality illustrations and photographs, print bleedthrough, substandard margins, and improper alignment can adversely affect reproduction.

In the unlikely event that the author did not send UMI a complete manuscript and there are missing pages, these will be noted. Also, if unauthorized copyright material had to be removed, a note will indicate the deletion.

Oversize materials (e.g., maps, drawings, charts) are reproduced by sectioning the original, beginning at the upper left-hand corner and continuing from left to right in equal sections with small overlaps. Each original is also photographed in one exposure and is included in reduced form at the back of the book.

Photographs included in the original manuscript have been reproduced xerographically in this copy. Higher quality 6" x 9" black and white photographic prints are available for any photographs or illustrations appearing in this copy for an additional charge. Contact UMI directly to order.

UMI

A Bell & Howell Information Company
300 North Zeeb Road. Ann Arbor. MI 48106-1346 USA
313/761-4700 800/521-0600

Order Number 9518372

Study of directionally solidified eutectics with emphasis on oscillatory instabilities

Diesslin, Brenda Wolfe, Ph.D.

Iowa State University, 1994

U·M·I
300 N. Zeeb Rd.
Ann Arbor, MI 48106

Study of directionally solidified eutectics with emphasis on oscillatory instabilities

by

Brenda Wolfe Diesslin

A Dissertation Submitted to the
Graduate Faculty in Partial Fulfillment of the
Requirements for the Degree of
DOCTOR OF PHILOSOPHY
Department: Mathematics
Major: Applied Mathematics

Approved:

Signature was redacted for privacy.

Signature was redacted for privacy.

In Charge of Major Work

Signature was redacted for privacy.

For the Major Department

Signature was redacted for privacy.

For the Graduate College

Iowa State University
Ames, Iowa
1994

Dedicated to two role models, my maternal grandmother and my mom.

TABLE OF CONTENTS

NOMENCLATURE viii
ACKNOWLEDGEMENTS xii
CHAPTER 1. GENERAL INTRODUCTION 1
Background 1
Thesis organization 3
CHAPTER 2. PREVIOUS MODELS 5
CHAPTER 3. OSCILLATORY INSTABILITIES IN DIRECTIONALLY SOLIDIFIED EUTECTICS 9
Abstract 9
I. INTRODUCTION 9
II. THE MODEL 11
III. STEADY-STATE SOLUTION 14
IV. LINEAR STABILITY ANALYSIS 14
V. EXAMPLES AND DISCUSSION 18
APPENDIX: DATYE AND LANGER MODEL 23
CHAPTER 4. ASYMPTOTICS 25
Acoustic oscillations ($N = 2$) 25
Condition one, $B = 0$ 27
Condition two, $AC > 0$ 29
The error term, ε_4 32
Optical oscillations ($N = 1$) 33
CHAPTER 5. HIGH PÉCLET NUMBER MODEL NEAR THE EUTECTIC CONCENTRATION 37

P dependent partition coefficient 37
Nonequilibrium interface concentration 38
High Péclet number model 41
Linear stability analysis 42
Effects of the high Péclet number model 44
CHAPTER 6. RANDOM WALK SIMULATIONS 48
Literature review 48
The random walk model 50
Random walk probabilities 53
After a walker hits the interface 55
Simulation results 56
CHAPTER 7. GENERAL CONCLUSIONS 64
BIBLIOGRAPHY 67
APPENDIX A: THE REAL AND IMAGINARY EQUATIONS AND THE CORRESPONDING FORTRAN PROGRAMS 71
APPENDIX B: ADDITIONAL INFORMATION PERTAINING TO CHAPTER 3 (THE OSCILLATORY PAPER) 87
APPENDIX C: SAMPLE RUNS AND THE FORTRAN PROGRAM FOR THE RANDOM WALK SIMULATIONS 93

LIST OF FIGURES

Figure 1.1: Schematic drawing of directional solidification. 2

Figure 2.1: Schematic illustration of a lamellar eutectic with a flat interface. 8

Figure 3.1: Schematic illustration of a lamellar eutectic using (a) dimensional units and (b) nondimensional units. 13

Figure 3.2: Portion of the phase diagram for the binary eutectic using (a) dimensional units and (b) nondimensional units. 13

Figure 3.3: Schematic illustration of a perturbed lamellar eutectic. 15

Figure 3.4: (a) Plot of real and imaginary equations, 2η vs P, for $N = 2$, $\Omega = 0.1045$, and $\theta = 65^{\circ}$ and (b) real-space trajectories of the triple points for $b = 0.01$, $P = 0.0067$, and $2\eta = 0.8015$ after 1000 units of time for the Al-Al_2Cu eutectic system with eutectic composition corresponding to $2\eta = 0.54$. 19

Figure 3.5: (a) Plot of real and imaginary equations, 2η vs P, for $N = 2$, $\Omega = 0.0447$, and $\theta = 60^{\circ}$ and (b) real-space trajectories of the triple points for $b = 3$, $P = 1.3015$, and $2\eta = 0.3595$ after 10 units of time for the CBr_4-C_2Cl_6 eutectic system with eutectic composition corresponding to $2\eta = 0.676$. 20

Figure 3.6: (a) Plot of real and imaginary equations, 2η vs P, for $N = 1$, $\Omega = 0.1045$, and $\theta = 65^{\circ}$ and (b) real-space trajectories of the triple points for $b = 1$, $P = 2.497$, and $2\eta = 0.7191$ after 15 units of time, and (c) real-space trajectories of the triple points for $b = 5.49$, $P = 0.0095$, and $2\eta = 0.9285$ after 10 units of time for the Al-Al_2Cu eutectic system with eutectic composition corresponding to $2\eta = 0.54$. 21

Figure 3.7: (a) Plot of real and imaginary equations, 2η vs P, for $N = 1$, $\Omega = 0.0447$, and $\theta = 60^{\circ}$ and (b) real-space trajectories of the triple points for $b = 5$, $P = 2.068$, and $2\eta = 0.7656$ after 5 units of time for the CBr_4-C_2Cl_6 eutectic system with eutectic composition corresponding to $2\eta = 0.676$. 22

Figure 3.8: Plot of Concentration (wt %) vs Velocity (cm/s) for $N = 1$ ($\triangle$) and $N = 2$ ($\bullet$) and the CBr_4-C_2Cl_6 eutectic system with $\Omega = 0.0447$, and $\theta = 60^{\circ}$. 22

Figure 3.9: Plot of Concentration (wt %) vs Velocity (m/s) for $N = 1$ ($\triangle$) and $N = 2$ ($\bullet$) and the Al-Al_2Cu eutectic system with $\Omega = 0.1045$ and $\theta = 65^{\circ}$. 23

Figure 4.1: $\Psi_j(\eta)$ for $j = 4$ and 6 using the first 200 terms (solid line) and $\Psi_4(\eta)$ using the first term only (dashed line). 28

Figure 4.2: P vs. 2η for $N = 2$ and for Al-Al_2Cu (solid line) and CBr_4-C_2Cl_6 (dashed line). 28

Figure 4.3: Inequality for the condition $C > 0$ for Al-Al_2Cu ($\theta_\alpha = 65^{\circ}$) and CBr_4-C_2Cl_6 ($\theta_\alpha = 60^{\circ}$). 30

Figure 4.4: 2η vs b where $\omega = \pm ib$ for Al-Al_2Cu (solid line) and CBr_4-C_2Cl_6 (dashed line). 31

Figure 4.5: P vs 2η for Al-Al_2Cu ($N = 1$) and various values of b. 35

Figure 4.6: P vs 2η for CBr_4-C_2Cl_6 ($N = 1$) and various values of b. . . 35

Figure 4.7: $-\sqrt{2}\,A\,b^{7/2} + D\,b^{3/2} + 2\eta\,b = \tan(\theta_\alpha)$ for Al-Al_2Cu. . . . 36

Figure 4.8: $-\sqrt{2}\,A\,b^{7/2} + D\,b^{3/2} + 2\eta\,b = \tan(\theta_\alpha)$ for CBr_4-C_2Cl_6. . 36

Figure 5.1: $(\Omega h)/(f\nu)$ vs P for Al-Al_2Cu and various values of P_D. . . . 44

Figure 5.2: $(\Omega h)/(f\nu)$ vs P for CBr_4-C_2Cl_6 and various values of P_D. . 45

Figure 5.3: (a) Plot of Concentration (wt %) vs Velocity (m/s) for $N = 1$ ($\triangle$ and a–d) and $N = 2$ ($\bullet$) and the Al-Al_2Cu eutectic system with $\Omega = 0.1045$, $\theta = 65^{\circ}$, and $P_D = \infty$, 100, 50 and 25 corresponding to the a–d. (b) Enlarged view of the boxed in region. 46

Figure 5.4: (a) Plot of Concentration (wt %) vs Velocity (cm/s) for $N = 1$ (a–d) and $N = 2$ (1-3) and the CBr_4-C_2Cl_6 eutectic system with $\Omega = 0.0447$, $\theta = 60°$, and $P_D = \infty$, 100, 50 and 25 corresponding to a–d and $P_D = \infty$, 100 and 50 corresponding to 1–3. (b) Enlarged view of the boxed in region. 47

Figure 6.1: Schematic drawing of the grid. 51

Figure 6.2: Schematic drawing of a portion of the grid. 51

Figure 6.3: Flowchart for random walk simulation. 57

Figure 6.4: Simulation runs for the Al-Al_2Cu system with $W = 100$, $H = 500$, countA = 13, countB = -10, $P = 0.0067$, $2\eta = 0.7$, seed = 0.54, incrementing 5 units every 500 sweeps and plotting the interface every 15,000 sweeps. 60

Figure 6.5: Simulation runs for the Al-Al_2Cu system with $W = 100$, $H = 500$, $P = 0.0067$, countA = 13, countB = -10, $2\eta = 0.4$, seed = 0.54, incrementing 5 units every 500 sweeps and plotting the interface every 15,000 sweeps. 61

Figure 6.6: Simulation run for the Al-Al_2Cu system with $W = 100$, $H = 500$, $P = 0.0067$, countA = 13, countB = -10 and $2\eta = 0.8015$ with an initial perturbation corresponding to $N = 2$. Increments are taken 5 units every 500 sweeps and the interface is plotted every 15,000 sweeps. 62

Figure 6.7: Simulation runs for the Al-Al_2Cu system with $W = 100$, $H = 500$, $P = 0.0095$, countA = 18, countB = -13 and $2\eta = 0.9285$ with an initial perturbation corresponding to $N = 1$. Increments are taken 5 units every 50 sweeps and the interface is plotted every 1500 sweeps. 63

NOMENCLATURE

α	subscript corresponding to the alpha phase
β	subscript corresponding to the beta phase
E	subscript corresponding to eutectic
L	subscript corresponding to the liquid
S	subscript corresponding to the solid
e	subscript or superscript corresponding to equilibrium
1	subscript corresponding to the alpha phase, except in Chap. 6 where it corresponds to the x-direction
2	subscript corresponding to the beta phase, except in Chap. 6 where it corresponds to the z-direction
i	subscript corresponding to the interface
V	constant mean velocity of the interface
G	imposed temperature gradient
λ	wavelength of the lamellar pattern
D	diffusion coefficient
P	Péclet number, $\equiv (\lambda V)/(2D)$
T	temperature
C	concentration of component B
m^{solid}, $m^{liq} = m$	absolute value of the slope of the solidus/liquidus line of the phase diagram
σ_α, σ_β, $\sigma_{\alpha\beta}$	alpha-liquid, beta-liquid and alpha-beta surface tension
L	latent heat of fusion per unit volume
κ	curvature, taken to be plus when the solid bulges into the liquid
ΔC_i	$\equiv (C_L - C_S)_i$

V_n	normal component of the interface velocity
C_∞	far-field concentration
ΔT	$\equiv T_E - T$
ΔC	miscibility gap, $\equiv C_{\beta E} - C_{\alpha E}$
U	dimensionless concentration field, $\equiv (C - C_E)/\Delta C$
ΔU_i	$\equiv U_i - U_\alpha$ for the α phase; $\equiv U_i - U_\beta$ for the β phase
Γ	capillary constant,$\equiv \sigma T_E/L$
θ	contact angle, measured from the horizontal
U_∞	dimensionless far-field concentration
$\bar{\zeta}$	average interface position (z direction)
2η	volume fraction of the α phase
ρ	volume fraction of the β phase
τ	$\equiv -2\eta\, U_{\alpha E} - \rho\, U_{\beta E}$
N	= 1 for the optical oscillations; = 2 for the acoustic oscillations
σ	multiple of π/N
ω	wavelength of the oscillation
$\pm\hat{x}\, e^{i\sigma 2\,(j+\eta)+\omega t}$	perturbation of the $\alpha\beta$ and $\beta\alpha$ triple points
$\hat{\eta} + \hat{\delta}$	volume fraction of the perturbed α phase
$\hat{\rho}$	volume fraction of the perturbed β phase
ϕ	dimensionless version of θ, $= \tan^{-1}[\tan(\theta)/\sqrt{P}]$
$\Delta\phi$	change in ϕ
$\langle\kappa\rangle$	average curvature over a phase
$S(\eta)$	$= 2\sum_{n=1}^{\infty} \frac{\sin^2(2n\pi\eta)}{(n\pi)^2}\left\{\frac{P}{2} + \left[\left(\frac{P}{2}\right)^2 + (n\pi)^2\right]^{1/2}\right\}^{-1}$
$R(\eta)$	$= \sum_{n=1}^{\infty} \frac{\sin(4n\pi\eta)}{(n\pi)}\left\{\frac{P}{2} + \left[\left(\frac{P}{2}\right)^2 + (n\pi)^2\right]^{1/2}\right\}^{-1}$
Ω	$\equiv (2\Gamma)/(m\Delta C\lambda P)$
b	$\equiv \mathrm{Im}(\omega)$ when the $\mathrm{Re}(\omega) = 0$
$Q(\eta)$	$\approx 2\sum_{n=1}^{\infty} \sin^2(2n\pi\eta)/(n\pi)^3$
$\tilde{S}(\eta)$	$= 2\sum_{n=1}^{\infty} \sin^2(2n\pi\eta)/(n\pi)^3$

$\tilde{R}(\eta)$	$= \sum_{n=1}^{\infty} \sin(4n\pi\eta)/(n\pi)^2$
$\Psi_j(\eta)$	$= \sum_{\text{odd } n=1}^{\infty} \sin(2n\pi\eta)/(n\pi)^j$
ε_4	error term
$\Phi_j(\eta)$	$= \sum_{n=1}^{\infty} \sin(4n\pi\eta)/(n\pi)^j$
k_1, k_2	partition coefficients defined by a ratio of concentrations
k^{eA}	equilibrium partition coefficient of component A
$k(P)$	P dependent partition coefficient
Λ_e	measure of the driving force for redistribution,$= k^e/k^{eA}$
V_D	diffusive speed
P_D	$= (\lambda V_D)/(2D)$
ΔG	free energy change of the solid
μ^0	chemical potential of the pure substance
R	gas constant
γ	activity coefficient
μ	chemical potential, $= \mu^0 + RT \ln[\gamma C]$
$\Delta\mu$	$= \mu_S - \mu_L$
δC	$= C_L - C_E$
g, h, f	high velocity functions
$\tau(P)$	$\equiv 2\eta \frac{C_E}{\Delta C}(1 - k_1(P)) - \rho \frac{(1 - C_E)}{\Delta C}(1 - k_2(P))$
$\nu(P)$	$\equiv \frac{C_E}{\Delta C}(1 - k_1(P)) + \frac{(1-C_E)}{\Delta C}(1 - k_2(P))$
$\langle U \rangle$	average concentration
W	number of grid sites in the x-direction
H	number of grid sites in the z-direction
$U(i)$	concentration of the i^{th} particle on the interface
n_L, n_α, n_β	number of liquid, α solid and β solid sites in a circle of a fixed radius
Q^*	probability of an "infinity" walk occuring
U_{ave}	average absolute value of the concentration across the interface
q_i	probability of walking from a neighboring site to (x, z)
Q_j	probability of an interface walk occuring for the j^{th} solid interface particle

Δt	change in time
δ_1	distance between neighboring sites in the x-direction
δ_2	distance between neighboring sites in the z-direction
c_1	nonzero constant, $= \lim({\delta_1}^2/\Delta t)$ as δ_1 and $\Delta t \rightarrow 0$
c_2	nonzero constant, $= \lim({\delta_2}^2/\Delta t)$ as δ_2 and $\Delta t \rightarrow 0$
$U(x,z,t)$	particle at the site (x,z) at time t
F_L^i	flux of the i^{th} interface liquid
F_S^j	flux of the j^{th} interface solid
$\rho\alpha$, ρ_β	density for the alpha and beta phases
k_α, k_β	partition coefficients defined by a ratio of slopes, m^{liq}/m^{solid}
$\bar{k}$	$\equiv 2\eta\, k_\alpha + \rho\, k_\beta$
Δk	$\equiv k_\beta - k_\alpha$

ACKNOWLEDGEMENTS

I would like to thank Dr. Grayhack for his willingness to accept me as his student, for his guidance and encouragement and for the many hours of teaching and discussion. I would also like to thank the other members of my committee, Dr. Heimes, Dr. Evans, Dr. Song and Dr. Trivedi; with special thanks to Dr. Trivedi for his material science assistance. In addition, I would like to acknowledge and thank Iwan Alexander, Franz Rosenberger and Alain Karma for their helpful discussions.

I would also like to thank my family and friends who supported and encouraged me over the years. A special thanks to my two sets of parents, Mom and Dad Wolfe and Mom and Dad Diesslin, for all their encouragement, and to the Grayhack family; Bill, Judy, Sean and Clara, for sharing a part of their lives while in Ames. Most importantly, I would like to say thank you to my husband, Bill, for everything he has done for me each and every day, specially for telling me we could have a big failure party if needed. (Thank the Lord that we get to have a graduation party instead!)

This work and my graduate studies leading to this work were fiancially supported by the Iowa State University Mathematics department, the Association for Women in Science Educational Foundation, the Dr. Aggie Ho Foundation, and of course, my husband, Bill. I am very grateful to all of them.

CHAPTER 1. GENERAL INTRODUCTION

Background

Each day we are surrounded by materials such as ice, glass, concrete, and metals, which result from a process known as solidification. Due to the ever increasing use of such materials and interest in understanding these materials, solidification has become an important topic worth studying.

The process of solidification can be catagorized under one of two methods. In both cases the melt or liquid is contained in a vessel and heat is extracted. For the first method, referred to as unconstrained, the liquid is initially undercooled (i.e., the initial temperature of the liquid is less than or equal to the melting temperature of the liquid). Solidification begins with a seed crystal at the center of the vessel. The solid grows outward from this crystal with the latent heat generated at the interface being conducted through the liquid. For the second method, referred to as constrained, the melt is contained in a vessel with one wall chilled allowing the solid to grow out from the wall. The liquid is initially at a temperature which is greater than or equal to the melting temperature of the liquid. The heat generated at the interface must be conducted through the solid without melting the solid.

A variation of the second method is directional (Bridgman-type) solidification as shown in Fig. 1.1. A melt such as Al-Al_2Cu or CBr_4-C_2Cl_6 with a fixed composition is contained in a cell made up of two slides (each typically 0.2 cm thick [1]) seperated by narrow strips of thin glass (typically 150 μm thick [1]) placed between the long edges of the slides. The directional solidification system consists of hot and cold chambers positioned a fixed distance apart with the thin cell containing the melt drawn at a velocity, V, through a fixed temperature gradient, G. Before an experiment is run, the cell is held in the hot chamber to ensure thermal and solutal

equilibrium. A small portion of the cell is then moved into the cold chamber so that a planar interface can form between the chambers. Then the melt is drawn at a velocity, V, through a fixed temperature gradient, G. If the fixed composition of the melt is in a region near the eutectic composition (i.e., near the composition where the components are in such proportions that the melting point is the lowest possible with those components), the sample forms lamella of alternating alpha (α) and beta (β) phases, that is, the sample forms as a eutectic (see Fig. 1.1). In addition to regular eutectic growth, different types of oscillatory instabilities, formed at off-eutectic and eutectic concentrations, have been experimentally found at low and high velocities, respectively [2, 3]. At high velocities the crystal may take on a banded structure [2, 4–6] and at even higher velocities the growth may become single phased [6].

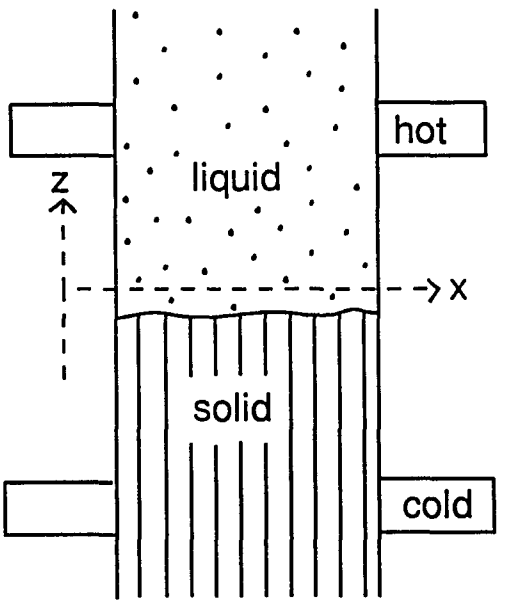

Figure 1.1: Schematic drawing of directional solidification.

This thesis will investigate the phenomenon of thin-film directional solidification of a binary alloy during eutectic growth through the process of mathematical modeling. In particular, emphasis will be placed on capturing two experimentally observed oscillatory instabilities, the "acoustic" mode and the "optical" mode [2, 3], defined in Sec. I of Chap. 3.

The process begins by identifying directional solidification of a binary alloy during eutectic growth as a Stefan-type problem, that is, a change of phase problem where the location or shape of the interface is not known in advance and must be determined as part of the solution. After the presentation of background material, the mathematical representation of the problem is presented. Then, after finding the steady state solution of the problem, a system of nonlinear equations are found from a linear stability analysis. Each equation relates the velocity to the far-field concentration for either the "acoustic" mode or the "optical" mode. The nonlinear equations are studied further using asymptotic expansions, and the mathematical model and linear stability analysis are revised to take high velocity (i.e., rapid solidification) conditions into account.

Finally, the mathematical modeling process continues with a Monte Carlo simulation applied to this solidification problem. Using a probability distribution, difference equations and Taylor's Theorem, the model presented in Chap. 3 is rewritten in terms of a probabilistic process. Simulation runs are presented, compared to each other and the previous assumptions and findings of the model, with the intention of testing the model against the simulations.

Thesis organization

The organization of this thesis is as follows. Chapter 2 contains a brief history of previous models for directional solidification of a binary alloy during eutectic growth. Chapter 3 contains the inclusion of a paper with five sections and an appendix. Section I contains an introduction and literature review. Section II contains a model of the eutectic system based on the Jackson and Hunt [7] model and Sec. III contains the steady-state solution of the system. A linear stability analysis is performed in Sec. IV, and Sec. V contains examples of oscillatory instabilities predicted by

the linear stability analysis and a discussion. The Fortran programs used for these examples are contained in Appendix A of the thesis. Comments concerning the Datye and Langer [8] model are found in the Appendix of the paper. Additional information, including explanatory steps and comments concerning the Donaghey and Tiller [9] model are contained in Appendix B of the thesis. Chapter 4 contains asymptotics which are shown to be valid for oscillations with a small wavelength and a small Péclet number, P, where $P = (\lambda V)/(2D_L)$, λ is the lamellar spacing and D_L is the diffusion coefficient for the liquid phase. Chapter 5 contains a high Péclet number model which applies when the system has a concentration near the eutectic concentration. Chapter 5 also contains the linear stability results for this new model. Chapter 6 begins with a literature review for a random walk used to simulate eutectic growth. The remainder of Chap. 6 contains the development of the random walk and results of runs of the Fortran program found in Appendix C of the thesis. Finally, Chap. 7 contains general conclusions and remarks. A comprehensive bibliography follows the chapters.

CHAPTER 2. PREVIOUS MODELS

The basic model for growth of a binary alloy during directional solidification was presented as early as 1964 by Mullins and Sekerka [10]. Other authors, Wollkind and Segel [11] and Langer [12] for example, have also contributed to modeling this solidification problem. The basic features of the model, applied to eutectic growth, are developed in [7–13]. A two-dimensional model is used with the assumptions that convection in the liquid is negligible, the extent of the liquid and solid phases is infinite and interface kinetics are negligible. Other assumptions made are that the hot and cold chambers set up a linear temperature gradient, thermal conductivities of the liquid and solid phases are about the same and small corrections due to latent heat generated at the interface are neglected. With the above assumptions, we write

$$T = T_E + Gz$$

where T is the interface temperature, T_E is the eutectic temperature and z is the interface position. Note that the imposed temperature gradient, G, is considered to be a constant due to the assumptions used.

The melt is composed of components A and B. Diffusion of component B in the liquid is modeled by the equation

$$D_L \nabla^2 C_L = \frac{\partial C_L}{\partial t} \tag{2.1}$$

where C_L is the concentration of component B in the liquid and D_L is the diffusion coefficient in the liquid. Note that in this model it has been assumed that D_L is a constant, although, in general, D_L may be dependent on time, temperature or concentration.

Likewise, diffusion of component B in the solid is modeled by

$$D_S \nabla^2 C_S = \frac{\partial C_S}{\partial t}$$

where C_S is the concentration of component B in the solid and D_S is the diffusion coefficient in the solid. Typically, $D_L \sim 10^{-5}\text{cm}^2/\text{s}$ and D_S is of order $10^{-10}\text{cm}^2/\text{s}$ (see Caroli, Caroli and Roulet [14]). Since D_S is much smaller than D_L, diffusion in the solid is much slower than diffusion in the liquid and D_S is taken as zero. Based on this assumption a one-sided model is used.

To relate temperature to concentration, an equilibrium or phase diagram is used. The alpha and beta phase liquidus lines of the phase diagram are assumed to be straight, at least near the eutectic concentration, C_E (see Fig. 3.2). With this assumption the equation of the alpha phase liquidus line is given by

$$T_\alpha = -m_\alpha (C_{L\alpha} - C_E) + T_E$$

and the equation of the beta phase liquidus line is given by

$$T_\beta = m_\beta (C_{L\beta} - C_E) + T_E.$$

Note that these equations do not take the curvature of the interface into account. To do this, the temperature at the interface is given by a form of the Gibbs-Thomson relation so that

$$T = \begin{cases} \left[-m_\alpha (C_{L\alpha} - C_E) + T_E\right]\left[1 - \frac{\sigma_\alpha}{L_\alpha}\kappa_\alpha\right] & \text{in the } \alpha \text{ phase} \\ \left[m_\beta (C_{L\beta} - C_E) + T_E\right]\left[1 - \frac{\sigma_\beta}{L_\beta}\kappa_\beta\right] & \text{in the } \beta \text{ phase} \end{cases} \tag{2.2}$$

where σ is the liquid-solid surface tension, L is the latent heat per unit volume and κ is the curvature. Equation (2.2) is referred to as the thermal boundary condition at the interface.

A second boundary condition at the interface comes from considering conservation of mass. If $\Delta C_i = (C_L - C_S)_i$ is the miscibility gap at the interface and V_n is the normal component of the interface velocity, then $V_n \Delta C_i$ is the quantity of component B rejected by the solid per unit area per unit time. This is set equal to the negative of the diffusion coefficient times the normal component of the concentration gradient at the interface. Thus the conservation of mass boundary condition at the interface is written as

$$V_n \Delta C_i = -D_L (\vec{n} \bullet \nabla C)_i \tag{2.3}$$

where $(\vec{n} \bullet \nabla C)_i$ is the normal component of the concentration gradient at the interface. In addition to the two boundary conditions at the interface, the model also incorporates a condition at infinity such that

$$\lim_{z \to \infty} C(z) = C_\infty. \tag{2.4}$$

Due to the complexity of the eutectic system, various additional simplifications and assumptions have been applied to the model. In 1966, Jackson and Hunt [7] assumed a flat eutectic interface. Thus the normal to the interface was taken as parallel to the direction of the growth velocity. In addition, C_L and C_S were assumed to be constants in the ΔC_i term of the conservation of mass boundary condition such that $C_L = C_E$, $C_S = C_{\alpha E}$ in the alpha phase and $C_S = C_{\beta E}$ in the beta phase. Jackson and Hunt argued that the variations of composition with position across the interface were small and could be dismissed in the ΔC_i term. These simplifications were used to write down their solution for the concentration of component B in the liquid as a Fourier Series. Note that during a later calculation, involving the thermal boundary condition, the average curvature of the interface was used and departures form the eutectic composition were considered important.

As part of the Jackson and Hunt analysis, they also assumed that $T_\alpha - T_E \equiv \Delta T_\alpha$ equals $T_\beta - T_E \equiv \Delta T_\beta$, that is, they made an equal-average-undercooling assumption. With this model, they found a relationship between the lamellar spacing, λ, and the average undercooling, ΔT, for a fixed velocity. They then picked out a unique lamellar spacing, λ_{min}, based on the minimum of the λ-ΔT curve.

Two years later, Donaghey and Tiller [9] maintained the assumption of a flat eutectic interface. However, they did not make the assumption that C_L and C_S can be taken as constants in the conservation of mass boundary condition. This complicated the procedure used to find the Fourier coefficients for their solution (for the concentration of component B in the liquid), in the respect that during the calculations involving the conservation of mass boundary condition an infinite system of equations was derived. This infinite system was then solved using the assumption that $(\lambda V)/(2D_L) \ll n\pi$ where n is a positive integer.

More recently, in 1981, Datye and Langer [8] proceeded with their analysis as Jackson and Hunt did except that C_L was not taken as C_E in the conservation of mass

boundary condition. Due to this change, they used the equal-average-undercooling assumption to complete their solution (for the concentration of component B in the liquid). Once they found their Fourier coefficients they then perturbed the interface in directions tangential and parallel to the interface, using a quasistationary assumption in their calculations.

The remainder of the dissertation will follow the models just presented in that a one-sided two-dimensional model will be used with the assumption of a planar interface (see Fig. 2.1) except in the thermal boundary condition where a curvature term appears. However, we will not assume equal-average-undercooling in the stability analysis except in the appendix of the paper presented in Chap. 3 where the Datye and Langer model is discussed nor will we use the quasistationary assumption of Datye and Langer [8]. The Jackson and Hunt [7] conservation of mass boundary condition and thermal boundary condition will be used throughout the main body of the thesis with comments concerning the Datye and Langer [8] model and the Donaghey and Tiller [9] model contained in the appendicies.

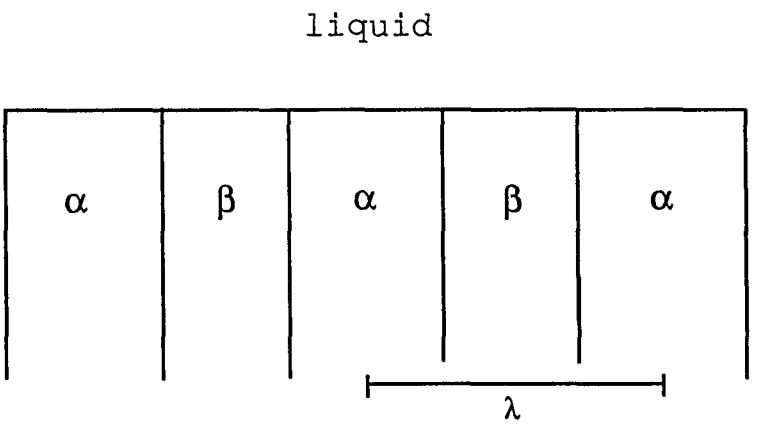

Figure 2.1: Schematic illustration of a lamellar eutectic with a flat interface.

CHAPTER 3. OSCILLATORY INSTABILITIES IN DIRECTIONALLY SOLIDIFIED EUTECTICS

A paper published in Physical Review B.[1]

Brenda A. Wolfe Diesslin and William T. Grayhack

Abstract

The presence of oscillatory instabilities during directional solidification of thin lamellar eutectics is explored. A linear stability analysis is performed in which the triple points are perturbed tangential to the interface, i.e., no Mullins-Sekerka type of morphological instabillity is allowed. A locally planar interface is assumed except in the thermal boundary condition where a curvature term is included. Neither the quasistationary approximation nor the equal-average-undercooling assumption is used; instead, the average concentration over a phase is forced to be consistent with the thermal boundary condition. This analysis reveals two oscillatory modes, an "acoustic" mode of wavelength twice that of the lamellar spacing and an "optical" mode of wavelegth equal to the lamellar spacing.

I. INTRODUCTION

Over the past 30 years directionally solidified eutectics have attracted considerable attention. Jackson and Hunt [7] (1966) extended a two-dimensional, one-sided model of a directionally solidified binary alloy (see, e.g., Mullins and Sekerka [10] and Langer [12]) to the eutectic case. Aside from the standard assumptions, their

[1]Reprinted with permission from *Physical Review B*, **50** (13) (1994), pp. 9111-9117.

analysis made use of an approximation in the conservation of mass boundary condition and, most significantly, equal average undercooling. Since then, other authors [15–21] have relaxed or revised some of the assumptions and analyzed the linear stability of these systems. Cline [15] (1968) carried out a linear stability analysis using a long- wavelength perturbation perpendicular to the interface where he treated the eutectic as a single phase and used an "effective" liquidus slope. He found a range of compositions in which stable growth may occur with a zero temperature gradient. Hurle and Jackman [16] (1968) also treated the eutectic as a single phase, averaging over the properties of the two phases. They found that in certain eutectic systems, the presence of a boundary layer leads to a morphological instability of the interface, at a wavelength comparable to that of a cellular single-phase material.

Strässler and Schneider [17] (1973) and Cline [18] (1979) approached the analysis by allowing variations of the lamellar spacing but did not consider any curvature effects. It was found that both short- and long-wavelength perturbations determine the growth conditions and that for spacings larger than a critical value, the growth of the eutectic was stable. Using an equal average undercooling assumption and a quasistationay approximation, Datye and Langer [8] (1981) perturbed the triple points of a eutectic in directions both tangential and perpendicular to the interface. At sufficiently off-eutectic melt compositions, an oscillatory instability with a wavelength approximately twice the lamellar spacing was found. This instability is referred to as an "acoustic" mode in which adjacent triple points oscillate in phase, tangential to the interface, so that the volume fractions of the two solid phases remain constant along the interface [see Fig. 3.4(b)]. They also found long-wavelength instabilities at lamellar spacings less than a critical value. Karma [19] (1987) duplicated the oscillatory instabilities found by Langer using a Laplacian approximation and a random walk model.

Caroli, Caroli, and Roulet [20] (1990) did an analysis in the large thermal gradient limit and small Péclet number limit using planar front and quasitationary approximations. They found long-wavelength instabilities for lamellar spacings on the same order of magnitude as the lamellar spacing corresponding to a minimum undercooling criteria. They also found two instabilities which are mixtures of interface modulations and "optical" modes [see Fig. 3.6(b)]. The term "optical" refers to an

oscillation in which adjacent triple points oscillate out of phase so that the volume fractions of the two solid phases also oscillate in time. Kassner and Misbah [21] (1991) studied lamellar eutectic growth in directional solidification by analyzing the pertinent boundary integral equation using a small Péclet number. They showed that average undercoolings are, in general, not equal. They also showed that for their model equations and for average undercooling as a function of the lamellar spacing, there are four branches of axi-symmetric solutions and one branch of tilted solutions.

In this paper, both the equal average undercooling and quasistationary approximations used by previous authors are relaxed. Though only perturbations tangential to the interface are considered, both an optical mode independent of interface modulations as well as the acoustic mode of Datye and Langer [8] are found. For a fixed thermal gradient G the acoustic modes occur in a region of low Péclet numbers (low velocities) and off-eutectic compositions (see Figs. 3.8 and 3.9). However, the optical modes appear in a region which ranges from low velocities, with compositions further from the eutectic composition; to higher velocities, with compositions closer to or at the eutectic composition depending on the particular eutectic system being considered (see Figs. 3.8 and 3.9).

The scheme of this paper is as follows. In Sec. II the model for the directional solidification of thin lamellar eutectics is described and in Sec. III the steady-state solution is given. Here we have chosen to follow Jackson and Hunt (JH) [7], but without the equal average undercooling assumption. The Appendix contains the parallel results for the Datye and Langer [8] (DL) model. Section IV consists of a linear stability analysis where a set of equations are found, which relate the pulling velocity (Péclet number) to the far-field concentration (volume fraction) and Sec. V contains examples of this relationship.

II. THE MODEL

To construct a model for the directional solidification of thin lamellar eutectic growth, the following assumptions are used: constant thermal gradient, G; equal thermal conductivities in the liquid and solids; negligible latent heat production and attachment kinetics; linear liquidus and solidus lines near the eutectic temperature;

and negligible diffusion in the solid phases. As in the JH model [7], the lamellar fronts are taken to be locally planar when the concentration field is calculated and the curvature of the interface is considered only in the thermal boundary condition.

Let V be the velocity, D the diffusion coefficient in the liquid phase, and λ the lamellar spacing [see Fig. 3.1(a)]. The Péclet number, P, is defined as $\lambda V/2D$. Tangential to the interface, lengths are scaled on $\lambda/2$, the half width of the eutectic spacing. Perpendicular to the interface, lengths are also scaled by a $\sqrt{P}$ factor, taking into account the diffusion-limited growth in the z direction. In particular, this will bring out the dependence on P of the rate of change of the average curvature (see Sec. IV). Time is scaled by $\lambda P/2V$. The dimensionless concentration in the liquid is $U \equiv (C - C_E)/\Delta C$ where C is the concentration, C_E is the eutectic concentration, and ΔC is the miscibility gap shown in Fig. 3.2(a).

In a frame of reference moving at the pulling velocity, diffusion of solute in the liquid is modeled by the differential equation:

$$P\frac{\partial^2 U}{\partial x^2} + \frac{\partial^2 U}{\partial z^2} + P^{3/2}\frac{\partial U}{\partial z} = P\frac{\partial U}{\partial t}. \tag{3.1}$$

Conservation of mass at the interface (indicated by the subscript i) requires that

$$-\left.\frac{\partial U}{\partial z}\right|_i = P^{3/2}\,\Delta U_i = P^{3/2}\begin{cases} U_i - U_\alpha & \text{in the } \alpha \text{ phase} \\ U_i - U_\beta & \text{in the } \beta \text{ phase.} \end{cases} \tag{3.2}$$

Note that U_α and U_β, as shown in Fig. 3.2(b), are in general not equal to $U_{\alpha E}$ and $U_{\beta E}$.

Thermal continuity at the interface requires that

$$-\frac{\lambda\sqrt{P}}{2}\,G\,z = T_E - T = \begin{cases} m_\alpha\, U_i\,\Delta C + \dfrac{2}{\lambda}\,\Gamma_\alpha\,\kappa & \text{in the } \alpha \text{ phase} \\ -m_\beta\, U_i\,\Delta C + \dfrac{2}{\lambda}\,\Gamma_\beta\,\kappa & \text{in the } \beta \text{ phase,} \end{cases} \tag{3.3}$$

where κ is the interface curvature, m is the absolute value of the slope of the liquidus line, Γ is the Gibbs-Thomson coefficient such that Γ equals $\sigma T_E/L$, σ being the liquid-solid surface tension, T_E being the euctectic temperature, and L being the latent heat per unit volume. Local equilibrium at the triple points requires that

$$\sigma_\alpha \sin\theta_\alpha + \sigma_\beta \sin\theta_\beta = \sigma_{\alpha\beta} \quad \text{and} \quad \sigma_\alpha \cos\theta_\alpha - \sigma_\beta \cos\theta_\beta = 0$$

where θ_α and θ_β are shown in Fig. 3.1(a) and $\sigma_{\alpha\beta}$ is the α-β surface tension.

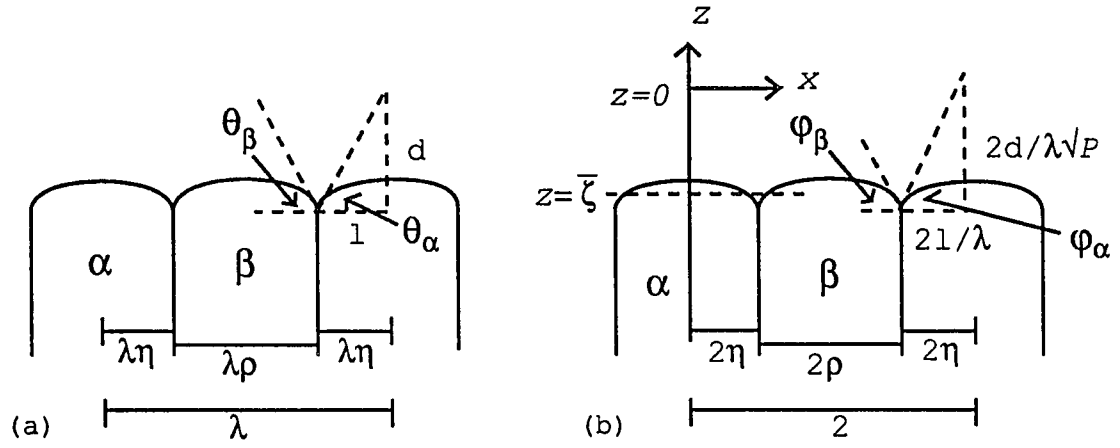

Figure 3.1: Schematic illustration of a lamellar eutectic using (a) dimensional units and (b) nondimensional units.

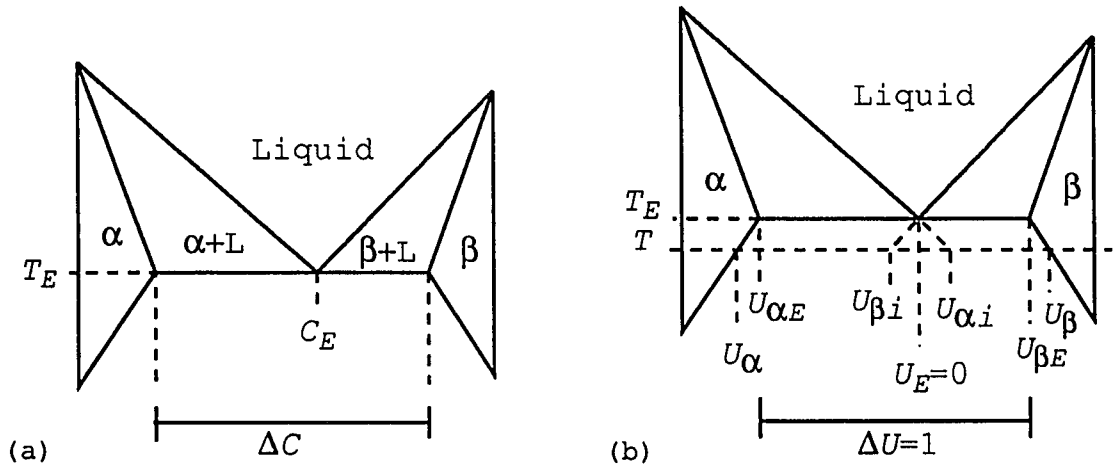

Figure 3.2: Portion of the phase diagram for the binary eutectic using (a) dimensional units and (b) nondimensional units.

III. STEADY-STATE SOLUTION

We seek a solution to the the steady-state system, Eqs. (3.1)-(3.3) with $\partial U/\partial t = 0$, in the form of a Fourier series

$$U(x,z) = U_\infty + \sum_{n=-\infty}^{\infty} E_n \, e^{iqnx} \, e^{-F_n(z-\bar{\zeta})} \tag{3.4}$$

where

$$q_n = n\pi, \quad F_n = P^{1/2} \left\{ \frac{P}{2} + \left[\left(\frac{P}{2}\right)^2 + (n\pi)^2 \right]^{1/2} \right\}, \tag{3.5}$$

$\bar{\zeta}$ is the average interface position as shown in Fig. 1(b), and U_∞ is the dimensionless far-field concentration. In the above calculations and throughout the paper we follow JH [7], for simplicity, such that U_i is approximated by U_E, U_α is approximated by $U_{\alpha E}$, and U_β is approximated by $U_{\beta E}$ [see Fig. 3.2(b)] in the conservation of mass boundary condition, Eq. (3.2).

To find E_n, substitute Eq. (3.4) into Eq. (3.2) and set $z_i = \bar{\zeta}$. Then the Fourier coeffiecients are found such that

$$E_0 = -2\eta \, U_{\alpha E} - \rho \, U_{\beta E} \equiv \tau, \tag{3.6}$$

$$E_n = P \left\{ \frac{P}{2} + \left[\left(\frac{P}{2}\right)^2 + (n\pi)^2 \right]^{1/2} \right\}^{-1} \frac{\sin(2n\pi\eta)}{n\pi} \quad \text{for } n \neq 0, \tag{3.7}$$

where 2η is the volume fraction of the α phase and ρ is the volume fraction of the β phase such that $2\eta + \rho = 1$ [see Figs. 3.1(a) and (b)] and $U_\infty = 2\eta \, U_{\alpha E} + \rho \, U_{\beta E}$ where the units of U are given in volume percent. If $P << 1$ then the DL model [8] agrees, to order P^2, with Eq. (3.5) and (3.7); however, the expressions for E_0 differ. [See the Appendix, Eqs. (3.A1)-(3.A3).]

IV. LINEAR STABILITY ANALYSIS

For the linear stability analysis, we do not use an equal average undercooling or a quasistationary approximation. We assume that the average front position remains

at $\bar{\zeta}$ and consider perturbations in the x direction only so that the $\alpha\beta$ and $\beta\alpha$ triple points are perturbed by

$$x_j^{\alpha}\, e^{i\sigma 2(j+\eta)+\omega t} \quad \text{and} \quad x_j^{\beta}\, e^{i\sigma 2(j+\eta)+\omega t}$$

respectively (see Fig. 3.3), where σ is a multiple of π/N and x_j^{α} and x_j^{β} are small. The volume fractions are allowed to change with time, subject to λ remaining constant. We consider the following cases:

$$(1)\ \mathrm{N}=1,\ -x_j^{\alpha} = x_j^{\beta} = \hat{x} \quad \text{and} \quad (2)\ \mathrm{N}=2,\ -x_j^{\alpha} = -x_j^{\beta} = \hat{x}$$

and write the perturbed volume fractions as $\hat{\eta} = \eta + \frac{1}{2}\, x_j^{\alpha}\, e^{i\sigma 2(j+\eta)+\omega t}$, $\hat{\rho} = \rho - \frac{1}{2}\,(x_j^{\alpha} - x_j^{\beta})\, e^{i\sigma 2(j+\eta)+\omega t}$ and $\hat{\delta} = \eta - \frac{1}{2}\, x_j^{\beta}\, i\sigma 2(j+\eta)+\omega t$, where $\hat{\eta}$, $\hat{\rho}$, and $\hat{\delta}$ represent the time-dependent volume fractions such that $\hat{\eta} + \hat{\rho} + \hat{\delta} = 1$ (see Fig. 3.3). Note that the coordinate system, which is different than the one used by DL [8], has been chosen so that both the α-phase and β-phase volume fractions can vary independently, allowing for the possibility of the optical mode to occur.

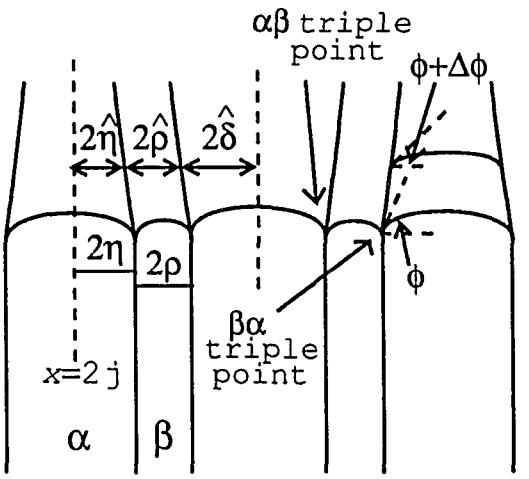

Figure 3.3: Schematic illustration of a perturbed lamellar eutectic.

We seek a solution to the perturbed system in the form

$$U(x,z,t) = U(x,z) + \sum_{n=-\infty}^{\infty} \hat{E}_n(t)\, e^{i\hat{q}nx}\, e^{-\hat{F}n(z-\bar{\zeta})} \tag{3.8}$$

where $U(x,z)$ is the JH steady-state solution and $\hat{q}_n = n\pi/N$. Using the conservation of mass boundary condition, Eq. (3.2), and setting

$$\frac{1}{2N}\int_{2j}^{2(j+N)} \left[\left.\frac{\partial U}{\partial z}\right|_i + P^{3/2}\,\Delta U_i \right] e^{-i\hat{q}mx}\, dx = 0, \tag{3.9}$$

it is found that for $N = 1$

$$\hat{E}_0(t) = \frac{-P^{3/2}}{\hat{F}_0}\,\hat{x}\, e^{i\sigma 2(j+\eta)+\omega t} + O(\hat{x}^2),$$
$$\hat{E}_n(t) = -P^{3/2}\left(\frac{\cos(2n\pi\eta)}{\hat{F}_n}\right)\hat{x}\, e^{i\sigma 2(j+\eta)+\omega t} + O(\hat{x}^2) \quad \text{for } n \neq 0,$$

and for $N = 2$

$$\hat{E}_n(t) = 0 + O(\hat{x}^2) \quad \text{when } n \text{ is even},$$
$$\hat{E}_n(t) = (-1)^{j+1}\, P^{3/2}\left(\frac{\cos(n\pi\eta)}{\hat{F}_n}\right)\hat{x}\, e^{i\sigma 2(j+\eta)+\omega t} + O(\hat{x}^2) \quad \text{when } n \text{ is odd},$$

where $\hat{F}_n$ satisfies

$$\hat{F}_n = P^{1/2}\left\{\frac{P}{2} + \left[\left(\frac{P}{2}\right)^2 + \left(\frac{n\pi}{N}\right)^2 + \omega\right]^{1/2}\right\}.$$

When $P << 1$ and $(n\pi/N)^2 + \omega \gg (P/2)^2$ for $N = 1, 2$, the previous Fourier coefficients agree, to order P^2, with those found by using the DL model [8]. Note that the differences in E_0 have no affect on these coefficients.

To find an expression for ω in terms of 2η the thermal boundary condition, Eq. (3.3), is used to solve for U_i and the average concentration over a phase is found. Since Eq. (3.3) contains a curvature term, we need the average curvature over a

phase. Using an α phase centered at $x = 2j$, the average curvature is calculated as $\sin(\phi + \Delta\phi)/(2\hat{\eta})$ where $\Delta\phi$ is the change in the angle measured from the horizontal (see Fig. 3). For small $\Delta\phi$,

$$\Delta\phi \approx \tan\Delta\phi = dx/d\tilde{z} = -\left(\frac{\omega}{\sqrt{P}}\right)\hat{x}\, e^{i\sigma 2(j+\eta)+\omega t}$$

where $\tilde{z} = z + \sqrt{P}t$. Thus

$$\langle\kappa\rangle_\alpha = \frac{\sin(\phi_\alpha)}{2\eta} + \left(\frac{\sin(\phi_\alpha)}{(2\eta)^2} - \frac{\cos(\phi_\alpha)}{2\eta}\frac{\omega}{\sqrt{P}}\right)\hat{x}\, e^{i\sigma 2(j+\eta)+\omega t} + O(\hat{x}^2).$$

Then the average concentration over the same region is found using the concentration equation, Eq. (3.8), and the two averages are set equal to one another. The zero-order terms relate E_0 to $\bar{\zeta}$. Thus the differences in E_0 affect the initial placement of the interface but do not affect the perturbation. From the first-order terms the following equations result such that for $N = 1$

$$\frac{S(\eta)}{(2\eta)^2} - \frac{R(\eta)}{2\eta} + \frac{2\,\Gamma_\alpha \sin(\phi_\alpha)}{(2\eta)^2\, m_\alpha\, \Delta C\, \lambda P} - \omega\frac{2\,\Gamma_\alpha \cos(\phi_\alpha)}{(2\eta)\, m_\alpha\, \Delta C\, \lambda P}\frac{1}{\sqrt{P}}$$

$$= \left\{\frac{P}{2} + \left[\left(\frac{P}{2}\right)^2 + \omega\right]^{1/2}\right\}^{-1}$$

$$+ \frac{1}{2\eta}\sum_{n=1}^{\infty}\frac{\sin(4n\pi\eta)}{n\pi}\left\{\frac{P}{2} + \left[\left(\frac{P}{2}\right)^2 + (n\pi)^2 + \omega\right]^{1/2}\right\}^{-1} \tag{3.10}$$

and for $N = 2$

$$\frac{S(\eta)}{(2\eta)^2} - \frac{R(\eta)}{2\eta} + \frac{2\,\Gamma_\alpha \sin(\phi_\alpha)}{(2\eta)^2\, m_\alpha\, \Delta C\, \lambda P} - \omega\frac{2\,\Gamma_\alpha \cos(\phi_\alpha)}{(2\eta)\, m_\alpha\, \Delta C\, \lambda P}\frac{1}{\sqrt{P}}$$

$$= \frac{1}{2\eta}\sum_{\text{odd } n=1}^{\infty}\frac{\sin(2n\pi\eta)}{n\pi/2}\left\{\frac{P}{2} + \left[\left(\frac{P}{2}\right)^2 + \left(\frac{n\pi}{2}\right)^2 + \omega\right]^{1/2}\right\}^{-1} \tag{3.11}$$

where

$$S(\eta) = 2\sum_{n=1}^{\infty} \frac{\sin^2(2n\pi\eta)}{(n\pi)^2} \left\{ \frac{P}{2} + \left[\left(\frac{P}{2}\right)^2 + (n\pi)^2 \right]^{1/2} \right\}^{-1}$$

and

$$R(\eta) = \sum_{n=1}^{\infty} \frac{\sin(4n\pi\eta)}{n\pi} \left\{ \frac{P}{2} + \left[\left(\frac{P}{2}\right)^2 + (n\pi)^2 \right]^{1/2} \right\}^{-1}.$$

Note that ϕ_α (or θ_α) and the quantity $(2\Gamma_\alpha)/(m_\alpha \Delta C \lambda P) \equiv \Omega$ are physical parameters dependent on the eutectic system under consideration. For $N = 1$, Eq. (3.10) yeilds a relationship between 2η, the α phase volume fraction, and P, the Péclet number. Similarly, for $N = 2$, Eq. (3.11) yields a different dependence of P on 2η.

V. EXAMPLES AND DISCUSSION

For the oscillations we consider, $\omega = ib$, i.e., ω is pure imaginary. Referring to Figs. 3.4(a)–3.7(a) we see how the real and imaginary equations are mapped out in terms of 2η and P for given Ω, θ, N, and b values. The parametric values needed for the computations are taken from experiments by Magnin and Trivedi [22]. All the summations are well-approximated by the first 200 terms (or less) in the series. For fixed Ω, θ, and N, the points of intersection map out a line segment of solutions as b varies; these lines move smoothly when Ω is varied, mapping a region in P-2η space where these oscillation occur. Figs. 3.4(b)–3.7(b) and Fig. 3.6(c) show the real space trajectories of the triple points for a particular set of solutions corresponding to Figs. 3.4(a)–3.7(a). Note that some solutions may be such that the P value is unrealistically large or small, and the system of equations is quite sensitive to the value of Ω.

For $N = 1$ there are variations with time in the volume fraction over one period from the middle of an α phase to the middle of the next α phase; however, for $N = 2$ these variations do not exist. The acoustic (2λ) oscillations shown occur at off-eutectic compositions and at low velocities (see Figs. 3.8 and 3.9). For the CBr_4-C_2Cl_6 system, the optical mode occurs at the eutectic composition or near

the eutectic composition with a higher velocity compared to the velocity for the acoustic modes (see Fig. 3.8). For the Al-Al_2Cu system, the optical modes occur at high velocities, close to the eutectic composition or at low velocities, but further from the eutectic composition; however, these oscillations with a low velocity may be difficult to see due to the size of b (see Fig. 3.9). The results agree qualitatively with experiments done on the Al-Al_2Cu system by Zimmermann *et al.* [2, 3].

For $\mathrm{Im}(\omega) \neq 0$ and $\mathrm{Re}(\omega) < 0$ (> 0), the perturbations may lead to growing and/or decaying oscillatory modes which result in a chaotic behavior, as discussed by Faivre, Guthman, and Mergy [23] or to oscillatory tilt waves as seen in the simulations of Xiao, Alexander, and Rosenberger [24]. For $\mathrm{Re}(\omega) > 0$ and $\mathrm{Im}(\omega) = 0$, these perturbations may lead to increased eutectic spacings or tilt waves. Further analysis is necessary to determine which, if any, of these dynamical states are present in our model. Currently, using the method presented in this paper, we are able to capture both previously observed oscillatory modes in a single, simpler (x perturbations only) analysis.

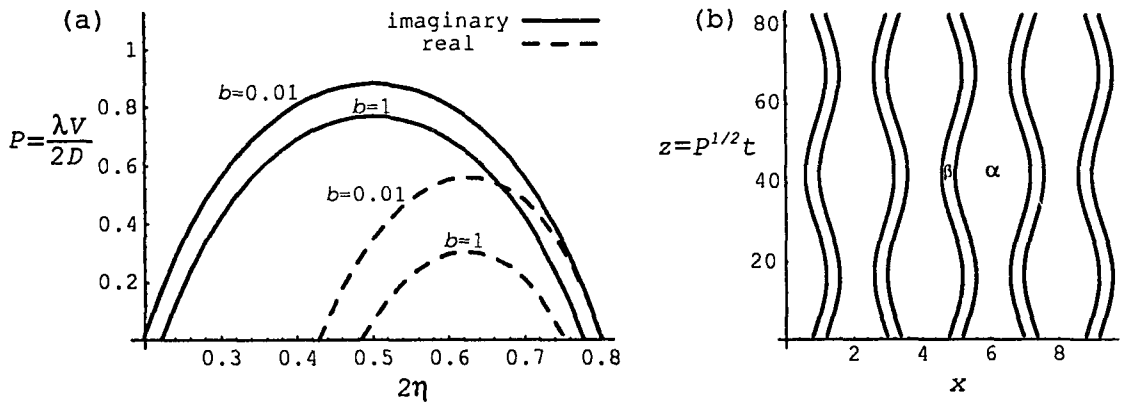

Figure 3.4: (a) Plot of real and imaginary equations, 2η vs P, for $N = 2$, $\Omega = 0.1045$, and $\theta = 65^\circ$ and (b) real-space trajectories of the triple points for $b = 0.01$, $P = 0.0067$, and $2\eta = 0.8015$ after 1000 units of time for the Al-Al_2Cu eutectic system with eutectic composition corresponding to $2\eta = 0.54$.

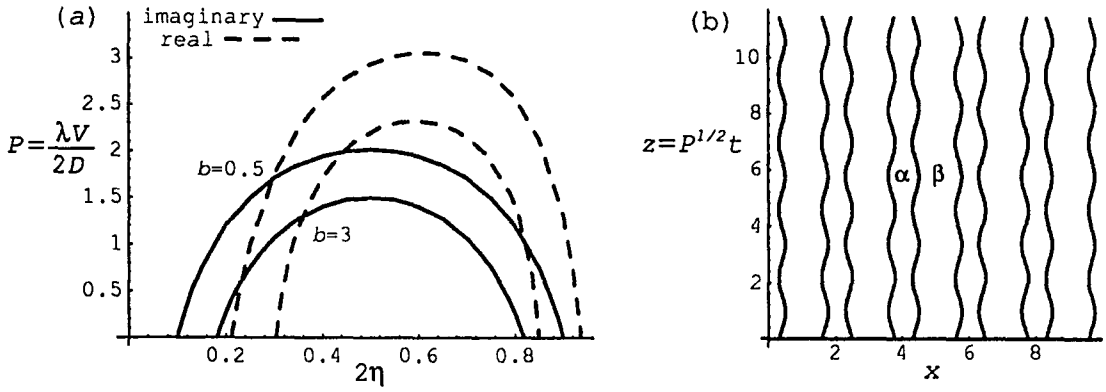

Figure 3.5: (a) Plot of real and imaginary equations, 2η vs P, for $N = 2$, $\Omega = 0.0447$, and $\theta = 60^{\circ}$ and (b) real-space trajectories of the triple points for $b = 3$, $P = 1.3015$, and $2\eta = 0.3595$ after 10 units of time for the CBr_4-C_2Cl_6 eutectic system with eutectic composition corresponding to $2\eta = 0.676$.

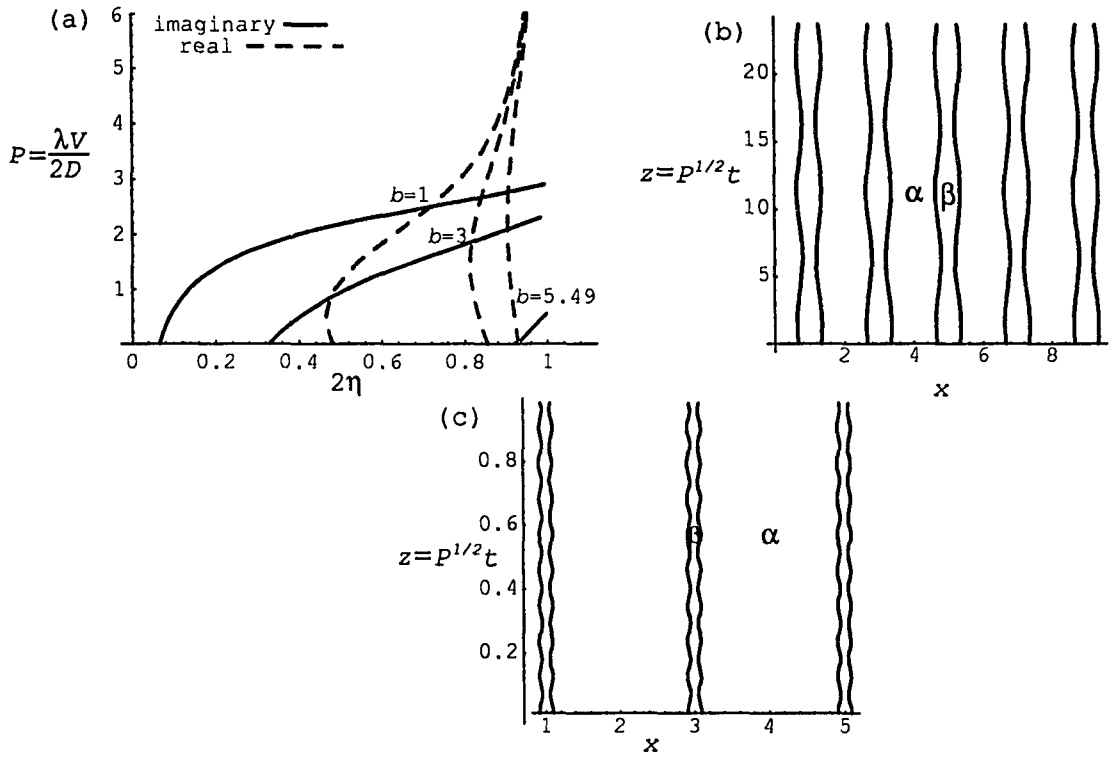

Figure 3.6: (a) Plot of real and imaginary equations, 2η vs P, for $N = 1$, $\Omega = 0.1045$, and $\theta = 65^{\circ}$ and (b) real-space trajectories of the triple points for $b = 1$, $P = 2.497$, and $2\eta = 0.7191$ after 15 units of time, and (c) real-space trajectories of the triple points for $b = 5.49$, $P = 0.0095$, and $2\eta = 0.9285$ after 10 units of time for the Al-Al_2Cu eutectic system with eutectic composition corresponding to $2\eta = 0.54$.

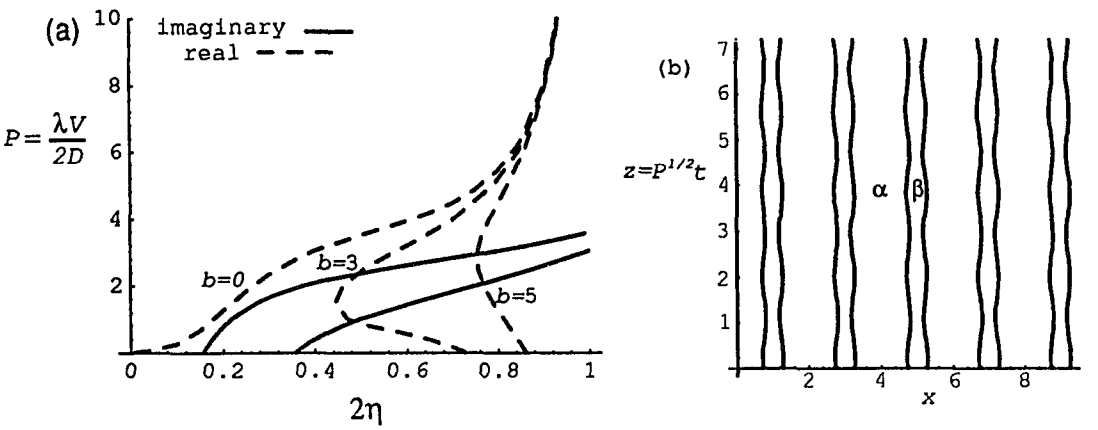

Figure 3.7: (a) Plot of real and imaginary equations, 2η vs P, for $N = 1$, $\Omega = 0.0447$, and $\theta = 60^{\circ}$ and (b) real-space trajectories of the triple points for $b = 5$, $P = 2.068$, and $2\eta = 0.7656$ after 5 units of time for the CBr_4-C_2Cl_6 eutectic system with eutectic composition corresponding to $2\eta = 0.676$.

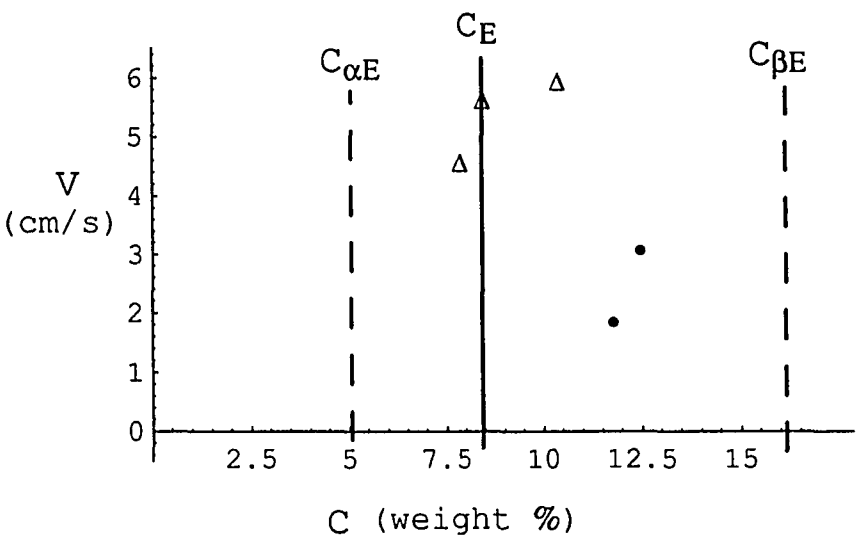

Figure 3.8: Plot of Concentration (wt %) vs Velocity (cm/s) for $N = 1$ (Δ) and $N = 2$ ($\bullet$) and the CBr_4-C_2Cl_6 eutectic system with $\Omega = 0.0447$, and $\theta = 60^{\circ}$.

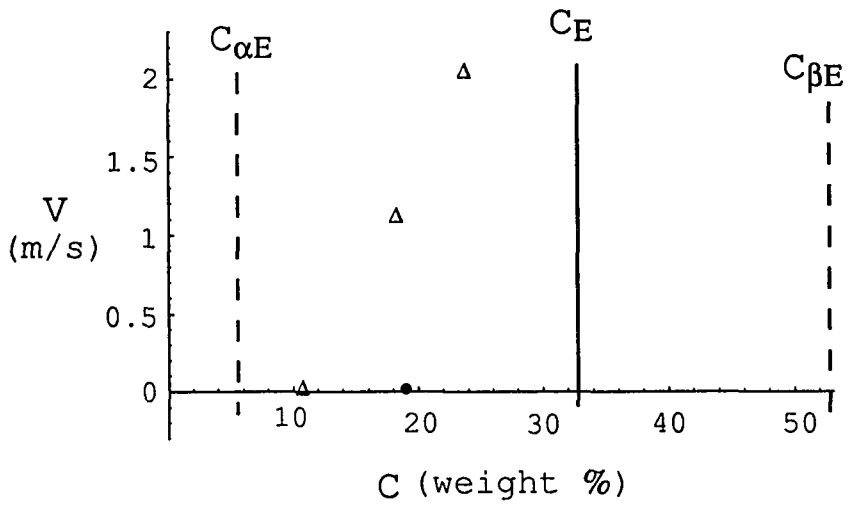

Figure 3.9: Plot of Concentration (wt %) vs Velocity (m/s) for $N = 1$ (Δ) and $N = 2$ ($\bullet$) and the Al-Al_2Cu eutectic system with $\Omega = 0.1045$ and $\theta = 65^\circ$.

APPENDIX: DATYE AND LANGER MODEL

The DL model differs from the JH model in the conservation of mass boundary condition, Eq. (3.2). DL [8] use two of the approximations made by JH ($U_\alpha \approx U_{\alpha E}$ and $U_\beta \approx U_{\beta E}$). For the DL model, E_0 can not be found in the same manner as the E_n's for $n \neq 0$ since the equation that results is $\tau + U_\infty = 0$. To find E_0, the average $\Delta T_\alpha \equiv T_E - T$ over an α phase is set equal to the average ΔT_β over a β phase. The remaining E_n's and the F_n's are found as in Sec. III. Thus,

$$F_n = P^{1/2} \left\{ \frac{P}{2} + \left[\left(\frac{P}{2} \right)^2 + (n\pi)^2 \right]^{1/2} \right\}, \tag{3.A1}$$

$$E_0 = -U_\infty + \frac{P\,Q(\eta)}{(m_\alpha + m_\beta)}\left(\frac{m_\beta}{\rho} - \frac{m_\alpha}{2\eta}\right) + \frac{2}{\lambda \Delta C\,(m_\alpha + m_\beta)}\left[\frac{\Gamma_\beta \sin(\phi_\beta)}{\rho} - \frac{\Gamma_\alpha \sin(\phi_\alpha)}{2\eta}\right], \tag{3.A2}$$

$$E_n = P\left\{\left[\left(\frac{P}{2}\right)^2 + (n\pi)^2\right]^{1/2} - \frac{P}{2}\right\}^{-1} \frac{\sin(2n\pi\eta)}{n\pi} \qquad \text{for } n \neq 0, \tag{3.A3}$$

where $\phi = \tan^{-1}[\tan(\theta)/\sqrt{P}]$ (see Fig. 3.1) and $Q(\eta) \approx 2\sum_{n=1}^{\infty} \sin^2(2n\pi\eta)/(n\pi)^3$. Note that for small P, the Fourier coefficients that affect the perturbation are the same for the DL model and the JH model. Thus Figs. 3.4(a)–3.7(a), in the small P range, and Figs. 3.4(b) and 3.6(c) also apply for the DL model.

CHAPTER 4. ASYMPTOTICS

It is difficult to evaluate the dependence of 2η and P on ω in the nonlinear Eqs. (3.10) and (3.11) in Chap. 3 due to the summation involving ω. In this chapter, simplier forms of Eqs. (3.10) and (3.11) are found under the assumption of a small Péclet number, using asymptotic expansions to rewrite the summations involving ω.

Acoustic oscillations ($N = 2$)

The small P approximation of Eq. (3.11) is written as

$$\frac{\tilde{S}(\eta)}{2\eta} - \tilde{R}(\eta) + \frac{\Omega \sin(\phi_\alpha)}{2\eta} - \omega \frac{\Omega \cos(\phi_\alpha)}{\sqrt{P}} = \sum_{\text{odd } n=1}^{\infty} \frac{\sin(2n\pi\eta)}{n\pi/2} \left[\left(\frac{n\pi}{2}\right)^2 + \omega \right]^{-1/2} \tag{4.1}$$

where

$$\tilde{S}(\eta) = 2 \sum_{n=1}^{\infty} \frac{\sin^2(2n\pi\eta)}{(n\pi)^3}$$

and

$$\tilde{R}(\eta) = \sum_{n=1}^{\infty} \frac{\sin(4n\pi\eta)}{(n\pi)^2}.$$

Note that $\tilde{S}(\eta)$, $\tilde{R}(\eta)$ and the sum on the right hand side of Eq. (4.1) are uniformly convergent series for $0 \leq 2\eta \leq 1$. Using a method based on improving the rate of convergence of Fourier Series as discussed by Kantorovich and Krylov [25] and Fulks [26], one lets

$$H(t) = \frac{4}{\pi^2} t^2 \left[1 + \frac{4\omega}{\pi^2} t^2 \right]^{-1/2}$$

where $0 \leq t \leq 1$. Then the right hand side of Eq. (4.1) is rewritten as

$$\sum_{\text{odd } n=1}^{\infty} H\left(\frac{1}{n}\right) \sin(2n\pi\eta).$$

Since $H(t)$ is at least eight times differentiable in the interval (0,1), one may use Taylor's Theorem with remainder to write

$$H(t) = \frac{4}{\pi^2}\, t^2 - \frac{8\omega}{\pi^4}\, t^4 + \frac{24\omega^2}{\pi^6}\, t^6 + \frac{H^{(8)}(t_k)}{8!}\, t^8$$

with

$$\frac{H^{(8)}(t_k)}{8!} = \frac{8\omega^3}{\pi^{16}} \left[a_1 + a_2\, t_k^2 + a_3\, t_k^4 + a_4\, t_k^6 + a_5\, t_k^8\right] \left[1 + \frac{4\omega}{\pi^2}\, t_k^2\right]^{-17/2},$$

$$\begin{aligned} a_1 &= -10\,\pi^8, \\ a_2 &= 1235\,\pi^6\,\omega, \\ a_3 &= -13920\,\pi^4\,\omega^2, \\ a_4 &= 25856\,\pi^2\,\omega^3, \\ a_5 &= -4096\,\omega^4 \end{aligned}$$

and $0 \le t_k \le 1$. Therefore

$$\sum_{\text{odd } n=1}^{\infty} H\left(\frac{1}{n}\right) \sin(2n\pi\eta) = 4\,\Psi_2(\eta) - 8\,\Psi_4(\eta)\,\omega + 24\,\Psi_6(\eta)\,\omega^2 + \varepsilon_4$$

where

$$\Psi_j(\eta) = \sum_{\text{odd } n=1}^{\infty} \frac{\sin(2n\pi\eta)}{(n\pi)^j}$$

is a uniformly convergent series for $j = 2$, 4 and 6; and the error term

$$\varepsilon_4 = \sum_{\text{odd } n=1}^{\infty} \frac{H^{(8)}(t_k)}{8!\, n^8} \sin(2n\pi\eta)$$

is a uniformly convergent series.

Thus, one rewrites the small P approximation of Eq. (3.11) as

$$A\omega^2 + B\omega + C + \varepsilon_4 = 0 \tag{4.2}$$

where

$$A = 24\,\Psi_6(\eta),$$

$$B = \frac{\Omega\,\cos(\phi_\alpha)}{\sqrt{P}} - 8\,\Psi_4(\eta)$$

and

$$C = 4\,\Psi_2(\eta) + \tilde{R}(\eta) - \frac{1}{2\eta}\left[\tilde{S}(\eta) + \Omega\sin(\phi_\alpha)\right].$$

If the error term is small enough to be ignored (see the error term section for further discussion), Eq. (4.2) is a quadratic equation in ω. Thus for ω to be pure imaginary (i.e., $\omega = bi$), two conditions must be satisfied, $B = 0$ and $AC \geq 0$.

Condition one, $B = 0$

Since $\cos(\phi_\alpha) = \sqrt{P}/\sqrt{P + \tan^2(\theta_\alpha)}$ (see Fig. 3.1 and the Appendix of the paper contained in Chap. 3), one finds from the first condition, $B = 0$, that the Péclet number satisfies the equation

$$P = \left[\frac{\Omega}{8\,\Psi_4(\eta)}\right]^2 - \tan^2(\theta_\alpha) \tag{4.3}$$

whenever $\Omega/(8\,\Psi_4(\eta)) > 0$ or since Ω is always positive, whenever $\Psi_4(\eta) > 0$. A plot of $\Psi_4(\eta)$ using the first term (dashed line) and the first 200 terms (solid line) is shown in Fig. 4.1, where it is seen that $\Psi_4(\eta) > 0$ and that there is little difference between using the first term or the first 200 terms of $\Psi_4(\eta)$ (due to $1/(n\pi)^4$). Note that as 2η approaches zero or one, $\Psi_4(\eta)$ approaches zero and from Eq. (4.3) one finds that P approaches infinity. Figure 4.2 shows a plot of P vs. 2η using Eq. (4.3) for Al-Al_2Cu (solid line) and CBr_4-C_2Cl_6 (dashed line) using the first 200 terms of $\Psi_4(\eta)$.

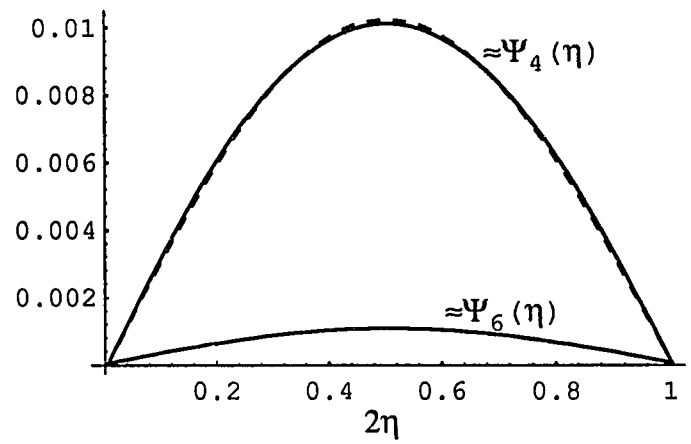

Figure 4.1: $\Psi_j(\eta)$ for $j = 4$ and 6 using the first 200 terms (solid line) and $\Psi_4(\eta)$ using the first term only (dashed line).

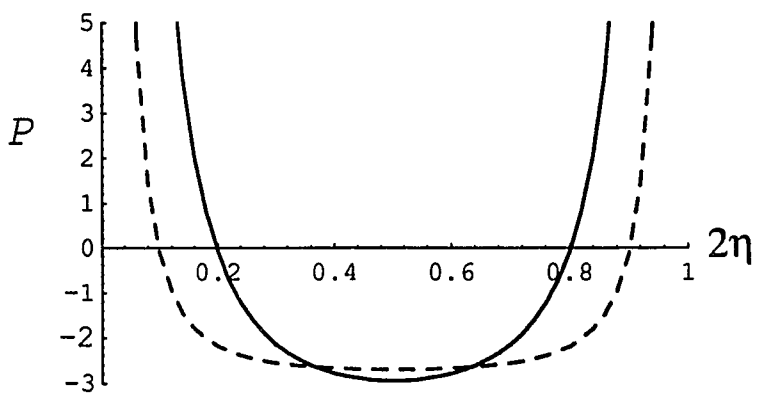

Figure 4.2: P vs. 2η for $N = 2$ and for Al-Al_2Cu (solid line) and CBr_4-C_2Cl_6 (dashed line).

To find the approximate 2η values where $P = 0$ one lets $\Psi_4(\eta) \approx \sin(2\pi\eta)/(\pi^4)$ and one sets $P = 0$ in Eq. (4.3). Then

$$2\eta \approx \begin{cases} \dfrac{1}{\pi}\sin^{-1}\left(\dfrac{\Omega\pi^4}{8\tan(\theta_\alpha)}\right) & \text{if} \quad 0 \le 2\eta \le \dfrac{1}{2} \\ \\ 1 - \dfrac{1}{\pi}\sin^{-1}\left(\dfrac{\Omega\pi^4}{8\tan(\theta_\alpha)}\right) & \text{if} \quad \dfrac{1}{2} \le 2\eta \le 1. \end{cases}$$

Using the above approximations, one finds that for P to be positive, 2η is restricted to the intervals

$$\left(0,\ \frac{1}{\pi}\sin^{-1}\left[\frac{\Omega\pi^4}{8\tan(\theta)}\right]\right) \quad \text{and} \quad \left(1 - \frac{1}{\pi}\sin^{-1}\left[\frac{\Omega\pi^4}{8\tan(\theta)}\right],\ 1\right)$$

referred to as region I and region II, respectively. Note that in the previous calculations it is assumed that λP is a nonzero constant as P varies. It may be that λP is a different constant for different values of concentration so that $\Omega = \Omega(\eta)$. Zimmerman *et al.* [3] claim that λP = constant decreases as one approaches the eutectic concentration (at least for the values documented).

If λP equals a constant corresponding to the eutectic concentration, then one finds that for Al-Al_2Cu with $\Omega = 0.1045$ and $\theta = 65^\circ$, 2η is restricted to the intervals $(0, 0.2022)$ and $(0.7978, 1)$ and that for CBr_4-C_2Cl_6 with $\Omega = 0.0447$ and $\theta = 60^\circ$, 2η is restricted to the intervals $(0, 0.1018)$ and $(0.8983, 1)$. Note that the 2η value for the CBr_4-C_2Cl_6 system in Fig. 3.5(b) does not fall into either of these intervals; however, this does not contradict the results from this section since the approximations made may not be valid when $P = 1.3015$ and $\omega = 3i$.

Condition two, $AC > 0$

The condition $AC > 0$ implies the condition $C > 0$ since $A = 24\,\Psi_6(\eta)$ and $\Psi_6(\eta) > 0$ (see Fig. 4.1). Thus, from the second condition one finds an inequality, which further restricts the possible 2η values, given by

$$4\,\Psi_2(\eta) + \tilde{R}(\eta) - \frac{1}{2\eta}\left(\tilde{S}(\eta) + \Omega\sin(\phi_\alpha)\right) > 0. \tag{4.4}$$

Since $\sin(\phi_\alpha) = \tan(\theta_\alpha)/\sqrt{P + \tan^2(\theta_\alpha)}$ (see Fig. 3.1 and the Appendix of the paper contained in Chap. 3) and P is given by Eq. (4.3), one rewrites Eq. (4.4) as

$$\frac{2\eta\left[4\,\Psi_2(\eta) + \tilde{R}(\eta)\right] - \tilde{S}(\eta)}{8\,\Psi_4(\eta)} > \tan(\theta_\alpha).$$

This inequality is plotted in Fig. 4.3 for Al-Al_2Cu and CBr_4-C_2Cl_6 using the first 200 terms of each series. For these two examples, the 2η values in region I, referred to earlier, do not satisfy the the above inequality. Thus 2η must be restricted to region II.

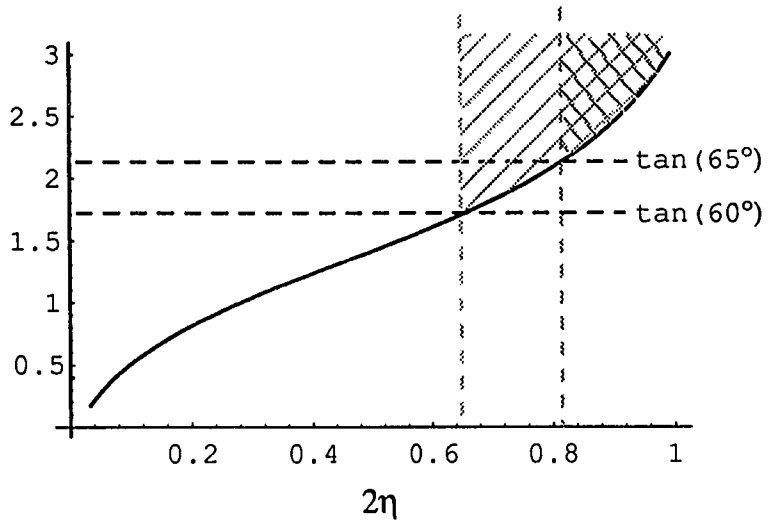

Figure 4.3: Inequality for the condition $C > 0$ for Al-Al_2Cu ($\theta_\alpha = 65^o$) and CBr_4-C_2Cl_6 ($\theta_\alpha = 60^o$).

Disregarding the error term is Eq. (4.2), with the conditions $B = 0$ and $AC > 0$ satisfied, one finds that

$$\omega = \pm i \sqrt{\frac{4\,\Psi_2(\eta) + \tilde{R}(\eta) - \left(\tilde{S}(\eta) + 8\,\Psi_4(\eta)\tan(\theta_\alpha)\right)/(2\eta)}{24\,\Psi_6(\eta)}}. \qquad (4.5)$$

Figure 4.4 shows 2η verses b where $\omega = bi$ as given by Eq. (4.5) for the Al-Al_2Cu eutectic system (solid line) and the CBr_4-C_2Cl_6 eutectic system (dashed line) using the first 200 terms of each series in Eq. (4.5).

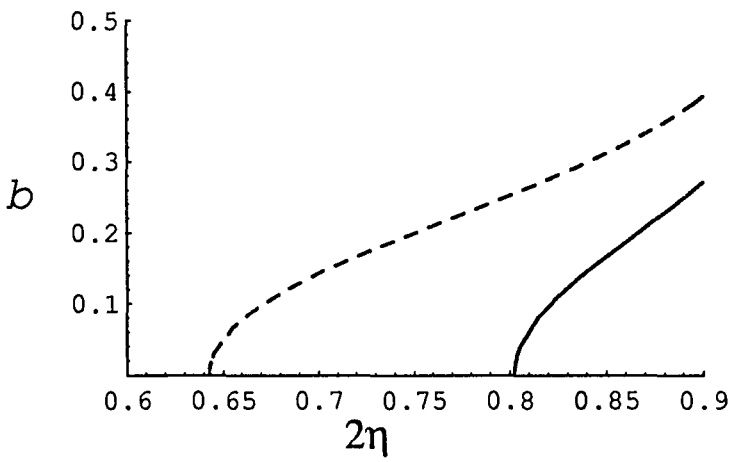

Figure 4.4: 2η vs b where $\omega = \pm ib$ for Al-Al_2Cu (solid line) and CBr_4-C_2Cl_6 (dashed line).

The error term, ε_4

To determine the error involved in treating Eq. (4.2) as a quadratic equation in ω, consider the absolute value of the error term such that:

$$|\varepsilon_4| \leq \sum_{\text{odd } n=1}^{\infty} \frac{8\,|\omega|^3}{\pi^{16}\, n^8} \left[|a_1| + |a_2| + |a_3| + |a_4| + |a_5| \right] \left[\left| 1 + \frac{4\omega}{\pi^2} t_k^2 \right| \right]^{-17/2}$$

$$\leq \left[O\left(|\omega|^3 \times 10^{-2} \right) + O\left(|\omega|^4 \times 10^{-1} \right) \right] \sum_{\text{odd } n=1}^{\infty} \frac{1}{n^8}$$

$$\leq \left[O\left(|\omega|^3 \times 10^{-2} \right) + O\left(|\omega|^4 \times 10^{-1} \right) \right] \left[1 + O\left(10^{-4} \right) \right].$$

For Al-Al_2Cu with $\Omega = 0.1045$ and $\theta = 65^\circ$, one finds that $P = 0.0067$, $\omega = 0.0498\,i$ and $2\eta = 0.8025$ satisfy Eqs. (4.3)-(4.5). Thus $|\varepsilon_4| \leq O(10^{-6})$. The corresponding results found earlier in Chap. 3 [see Fig. 3.4(a)] are $P = 0.0067$, $\omega = 0.01\,i$ and $2\eta = 0.8015$. Although the α phase volume fractions are quite close (0.8025 vs. 0.8015) for $P = 0.0067$, the wavelengths are not very close ($0.0498\,i$ vs. $0.01\,i$). This is due to the order of the terms in Eq. (4.2). Specifically, for this example, A is of the order 10^{-2} whereas B is of the order 10^{-6} and C is of order 10^{-5}. Thus, once B is taken as zero, Eq. (4.2) becomes $A\omega^2 + C + \varepsilon_4 = 0$ and using Eq. (4.5) to find ω causes some error. As discussed previously, the values found in Chap. 3 for the CBr_4-C_2Cl_6 system can not be compared with the values found by using the approximations in this section.

Thus for small P and ω the asymptotics done in this section appear to be quite reasonable for finding P and 2η although there is some error in finding the corresponding ω. At the very minimum the asymptotics clearly show the general region in P-2η space (at least for small P) where the acoustic oscillations occur without using the more complex equation given by Eq. (3.11).

Optical oscillations ($N = 1$)

Similiarly, Eq. (3.10) is rewritten as

$$A\omega^2 + B\omega + C + \frac{2\eta}{\sqrt{\omega}} + \varepsilon_4 = 0 \tag{4.6}$$

where

$$A = \frac{3}{8}\Phi_6(\eta),$$

$$B = \frac{\Omega\cos(\phi_\alpha)}{\sqrt{P}} - \frac{1}{2}\Phi_4(\eta) = \frac{\Omega}{\sqrt{P+\tan^2(\theta_\alpha)}} - \frac{1}{2}\Phi_4(\eta),$$

$$C = 4\,\Phi_2(\eta) + \tilde{R}(\eta) - \frac{1}{2\eta}\left[\tilde{S}(\eta) + \Omega\sin(\phi_\alpha)\right],$$

$$\Phi_j(\eta) = \sum_{n=1}^{\infty}\frac{\sin(4n\pi\eta)}{(n\pi)^j}$$

and the error term

$$\varepsilon_4 = \sum_{n=1}^{\infty}\frac{G^{(8)}(t_k)}{8!\,n^8}\sin(4n\pi\eta)$$

with all series involved uniformly convergent and with

$$\frac{G^{(8)}(t_k)}{8!} = \frac{\omega^3}{128\,\pi^{16}}\left[c_1 + c_2\,t_k^2 + c_3\,t_k^4 + c_4\,t_k^6 + c_5\,t_k^8\right]\left[1+\frac{\omega}{\pi^2}\,t_k^2\right]^{-17/2},$$

$$\begin{aligned} c_1 &= -40\,\pi^8, \\ c_2 &= 1235\,\pi^6\,\omega, \\ c_3 &= -3480\,\pi^4\,\omega^2, \\ c_4 &= 1616\,\pi^2\,\omega^3, \\ c_5 &= -64\,\omega^4 \end{aligned}$$

for $0 \le t_k \le 1$.

Equation (4.6) is not a quadratic equation in ω due to the $1/\sqrt{\omega}$ term; however, by setting $\omega = bi$ and again disregarding the error term, the real and imaginary components of Eq. (4.6) are written as

$$-A\,b^2 + C + \frac{2\eta}{\sqrt{2\,b}} = 0 \tag{4.7}$$

and

$$B\,b - \frac{2\eta}{\sqrt{2\,b}} = 0. \tag{4.8}$$

Using Eq. (4.8), one finds that the Péclet number must satisfy

$$P = \left[\frac{\Omega\sqrt{2}\,b^{3/2}}{2\eta + \frac{1}{\sqrt{2}}\,\Phi_4(\eta)\,b^{3/2}}\right]^2 - \tan^2(\theta_\alpha). \tag{4.9}$$

Note that Eq. (4.9) is dependent on b as well as η and that the parallel result for $N = 2$, given by Eq. (4.3), shows a dependence on η only. From Eq. (4.9) one finds that as 2η aprroaches zero, P approaches infinity and as 2η approaches one, P approaches $2\,b^2\,\Omega^2 - \tan^2(\theta_\alpha)$. Figures 4.5 and 4.6 show the b and η dependence of Eq. (4.9) for the Al-Al_2Cu and CBr_4-C_2Cl_6 systems using the first 200 terms of $\Phi_4(\eta)$.

From Eqs. (4.7) - (4.9), one finds that

$$-\sqrt{2}\,A\,b^{7/2} + D\,b^{3/2} + 2\eta\,b = \tan(\theta_\alpha) \tag{4.10}$$

where

$$D = \sqrt{2}\left(4\,\Phi_2(\eta) + \tilde{R}(\eta) - \frac{1}{2\eta}\left[\tilde{S}(\eta) + \frac{1}{2}\,\Phi_4(\eta)\tan(\theta_\alpha)\right]\right)$$

and A is the same as in Eq. (4.6). Using the first 200 terms of each series, Eq. (4.10) is plotted for various values of b for the Al-Al_2Cu system in Fig. 4.7 and the CBr_4-C_2Cl_6 system in Fig. 4.8.

Equations (4.9) and (4.10) clearly show that the equations found in this section are not as easily analyzed as those found for the acoustic mode. In addition to this difficulty, the approximations may have large errors associated with them because b and/or P tend to be quite large as seen in Figs. 4.5 - 4.8. Thus, the approximations of this section are not valid for the optical mode, and Eq. (3.10) must be used.

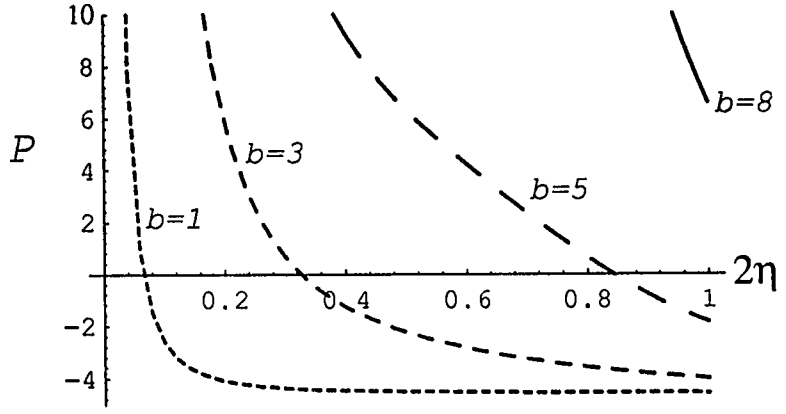

Figure 4.5: P vs 2η for Al-Al_2Cu ($N = 1$) and various values of b.

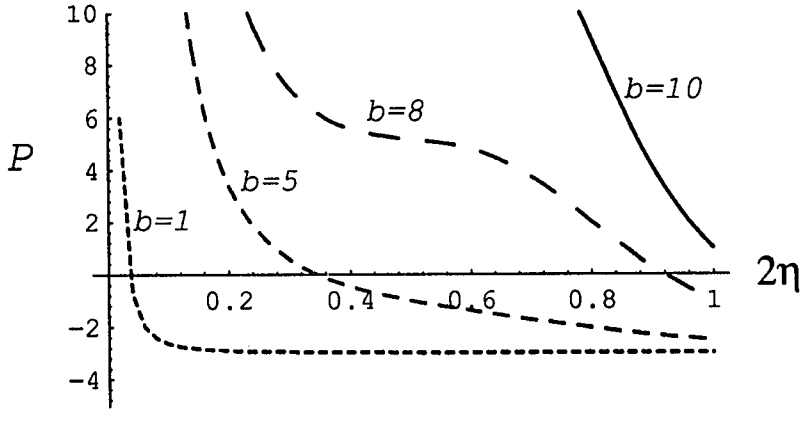

Figure 4.6: P vs 2η for CBr_4-C_2Cl_6 ($N = 1$) and various values of b.

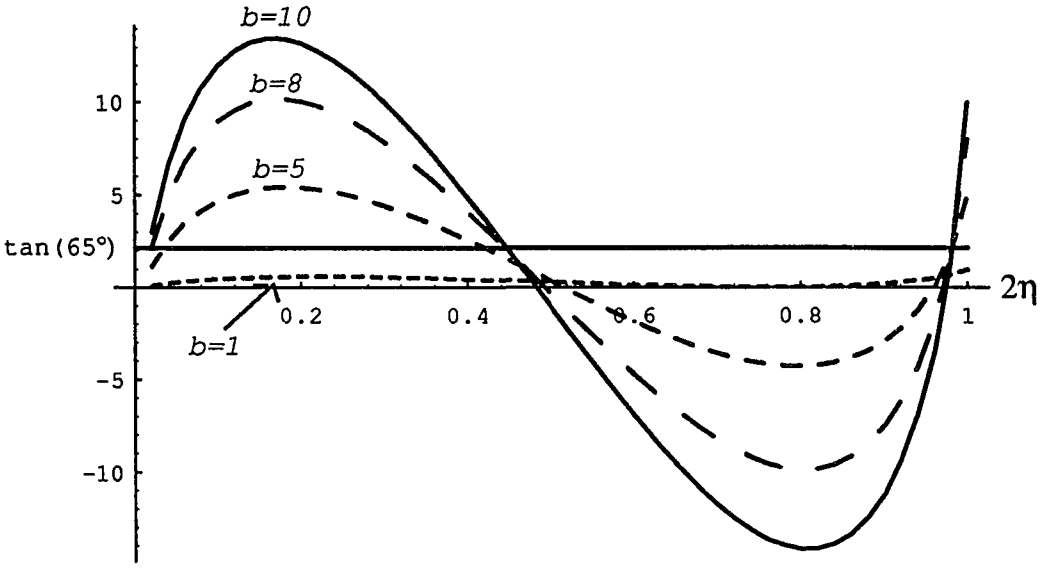

Figure 4.7: $-\sqrt{2}\,A\,b^{7/2} + D\,b^{3/2} + 2\eta\,b = \tan(\theta_\alpha)$ for Al-Al_2Cu.

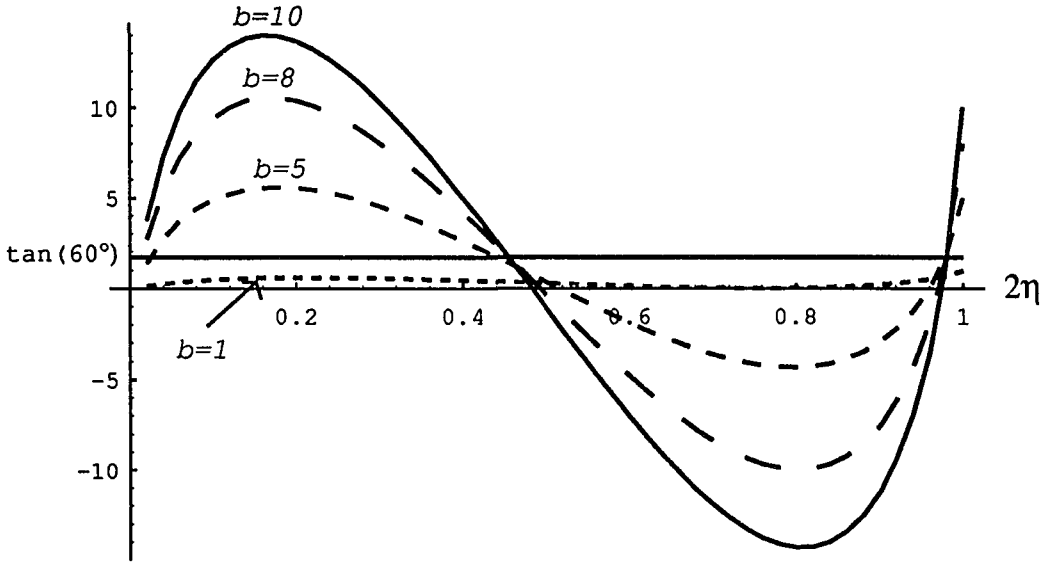

Figure 4.8: $-\sqrt{2}\,A\,b^{7/2} + D\,b^{3/2} + 2\eta\,b = \tan(\theta_\alpha)$ for CBr_4-C_2Cl_6.

CHAPTER 5. HIGH PÉCLET NUMBER MODEL NEAR THE EUTECTIC CONCENTRATION

Due to the moderately high Péclet numbers associated with the CBr_4-C_2Cl_6 oscillations (both acoustic and optical) and some of the Al-Al_2Cu optical oscillations, as shown in Figs. 3.5–3.9, it is appropriate to develop a high Péclet number model for the diffusion problem being considered.

P dependent partition coefficient

One noteable difference in the high Péclet number model is the dependence of the partition coefficient, k, on P. Following Aziz and Kaplan [27], one obtains the partition coefficient for the α phase as

$$k_1(P) = \frac{P/P_D + \Lambda_e}{P/P_D + 1 - (1 - \Lambda_e)\, C_L}$$

where Λ_e is a measure of the driving force for redistribution and $P_D = (\lambda V_D)/(2\, D)$ where V_D is the diffusive speed. Using $\Lambda_e = k_1^e/k_1^{eA}$ where k_1^e is the equilibrium partition coefficient of component B and k_1^{eA} is the equilibrium partition coefficient of component A defined by $k_1^{eA} = (1 - C_S)/(1 - C_L)$, one obtains

$$k_1(P) = \frac{C_S}{C_L} = \frac{P/P_D + k_1^e\,(1 - C_L)}{P/P_D + (1 - C_L)}.$$

Similiarly, for the β phase, one obtains

$$k_2(P) = \frac{1 - C_S}{1 - C_L} = \frac{P/P_D + k_2^e\, C_L}{P/P_D + C_L}.$$

For small P/P_D, $k(P)$ goes to the equilibrium partition coefficient, k^e, and for large P/P_D, $k(P)$ goes to one. The increase in $k(P)$ for increasing P/P_D is referred to

as solute trapping. For dilute concentrations (where C_L is taken as zero), one finds that

$$k_1(P) = \frac{P/P_D + k_1^e}{P/P_D + 1}$$

as demonstrated by previous authors [28, 29].

Nonequilibrium interface concentration

The P dependence also shows up in the interface concentration through the P dependent partition coefficients. Following Kurz and Trivedi [28], the free energy change of solid formed is given by

$$\Delta G = (1 - C_S)\,\Delta\mu^A + C_S\,\Delta\mu^B$$

where $\Delta\mu = \mu_S - \mu_L$ with μ as the chemical potential such that $\mu = \mu^0 + RT \ln[\gamma C]$, with μ^0 as the chemical potential of the pure substance, R as the gas constant and γ as the activity coefficient. Using equilibrium conditions, they obtain

$$\frac{\Delta G}{RT} = (1 - C_S) \ln\left[\frac{(1 - C_S)(1 - C_L^e)}{(1 - C_S^e)(1 - C_L)}\right] + C_S \ln\left[\frac{C_S\, C_L^e}{C_S^e\, C_L}\right]$$
$$+ (1 - C_S) \ln\left[\frac{\gamma_L^{A,e}\, \gamma_S^A}{\gamma_L^A\, \gamma_S^{A,e}}\right] + C_S \ln\left[\frac{\gamma_L^{B,e}\, \gamma_S^B}{\gamma_L^B\, \gamma_S^{B,e}}\right]. \qquad (5.1)$$

To evaluate Eq. (5.1) further, one may relate the concentration in the solid to the concentration in the liquid by $C_S = k_1(P)\, C_L$ and $C_S^e = k_1^e\, C_L^e$ in the α phase and by $[1 - C_S] = k_2(P)\,[1 - C_L]$ and $(1 - C_S^e) = k_2^e\,(1 - C_L^e)$ in the β phase. Taking the concentration of the two phases to be near the eutectic concentration one writes

$$\Delta C\, U_L \equiv C_L - C_E = \delta C \qquad (5.2)$$

$$C_L^e - C_E = \delta C_e \qquad (5.3)$$

where δC and δC_e are small.

Then, for the α phase, one finds that

$$\ln\left[\frac{C_S\,C_L^e}{C_S^e\,C_L}\right] = \ln\left[\frac{k_1(P)}{k_1^e}\right]$$

and

$$\ln\left[\frac{(1-C_S)(1-C_L^e)}{(1-C_S^e)(1-C_L)}\right] = \ln\left[\frac{1-k_1(P)\,C_E}{1-k_1^e\,C_E}\right] + \delta C\frac{1-k_1(P)}{(1-C_E)\left[1-k_1(P)\,C_E\right]}$$

$$-\delta C_e\frac{1-k_1^e}{(1-C_E)(1-k_1^e\,C_E)} + \text{higher order terms.}$$

Likewise, for the β phase, one finds that

$$\ln\left[\frac{(1-C_S)(1-C_L^e)}{(1-C_S^e)(1-C_L)}\right] = \ln\left[\frac{k_2(P)}{k_2^e}\right]$$

and

$$\ln\left[\frac{C_S\,C_L^e}{C_S^e\,C_L}\right] = \ln\left\{\frac{1-k_2(P)\left[1-C_E\right]}{1-k_2^e\left(1-C_E\right)}\right\} - \delta C\frac{1-k_2(P)}{C_E\left[1-k_2(P)\left(1-C_E\right)\right]}$$

$$+\delta C_e\frac{1-k_2^e}{C_E\left[1-k_2^e\left(1-C_E\right)\right]} + \text{higher order terms.}$$

If one now assumes for simplicity that the activity coefficients are constants near the eutectic concentration then the remaining logarithmic terms in Eq. (5.1) vanish and one may rewrite Eq. (5.1) for the α phase as

$$\frac{\Delta G}{RT} = \left[1-k_1(P)\,C_E\right]\ln\left[\frac{1-k_1(P)\,C_E}{1-k_e^\alpha\,C_E}\right] + k_1(P)\,C_E\ln\left[\frac{k_1(P)}{k_1^e}\right]$$

$$+\delta C\left(\frac{\left[1-k_1(P)\right]}{(1-C_E)} + k_1(P)\ln\left\{\frac{k_1(P)\left[1-k_1^e\,C_E\right]}{k_1^e\left[1-k_1(P)C_E\right]}\right\}\right)$$

$$-\delta C_e\frac{(1-k_1^e)\left[1-k_1(P)\,C_E\right]}{(1-C_E)(1-k_1^e\,C_E)} + \text{higher order terms.} \qquad (5.4)$$

To write the corresponding expression for $\Delta G/(RT)$ in the β phase the following substitutions are made in Eq. (5.4): $k_2(P)$ for $k_1(P)$, k_2^e for k_1^e, $(1-C_E)$ for C_E, $-\delta C$ for δC and $-\delta C_e$ for δC_e. Note that for dilute concentrations, one lets $C_E = 0$ in Eq. (5.4) so that

$$\frac{\Delta G}{RT} = C_i^e \left\{ \left[1 - k_1(P)\right] + k_1(P) \ln\left[\frac{k_1(P)}{k_1^e}\right] \right\} - \delta C_e \left(1 - k_1^e\right)$$

$$= -\frac{(1-k_1^e)}{m_\alpha}\left[T_E - T(P,C) - m_\alpha C_i\right] + C_i \left(k_1^e - k^\alpha(P)\left\{1 - \ln\left[\frac{k_1(P)}{k_1^e}\right]\right\}\right)$$

as demonstrated by Boettinger and Coriell [29].

From the equilibrium phase diagram, Fig. 3.2. one finds that

$$C_L^e - C_E = \begin{cases} \left[T_E - T(P,C_L)\right]/m_\alpha & \text{in the } \alpha \text{ phase} \\ -\left[T_E - T(P,C_L)\right]/m_\beta & \text{in the } \beta \text{ phase;} \end{cases}$$

however, due to the curvature, $T = T(P,C_L) - \frac{2}{\lambda}\Gamma_\alpha \kappa_\alpha$ and one writes

$$\delta C_e = C_L^e - C_E = \begin{cases} \left(\Delta T_\alpha - \frac{2}{\lambda}\Gamma_\alpha \kappa_\alpha\right)/m_\alpha & \text{in the } \alpha \text{ phase} \\ -\left(\Delta T_\beta - \frac{2}{\lambda}\Gamma_\beta \kappa_\beta\right)/m_\beta & \text{in the } \beta \text{ phase} \end{cases} \tag{5.5}$$

where $\Delta T = T_E - T$. Using Eq. (5.2)-(5.5), one writes the nondimensional interface concentration near the eutectic as

$$U_i = \begin{cases} \dfrac{g\left(k_1(P), k_1^e, C_E\right) + h\left(k_1(P), k_1^e, C_E\right)\left[\Delta T_\alpha - \frac{2}{\lambda}\Gamma_\alpha \kappa_\alpha\right]/m_\alpha}{\Delta C\, f\left(k^\alpha(P), k_e^\alpha, C_E\right)} & \text{in the } \alpha \text{ phase} \\ \dfrac{-g\left(k_2(P), k_2^e, 1-C_E\right) - h\left(k_2(P), k_2^e, 1-C_E\right)\left[\Delta T_\beta - \frac{2}{\lambda}\Gamma_\beta \kappa_\beta\right]/m_\beta}{\Delta C\, f\left(k_2(P), k_2^e, 1-C_E\right)} & \text{in the } \beta \text{ phase} \end{cases} \tag{5.6}$$

where

$$g\Big(k(P), k^e, C\Big) = -\left\{\Big[1 - k(P)\,C\Big]\,\ln\left[\frac{1 - k(P)\,C}{1 - k^e\,C}\right] + k(P)\,C\,\ln\left[\frac{k(P)}{k^e}\right] + \frac{\Delta G}{RT}\right\}(1 - C),$$

$$h\Big(k(P), k^e, C\Big) = \frac{(1 - k^e)\Big[1 - k(P)\,C\Big]}{1 - k^e\,C}$$

and

$$f\Big(k(P), k^e, C\Big) = [1 - C]\;k(P)\;\ln\left\{\frac{k(P)\Big[1 - k^e\,C\Big]}{k^e\Big[1 - k(P)\,C\Big]}\right\} + 1 - k(P).$$

Note that if $k(P) = k^e$ and $\Delta G = 0$ then $g(k^e, k^e, C_E) = 0$ and $h(k^e, k^e, C_E) = f(k^e, k^e, C_E) = 1 - k^e$ so that U_i is as in Chap. 3.

High Péclet number model

Using the same scaling as found in Chap. 3, diffusion of solute in the liquid is modeled by

$$P\,\frac{\partial^2 U}{\partial x^2} + \frac{\partial^2 U}{\partial z^2} + P^{3/2}\,\frac{\partial U}{\partial z} = P\,\frac{\partial U}{\partial t} \tag{5.7}$$

as before. The thermal boundary condition (written in terms of U_i) is given by Eq. (5.6) and conservation of mass at the interface is given by

$$\left.\frac{\partial U}{\partial z}\right|_i + P^{3/2}\,\Delta U_i = 0 \tag{5.8}$$

where

$$\Delta U_i = \begin{cases} U_i - U_\alpha = \Big[U_i + \dfrac{C_E}{\Delta C}\Big]\,[1 - k_1(P)] & \text{in the } \alpha \text{ phase} \\ \\ U_i - U_\beta = \Big[U_i + \dfrac{(1 - C_E)}{\Delta C}\Big]\,[1 - k_2(P)] & \text{in the } \beta \text{ phase.} \end{cases}$$

Note that if one assumes $U_i = U_E = 0$ and $k(P) = k^e$, then $\Delta U_i = U_E - U_{\alpha E}$ in the α phase and $U_E - U_{\beta E}$ in the β phase, as in Chap. 3 where we used the JH [7] equilibrium model.

Linear stability analysis

Proceeding as in the Chap. 3, taking U_i as $U_E = 0$, one writes for the $N = 1$ case (i.e., for the optical oscillations)

$$U(x,z) = U_\infty + \sum_{n=-\infty}^{\infty} E_n\, e^{iqnx}\, e^{-F_n(z-\bar{\zeta})} + \sum_{n=-\infty}^{\infty} \hat{E}_n(t)\, e^{i\hat{q}nx}\, e^{-\hat{F}n(z-\bar{\zeta})} \tag{5.9}$$

where q_n, F_n, $\hat{q}_n$ and $\hat{F}_n$ are as in Chap. 3,

$$E_0 = \tau(P),$$

$$E_n = \frac{P^{3/2}\,\nu(P)}{F_n}\,\frac{\sin(2n\pi\eta)}{n\pi} \quad \text{for } n \neq 0,$$

$$\hat{E}_0(t) = \frac{-P^{3/2}\,\nu(P)}{\hat{F}_0}\,\hat{x}\, e^{i\sigma 2(j+\eta)+\omega t} + O(\hat{x}^2)$$

and

$$\hat{E}_n(t) = -P^{3/2}\,\nu(P)\left[\frac{\cos(2n\pi\eta)}{\hat{F}_n}\right]\hat{x}\, e^{i\sigma 2(j+\eta)+\omega t} + O(\hat{x}^2) \quad \text{for } n \neq 0$$

with

$$\tau(P) \equiv 2\eta\,\frac{C_E}{\Delta C}\left[1 - k_1(P)\right] - \rho\,\frac{(1-C_E)}{\Delta C}\left[1 - k_2(P)\right]$$

and

$$\nu(P) \equiv \frac{C_E}{\Delta C}\left[1 - k_1(P)\right] + \frac{(1-C_E)}{\Delta C}\left[1 - k_2(P)\right].$$

Then one finds that the average concentration over an α phase centered at $x = 2j$ using Eq. (5.9) is given by

$$< U > = U_\infty + \tau(P) + \frac{P\,\sigma(P)\,S(\eta)}{2\eta}$$

$$- P\,\nu(P)\left[\frac{\sqrt{P}}{\hat{F}_0(\omega)} + \frac{R(\eta)}{2\eta} - \frac{S(\eta)}{(2\eta)^2} + \frac{1}{2\eta}\sum_{n=1}^{\infty}\frac{\sqrt{P}}{\hat{F}_n(\omega)}\,\frac{\sin(4n\pi\eta)}{n\pi}\right]\hat{x}\, e^{i\sigma 2(j+\eta)+\omega t}$$

$$+ O(\hat{x}^2);$$

whereas the average concentration using the thermal boundary condition, Eq. (5.6), is given by

$$< U > = \frac{g\left(k_1(P), k_1^e, C_E\right)}{\Delta C\, f\left(k_1(P), k_1^e, C_E\right)} + \frac{\Delta T_\alpha}{m_\alpha \Delta C} \frac{h\left(k_1(P), k_1^e, C_E\right)}{f\left(k_1(P), k_1^e, C_E\right)} - \frac{2\,\Gamma_\alpha}{\lambda\, m_\alpha\, \Delta C} \frac{h\left(k_1(P), k_1^e, C_E\right)}{f\left(k_1(P), k_1^e, C_E\right)} < \kappa_\alpha >$$

where $R(\eta)$, $S(\eta)$, and $< \kappa_\alpha >$ are given in Chap. 3. Equating the two averages, one finds a nonlinear equation similiar to Eq. (3.10) given by

$$\frac{S(\eta)}{(2\eta)^2} - \frac{R(\eta)}{2\eta} + \frac{\Omega \sin(\varphi_\alpha)\, h\left(k_1(P), k_1^e, C_E\right)}{(2\eta)^2 f\left(k_1(P), k_1^e, C_E\right) \nu(P)}$$

$$= \omega \frac{\Omega \cos(\phi_\alpha)\, h\left(k_1(P), k_1^e, C_E\right)}{(2\eta) f\left(k_1(P), k_1^e, C_E\right) \nu(P)} \frac{1}{\sqrt{P}} + \left\{ \frac{P}{2} + \left[\left(\frac{P}{2}\right)^2 + \omega \right]^{1/2} \right\}^{-1}$$

$$+ \frac{1}{2\eta} \sum_{n=1}^{\infty} \frac{\sin(4n\pi\eta)}{n\pi} \left\{ \frac{P}{2} + \left[\left(\frac{P}{2}\right)^2 + (n\pi)^2 + \omega \right]^{1/2} \right\}^{-1}. \qquad (5.10)$$

Proceding as in the $N = 1$ case, one finds a nonlinear equation similiar to Eq. (3.11) for the $N = 2$ case (i.e., the acoustic oscillations) given by

$$\frac{S(\eta)}{(2\eta)^2} - \frac{R(\eta)}{2\eta} + \frac{\Omega \sin(\phi_\alpha)\, h\left(k_1(P), k_1^e, C_E\right)}{(2\eta)^2 f\left(k_1(P), k_1^e, C_E\right) \nu(P)} - \omega \frac{\Omega \cos(\phi_\alpha)\, h(k_1(P), k_1^e, C_E)}{(2\eta) f\left(k_1(P), k_1^e, C_E\right) \nu(P)} \frac{1}{\sqrt{P}}$$

$$= \frac{1}{2\eta} \sum_{\text{odd } n=1}^{\infty} \frac{\sin(2n\pi\eta)}{n\pi/2} \left\{ \frac{P}{2} + \left[\left(\frac{P}{2}\right)^2 + \left(\frac{n\pi}{2}\right)^2 + \omega \right]^{1/2} \right\}^{-1}. \qquad (5.11)$$

Effects of the high Péclet number model

The nonlinear Eqs. (5.10) and (5.11) differ from the nonlinear Eqs. (3.10) and (3.11) by a factor, which we will refer to as the Péclet factor, of $h/(f\nu)$ in the terms involving $\sin(\phi_\alpha)$ and $\cos(\phi_\alpha)$. The Péclet factor times Ω is plotted in Figs. 5.1 and 5.2 for the Al-Al_2Cu and CBr_4-C_2Cl_6 systems with C_L taken as C_E in the expressions for the partition coefficients. The figures show that as P approaches zero, the Péclet factor times Ω approaches Ω and as P increases from zero to ten the Péclet factor also increases. Figures 5.3 and 5.4 show the effect of the Péclet factor on the plots of concentration verses velocity shown in Figs. 3.8 and 3.9. (See Appendix A for the Fortran programs and equations used in the calculations.) Each string of symbols (a–d for the optical oscillations or 1–3 for the acoustic oscillations) corresponds to a fixed wavelength of the oscillation with the symbols 'a' and '1' corresponding to $P_D = \infty$; 'b' and '2' corresponding to $P_D = 100$; 'c' and '3' corresponding to $P_D = 50$; and 'd' corresponding to $P_D = 25$. The small Péclet number solutions of Eqs. (3.10) and (3.11) remain plotted as they were in Figs. 3.8 and 3.9 using the $\triangle$ and $\bullet$ symbols.

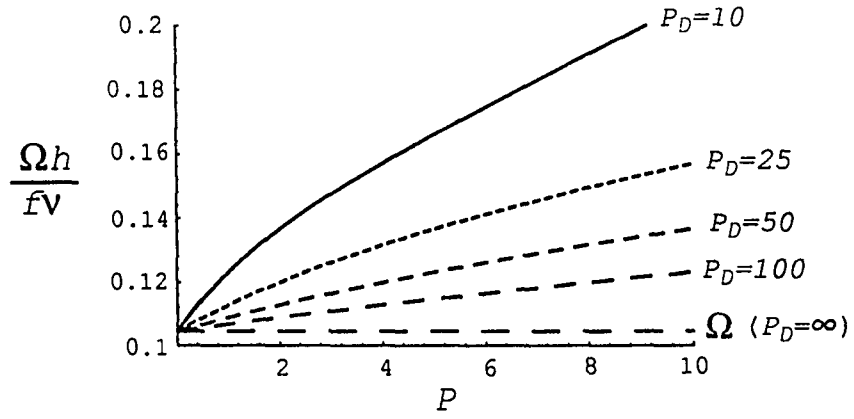

Figure 5.1: $(\Omega h)/(f\nu)$ vs P for Al-Al_2Cu and various values of P_D.

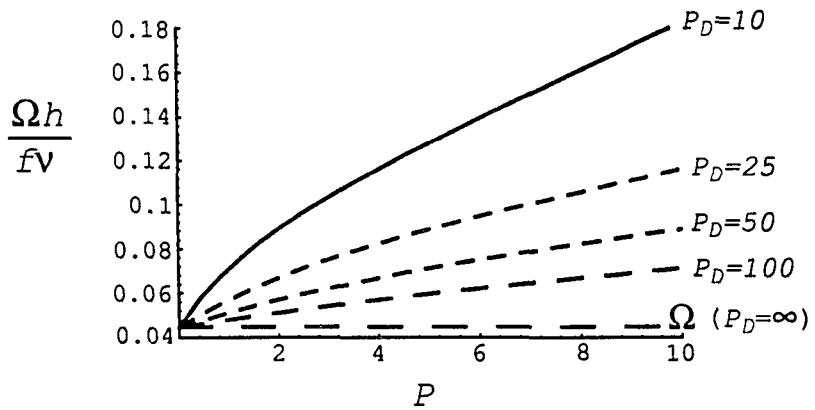

Figure 5.2: $(\Omega h)/(f\nu)$ vs P for CBr_4-C_2Cl_6 and various values of P_D.

A shown in Fig. 5.3 the optical oscillations of the Al-Al_2Cu system move further from the eutectic but decrease in velocity for a fixed wavelength and the range of P_D values shown. Likewise, under the same conditions, the optical oscillations of the CBr_4-C_2Cl_6 system decrease in velocity; however, these oscillations may move closer to or further from the eutectic, depending on the initial position (see Fig. 5.4). Figure 5.4 also shows that the acoustic oscillations of the CBr_4-C_2Cl_6 system decrease in velocity and move closer to the eutectic (for a fixed wavelength and the range of P_D values shown). Thus the high Péclet number model changes the previous mathematical model by moving the velocity values down and the concentration values to the left for an oscillation with a fixed wavelength.

In addition, Fig. 5.4 indicates that the optical oscillations of the CBr_4-C_2Cl_6 system move to a lower velocity and a lower wavelength for approximately the same concentration (compare 'a' of the $\omega = \pm 4.077i$ string to 'c' or 'd' of the $\omega = \pm 3i$ string). Thus the oscillations are stretched out more and may be easier to see. This may also be true for the optical oscillations of the Al-Al_2Cu system and the acoustic oscillations of the CBr_4-C_2Cl_6 system; however, there is not enough data at this time to make such a conclusion. Note that these calculations do not take into account the effect of P on λP (i.e., on Ω), which is assumed to be constant. A more extensive analysis would have to be done to take these changes into account.

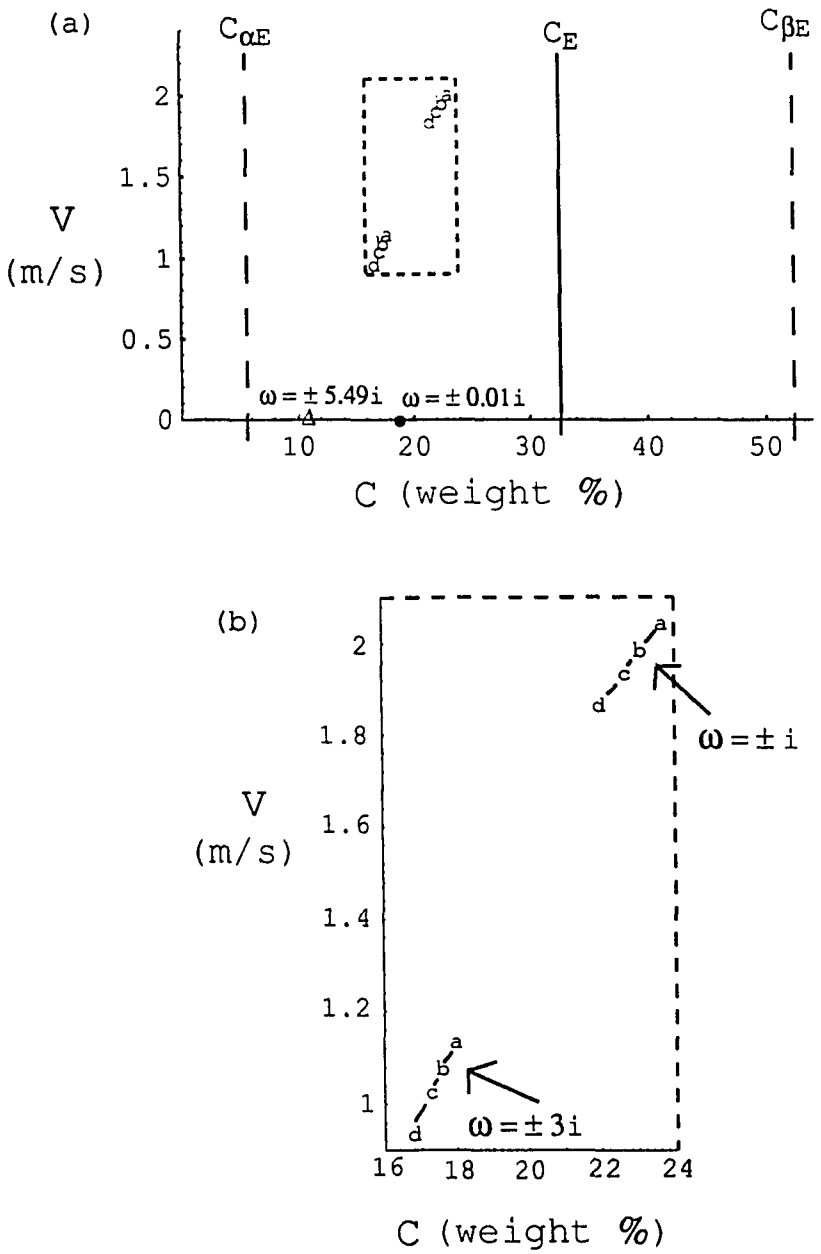

Figure 5.3: (a) Plot of Concentration (wt %) vs Velocity (m/s) for $N = 1$ (Δ and a–d) and $N = 2$ ($\bullet$) and the Al-Al_2Cu eutectic system with $\Omega = 0.1045$, $\theta = 65^\circ$, and $P_D = \infty$, 100, 50 and 25 corresponding to the a–d. (b) Enlarged view of the boxed in region.

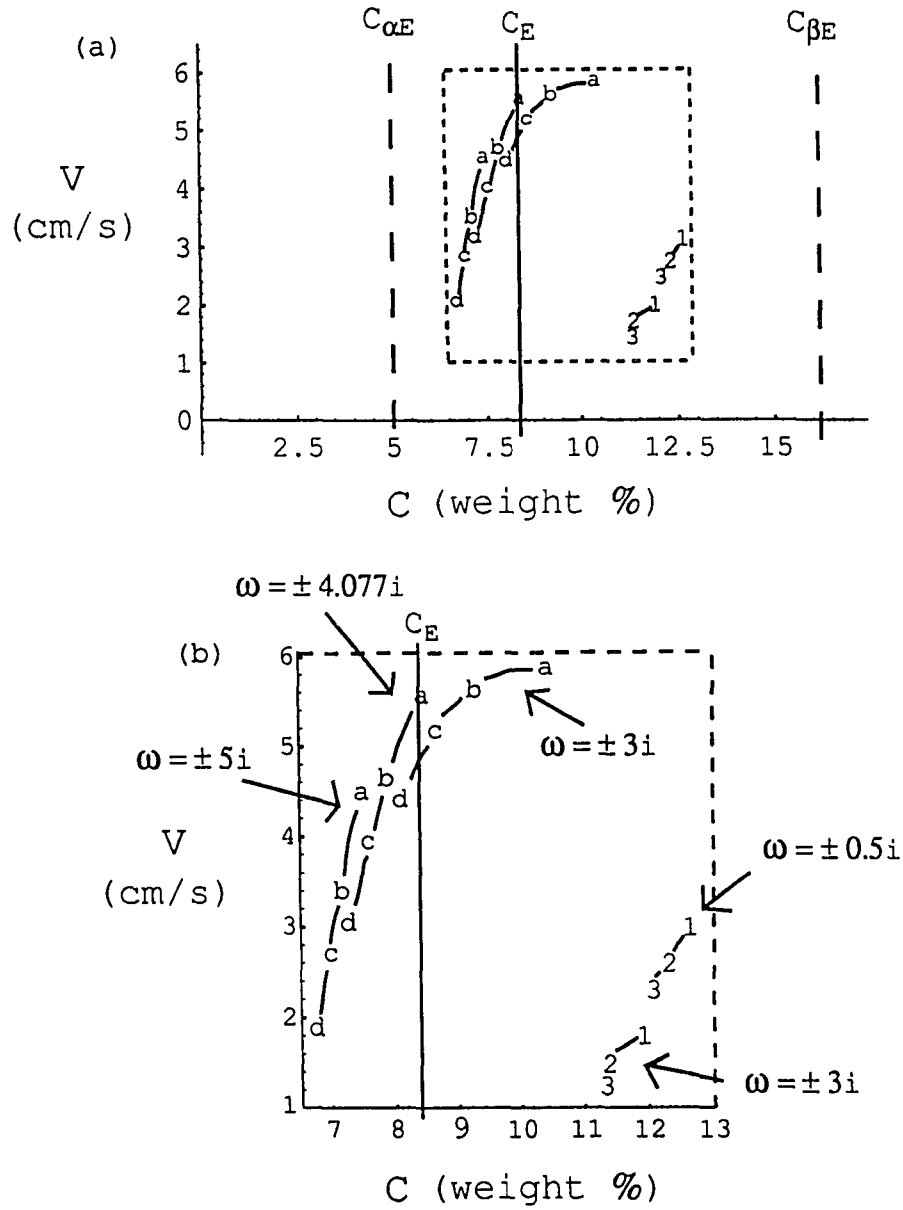

Figure 5.4: (a) Plot of Concentration (wt %) vs Velocity (cm/s) for $N = 1$ (a–d) and $N = 2$ (1-3) and the CBr_4-C_2Cl_6 eutectic system with $\Omega = 0.0447$, $\theta = 60°$, and $P_D = \infty$, 100, 50 and 25 corresponding to a–d and $P_D = \infty$, 100 and 50 corresponding to 1–3. (b) Enlarged view of the boxed in region.

CHAPTER 6. RANDOM WALK SIMULATIONS

Literature review

To further the understanding of the theoretical work and to test the previous assumptions of the model, numerous numerical techniques (i.e., finite-difference schemes, finite-element schemes, Monte Carlo simulations, etc.) may be applied to the boundary value problem being considered. Here we have chosen to use a Monte Carlo simulation following the lead of Karma [19] and Xiao, Alexander and Rosenberger [24, 30].

In 1987, Karma [19] constructed a random walk model to simulate eutectic solidification of a thin film. Incorporating the far-field concentration, "counters" and the curvature (including the triple points) and approximating the diffusion equation by the Laplacian, he found tilted lamella and acoustic oscillations. However, due to the Laplacian approximation, the results were applicable to low velocity systems only. Note that he used a two-dimensional square lattice and a walk occured in four possible directions, each with equal probability.

More recently, in 1994, Xiao, *et al.* [24] simulated directional solidification at high velocities. They approached the simulation from a molecular point of view using the kinetic effects of attachment, diffusion and detachment. Their Monte Carlo model is not derived from a continuum mathematical representation of the problem, as Karma's is. They consider the physical processes of binary growth written in terms of interfacial transition probabilities involving local configurations. The direction of a walk is chosen from 10^7 possibilities within 2π, each with equal probability. With their simulations restricted to high velocities, they observed lamellar tilting, optical oscillations and "divorced eutectics". The restriction to high velocities was made due to the amount of CPU time needed to carry out their simulations [31].

Before the work of Karma [19] and Xiao, *et al.* [24], Witten and Sander [32] studied a model for random aggregates using a computer simulation. From a seed particle at the center of a lattice, they grew a cluster by allowing particles to be randomly added a large distance from the center and then to randomly walk until they hit the cluster being formed. Their method generated sparse clusters with random branches. A year later, in 1982, Rikvold [33] extended this diffusion-limited-aggregation (DLA) model by taking into account surface tension, resulting in compact structures with no regular shape. In 1985 Vicsek [34] took the anisotropic surface tension into account by incorporating a sticking probability, dependent on the local orientation of the interface, into his algorithm. He obtained compact regular clusters from a seed particle and simulated directional solidification by using a biased random walk seeded on a line.

During the same time period, Kadanoff [35], Tang [36] and Liang [37] applied the random walk model to the growth of Saffman-Taylor fingers. Note that the Saffman-Taylor problem is quite comparable to directional solidification at low velocities in that both processes are boundary value problems which have been modeled using Laplace's equation, one in terms of pressure and the other in terms of concentration. In addition, there is a characteristic length (ratio of the finger width to the channel width vs. lamellar spacing) involved with both problems, simulations are carried out by growing the finger or crystal from an initial seed line and the movement of the interface (a fluid-fluid interface or a fluid-air interface vs. a solid-liquid interface) must be tracked in both cases. Tang [36] included a counter which increased whenever an interface site was hit by a walker, with a new particle added to the cluster only after the counter hit a predetermined number. Kadanoff [35] and Liang [37] allowed for walkers to walk from one interface site to another interface site, in addition to having walkers released from "infinity".

Between the work of Karma [19] and Xiao, *et al.* [24], Roberts and Knackstedt [38] used a random walk on a non-Laplacian partial differential equation. Specifically, they studied the diffusion equation in two dimensions and the concentration fields of ions in electrochemical deposition (ECD) by deriving rules goverening the motion of the walkers from a finite difference scheme. They then used a random walk to grow needle crystals.

In this chapter a random walk model will be constructed, based on the directional solidification model of Chap. 3. The model originates from the work of Karma [19]; however, the differential equation will not be approximated by the Laplacian and the velocity will be allowed to vary. The simulation results presented will be compared with various aspects of the model presented in Chap. 3.

The random walk model

Consider a two dimensional grid ($W \times H$ sites), occupied by three different particles, liquid, α-phase solid, and β-phase solid, such that the solid particles form the alternating α phase, β phase structure of a eutectic crystal of a fixed composition. Particles may "walk" from a liquid source at "infinity" (a finite distance for the simulation) or from the solid-liquid interface until they hit the interface or leave the grid through the top (see Fig. 6.1). This allows for simulation of the capillary effects at the solid-liquid interface and for simulation of the effect of the far-field concentration. As in Fig. 6.2, each solid site on the interface is bonded to at least one liquid site on the interface. Each bond has a corresponding flux which may change each time a walker from infinity hits the interface or each time a walker moves from one interface site to another interface site. No movement occurs until the flux reaches a number determined by the conservation of mass boundary condition. From the thermal boundary condition, Eq. (3.3), each solid particle on the interface has a concentration, $U(i)$, associated with it such that

$$U(i) = \begin{cases} \dfrac{\Delta T_\alpha}{m_\alpha \Delta C} - P\Omega_\alpha\left[(n_L - n_\alpha) - n_\beta\left(\dfrac{\sigma_\beta - \sigma_{\alpha\beta}}{\sigma_\alpha}\right)\right] & \text{in the } \alpha \text{ phase} \\ \dfrac{-\Delta T_\beta}{m_\beta \Delta C} + P\Omega_\beta\left[(n_L - n_\beta) - n_\alpha\left(\dfrac{\sigma_\alpha - \sigma_{\alpha\beta}}{\sigma_\beta}\right)\right] & \text{in the } \beta \text{ phase} \end{cases} \tag{6.1}$$

where the terms in brackets are a measure of the curvature (see Karma [19]) with n_L, n_α, and n_β being the number of liquid, α solid, and β solid sites divided by the total number of sites within a circle, of a fixed size, centered about the site being considered. The radius of the circle is chosen to be proportional to W, taken as $W/24$.

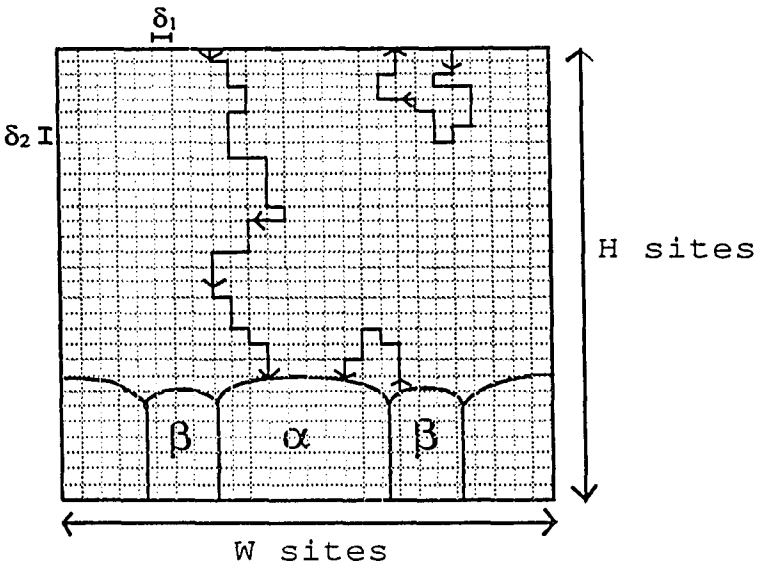

Figure 6.1: Schematic drawing of the grid.

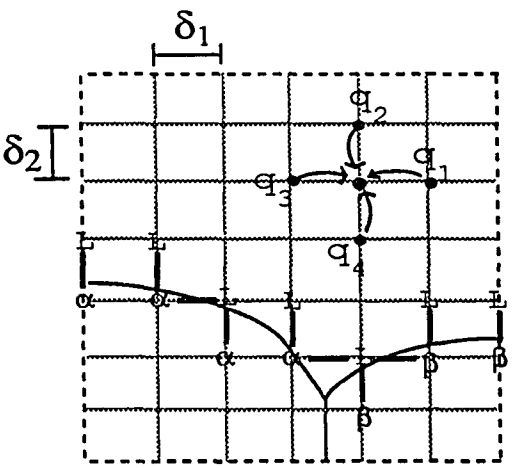

Figure 6.2: Schematic drawing of a portion of the grid.

For each solid walker on the interface, starting at one end of the interface and moving sequentially across the interface (referred to as one sweep of the interface), a random number, $r1$, is generated and compared with the probability, Q^*, of an infinity walk ocurring such that

$$Q^* = \frac{|U_\infty|}{|U_\infty| + U_{\text{ave}}}$$

(see Xiao, *et al.* [30]) where U_∞ is the nondimensional far-field concentration and

$$U_{\text{ave}} = \frac{\sum |U(i)|}{\sum}$$

where $U(i)$ is given by Eq. (6.1) and the sums are taken over all solid interface particles which may walk off the interface.

If $Q^* > r1$ then an infinity walk occurs. The x position of the infinity walker is randomly determined and the walker proceeds from site (x, H) according to the probabilities q_i given in the next section. Note that the notation (x, z) should be interpreted as the x^{th} site in the x-direction and the z^{th} site in the z-direction, with $(0, 0)$ being the left-hand corner of the grid. The walker continues until the z position becomes greater than H or until the walker hits the interface. Periodic conditions are imposed on the sides of the grid so that if a walker moves form $(1, z)$ to $(0, z)$, the new position is recorded as (W, z) or if a walker moves from (W, z) to $(W + 1, z)$, the new position is recorded as $(1, z)$ and the walker continues.

If $Q^* \leq r1$ then no infinity walk occurs but there is the possibility of an interface walk occurring based on the probability Q_j such that

$$Q_j = \frac{|U(j)|}{\max |U(i)|}$$

where $U(j)$ is given by Eq. (6.1) for the j^{th} solid walker on the interface and the maximum is taken over all solid interface particles which may walk. A random number, $r2$, is generated and compared with Q_j such that if $Q_j \leq r2$ no walk occurs and the next solid walker on the interface is considered and if $Q_j > r2$ the walker is released from the interface and walks in the liquid according to the probabilities q_i given in the next section (see Karma [19]).

Random walk probabilities

Each walk in the liquid is determined by the probability of walking right, left, up or down based on the differential equation

$$P\,U_{xx} + U_{zz} + P^{3/2}\,U_z = P\,U_t. \tag{6.2}$$

Similiar to the work of Zauder [39] and Sadeh and Franklin [40], one lets Δt be a change in time, δ_1 be the distance between neighboring sites in the x direction and δ_2 be the distance between neighboring sites in the z direction such that $(\delta_1)^2/\Delta t$ goes to a nonzero constant, c_1, and $(\delta_2)^2/\Delta t$ goes to a nonzero constant, c_2, as δ_1, δ_2 and Δt go to zero. Note that the previous sentence implies that $\delta_1/\Delta t$ and $\delta_2/\Delta t$ go to infinity as δ_1, δ_2 and Δt go to zero. Let q_i be the probability of walking from a neighboring site, $[(x+\delta_1, z)$, $(x, z+\delta_2)$, $(x-\delta_1, z)$ or $(x, z-\delta_2)]$, to the site (x, z) (see Fig. 6.2) and let the probability distribution $U(x, z, t)$ represent the particle at the site (x, z) at time t. Then one may write the difference equation

$$\begin{aligned} U(x, z, t+\Delta t) = {} & q_1\,U(x+\delta_1, z, t) + q_2\,U(x, z+\delta_2, t) \\ & + q_3\,U(x-\delta_1, z, t) + q_4\,U(x, z-\delta_2, t). \end{aligned} \tag{6.3}$$

For small Δt, δ_1 and δ_2 one may rewrite Eq. (6.3) as

$$\begin{aligned} & \frac{\partial U(x, z, t)}{\partial t} + O(\Delta t) = \frac{\delta_1}{\Delta t}\,[q_1 - q_3]\,\frac{\partial U(x, z, t)}{\partial x} \\ & + \frac{\delta_2}{\Delta t}\,[q_2 - q_4]\,\frac{\partial U(x, z, t)}{\partial z} + \frac{{\delta_1}^2}{2\Delta t}\,[q_1 + q_3]\,\frac{\partial^2 U(x, z, t)}{\partial x^2} \\ & + \frac{{\delta_2}^2}{2\Delta t}\,[q_2 + q_4]\,\frac{\partial^2 U(x, z, t)}{\partial z^2} + O\Big(\frac{{\delta_1}^3}{\Delta t}\Big) + O\Big(\frac{{\delta_2}^3}{\Delta t}\Big). \end{aligned} \tag{6.4}$$

Equating the coefficients of Eq. (6.2) with Eq. (6.4) in the limit as δ_1, δ_2 and Δt go to zero, one finds that to eliminate the $\partial U/\partial x$ term in Eq. (6.4), one needs to let $q_1 = q_3$ and to retain the $\partial U/\partial z$ term in Eq. (6.4), one needs to let $q_2 - q_4 = \gamma\,\delta_2$ for a nonzero γ. In addition, one finds that $c_1 = 1\,/\,q_1$, $c_2 = \sqrt{P}\,/\,\gamma$, and $q_2 + q_4 =$

$(2\gamma)/(P^{3/2})$. If one now uses the previous information with the condition that the sum of the q_i's equals one, it is found that

$$q_1 = q_3 = \frac{1}{2} - \frac{\gamma}{P^{3/2}},$$

$$q_2 = \frac{\gamma}{P^{3/2}} + \frac{\gamma}{2}\delta_2$$

and

$$q_4 = \frac{\gamma}{P^{3/2}} - \frac{\gamma}{2}\delta_2.$$

Then, one may chose γ as $(P^{3/2})/4$ so that $\delta_2 = \delta_1/\sqrt{P}$,

$$\begin{aligned} q_1 &= \mathrm{P}\left(\text{walking from } (x+\delta_1, z) \text{ to } (x, z)\right) \\ &= \mathrm{P}\left(\text{walker moves left from } (x, z) \text{ to } (x-\delta_1, z)\right) \\ &= \frac{1}{4}, \end{aligned}$$

$$\begin{aligned} q_2 &= \mathrm{P}\left(\text{walking from } (x, z+\delta_2) \text{ to } (x, z)\right) \\ &= \mathrm{P}\left(\text{walker moves down from } (x, z) \text{ to } (x, z-\delta_2)\right) \\ &= \frac{1}{4} + \frac{P}{8}\delta_1, \end{aligned}$$

$$\begin{aligned} q_3 &= \mathrm{P}\left(\text{walking from } (x-\delta_1, z) \text{ to } (x, z)\right) \\ &= \mathrm{P}\left(\text{walker moves right from } (x, z) \text{ to } (x+\delta_1, z)\right) \\ &= \frac{1}{4} \end{aligned}$$

and

$$\begin{aligned} q_4 &= \mathrm{P}\left(\text{walking from } (x, z-\delta_2) \text{ to } (x, z)\right) \\ &= \mathrm{P}\left(\text{walker moves up from } (x, z) \text{ to } (x, z+\delta_2)\right) \\ &= \frac{1}{4} - \frac{P}{8}\delta_1. \end{aligned}$$

After a walker hits the interface

Originally all flux values associated with the interface bonds are initialized to zero. Each time a walker from infinity hits the interface a random number, $r3$, is generated. If the volume fraction of the α phase, 2η, is greater than $r3$ the flux associated with the bond which was broken is increased by one and if $2\eta \leq r3$ the flux is decreased by one. Each time a walker from the interface hits the interface the flux associated with the hit site is decreased by $\mathrm{sgn}\, U(i) \times 1$ and the flux associated with the departure site is increased by $\mathrm{sgn}\, U(i) \times 1$ where $U(i)$ is given by Eq. (6.1) (see Karma [19]).

After a sweep of the interface, the flux value associated with each solid walker on the interface is compared with a value determined by the conservation of mass boundary condition given by

$$-\left.\frac{\partial U}{\partial z}\right|_i = P^{3/2} \begin{cases} U_i - U_\alpha & \text{in the } \alpha \text{ phase} \\ U_i - U_\beta & \text{in the } \beta \text{ phase} \end{cases} \tag{6.5}$$

with $U_i \approx U_E$, $U_\alpha \approx U_{\alpha E}$ and $U_\beta \approx U_{\beta E}$ as in the JH model [7]. Specifically, one rewrites Eq. (6.5) as

$$\begin{aligned} -[U(x, z+\delta_2, t) - U(x, z, t)] &= \delta_2 P^{3/2} \begin{cases} -U_{\alpha E} & \text{in the } \alpha \text{ phase} \\ -U_{\beta E} & \text{in the } \beta \text{ phase} \end{cases} \\ &= \delta_1 P \begin{cases} -U_{\alpha E} & \text{in the } \alpha \text{ phase} \\ -U_{\beta E} & \text{in the } \beta \text{ phase.} \end{cases} \end{aligned} \tag{6.6}$$

Note that in the simulations presented, the solid walkers on the interface are restricted to the solid interface sites which are bonded to a liquid interface site directly above so that the concentration at the interface changes with respect to z only as stated in the conservation of mass boundary condition at the interface.

From Eq. (6.6), the flux for the i^{th} liquid interface site bonded to a solid walker on the interface is considered. If the flux, given by F_L^i, satisfies

$$F_L^i \geq -\delta_1 P\, U_{\alpha E}\, M \equiv \mathrm{countA},$$

where M is a constant needed for the computations, and the liquid is connected to at least one alpha solid, then the liquid solidifies as alpha solid. If

$$F_L^i \leq -\delta_1 P U_{\beta E} M \equiv \text{countB}$$

and the liquid is connected to at least one beta solid then the liquid solidifies as beta solid.

Likewise, for the j^{th} solid walker on the interface, if the solid is alpha phase solid and the flux, F_S^j, satisfies

$$F_S^j \leq -\text{countA}$$

then the solid alpha melts and if the solid is beta phase solid and if

$$F_S^j \geq -\text{countB},$$

then the solid beta melts. In this manner, solidifying and melting at the interface are simulated according to the conservation of mass boundary condition given by Eq. (6.5).

After all interface changes are made the new interface is recorded with old bonds retaining their flux values and new bonds having zero flux. The simulation is repeated for the new interface and the process is continued a predetermined number of times.

Simulation results

A flowchart desribing the simulation procedure is shown in Fig. 6.3. The Fortran program used to carry out the simulations, sample runs and the Matlab program used for plotting the growth of the eutectics are contained in Appendix C. For comparison with the analytic results, the Fortran program was set up for the CBr_4-C_2Cl_6 and Al-Al_2Cu eutectic systems. In the figures presented the grid is seeded, with some initial curvature, to form a eutectic crystal of a fixed composition. Two periods of the initial crystal are seeded with the center of the first alpha phase at $x = 0$. The eutectic is then allowed to grow by a combination of infinity and interface walks as described earlier.

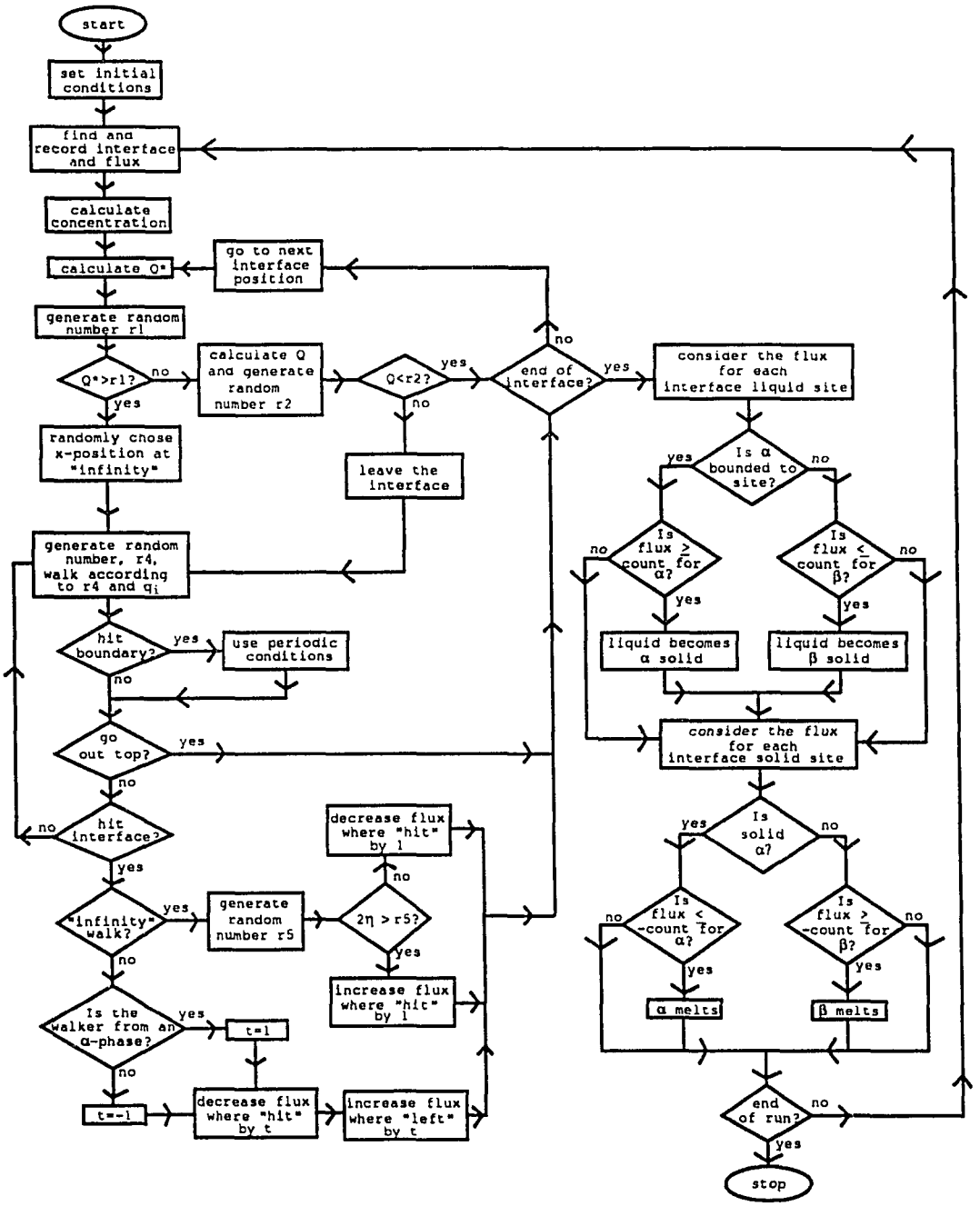

Figure 6.3: Flowchart for random walk simulation.

The triple point locations are recorded and plotted after a fixed number of sweeps of the interface. In addition, the location of the solid interface sites are periodically recorded and plotted as indicated in the figures presented. Note that due to the moving reference frame incorporated into the mathematical model, the z-coordinates of the triple points and the solid interface sites must be incremented to see the growth behavior over time. Also note that a subroutine is present in the code which restricts the interface to grow in a smooth manner (see Appendix C). The values needed to calculate $U(i)$ in Eq. (6.1) and the counters (countA $= \delta_1 P U_{\alpha E} M$ and countB $= \delta_1 P U_{\beta E} M$) were taken from Karma [19] and Magnin and Trivedi [22] and can be found in Appendix C. In the runs presented M is taken as $80,000$ to give reasonable values to countA and countB. If an initial seed value is not stated for a particular run it was taken as 2η.

Figure 6.4 shows a simulation run for the Al-Al_2Cu system with $W = 100$, $H = 500$, $P = 0.0067$, countA $= 13$, countB $= -10$, and $2\eta = 0.7$ with the eutectic seeded such that the alpha phase volume fraction is initially taken as 0.54. The triple points are plotted and the z-direction is incremented 5 units every 500 sweeps of the interface and the solid-liquid interface is plotted every 15,000 sweeps. Figure 6.5 shows a similiar simulation run for the Al-Al_2Cu system. All values are the same as in Fig. 6.4 except that $2\eta = 0.4$. Note that the volume fractions adjust so that the alpha phase volume fraction begins to change from the seeded value of 0.54 to 0.7 and 0.4 respectively and that the curvature of the solid-liquid interface becomes quite small. A closer look at the curvature of the interface indicates that the curvature in the simulations does not satisfy the assumption in Chap. 3 that the average curvature over a phase is $\sin\hat{\phi}$ divided by the volume fraction. Thus a discrepancy exists between the interface curvature found in the simulations and the interface curvature assumptions in Chap. 3.

Figure 6.6 shows a simulation run for comparison with Fig. 3.4(b) from the analytic results for the Al-Al_2Cu system with $P = 0.0067$ and $2\eta = 0.8015$ with a perturbation corresponding to $N = 2$ (the acoustic mode). In the simulation run the triple points are plotted and the z-direction is incremented 5 units every 500 sweeps of the interface, the solid-liquid interface is plotted every 15,000 sweeps, $W = 100$, $H = 500$, countA $= 13$ and countB $= -10$. Likewise Figure 6.7 shows a

simulation run for comparison with Fig. 3.6(c) for the same eutectic system except that $P = 0.0095$ and $2\eta = 0.9385$ with an initial perturbation corresponding to $N = 1$ (the optical mode). The change in P results in a change in countA and countB such that countA $= 18$ and countB $= -13$. The triple points are incremented 5 units and plotted every 50 sweeps of the interface and the solid-liquid interface is plotted every 1500 sweeps of the interface. Unfortunately, the analytic results of Chap. 3 are not duplicated in Figs. 6.6 and 6.7. The discrepency may be due to an incorrect combination of parameters used for the simulations or the discrepency may be due to an inconsistency in the assumptions made in the analytic model and the assumptions made in the simulation model (code).

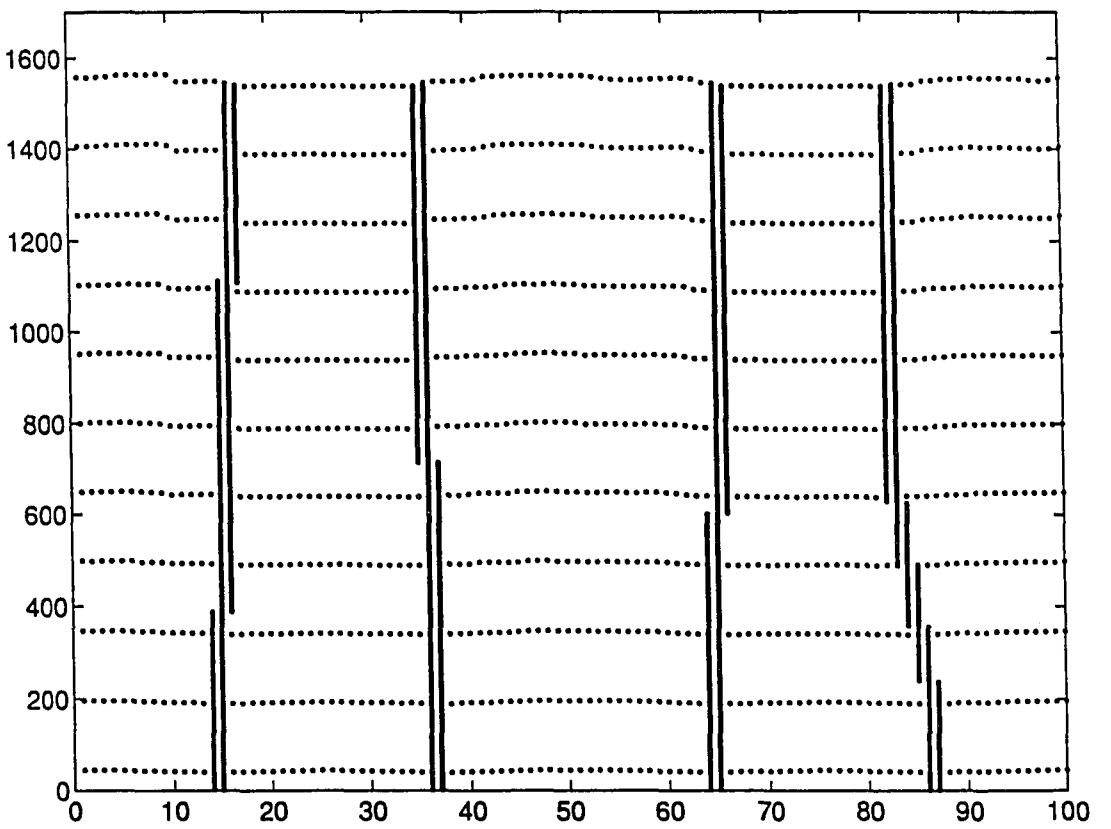

Figure 6.4: Simulation runs for the Al-Al_2Cu system with $W = 100$, $H = 500$, countA $= 13$, countB $= -10$, $P = 0.0067$, $2\eta = 0.7$, seed $= 0.54$, incrementing 5 units every 500 sweeps and plotting the interface every 15,000 sweeps.

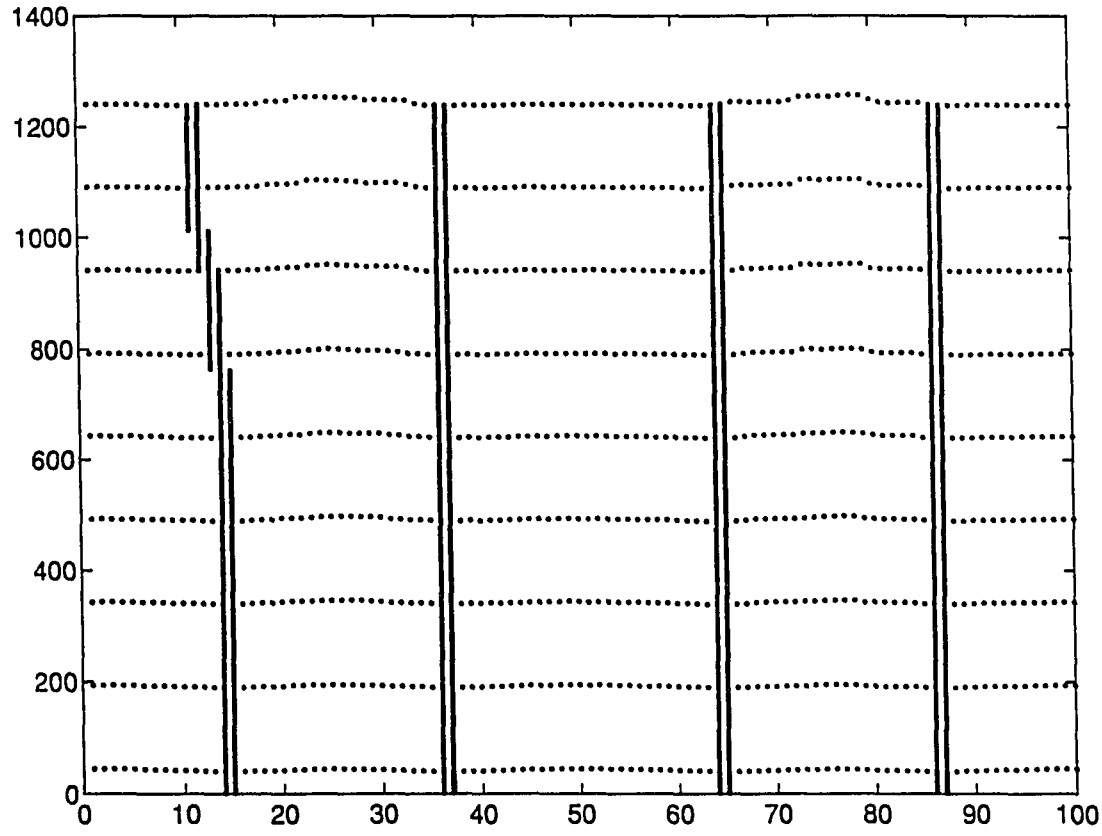

Figure 6.5: Simulation runs for the Al-Al_2Cu system with $W = 100$, $H = 500$, $P = 0.0067$, countA $= 13$, countB $= -10$, $2\eta = 0.4$, seed $= 0.54$, incrementing 5 units every 500 sweeps and plotting the interface every 15,000 sweeps.

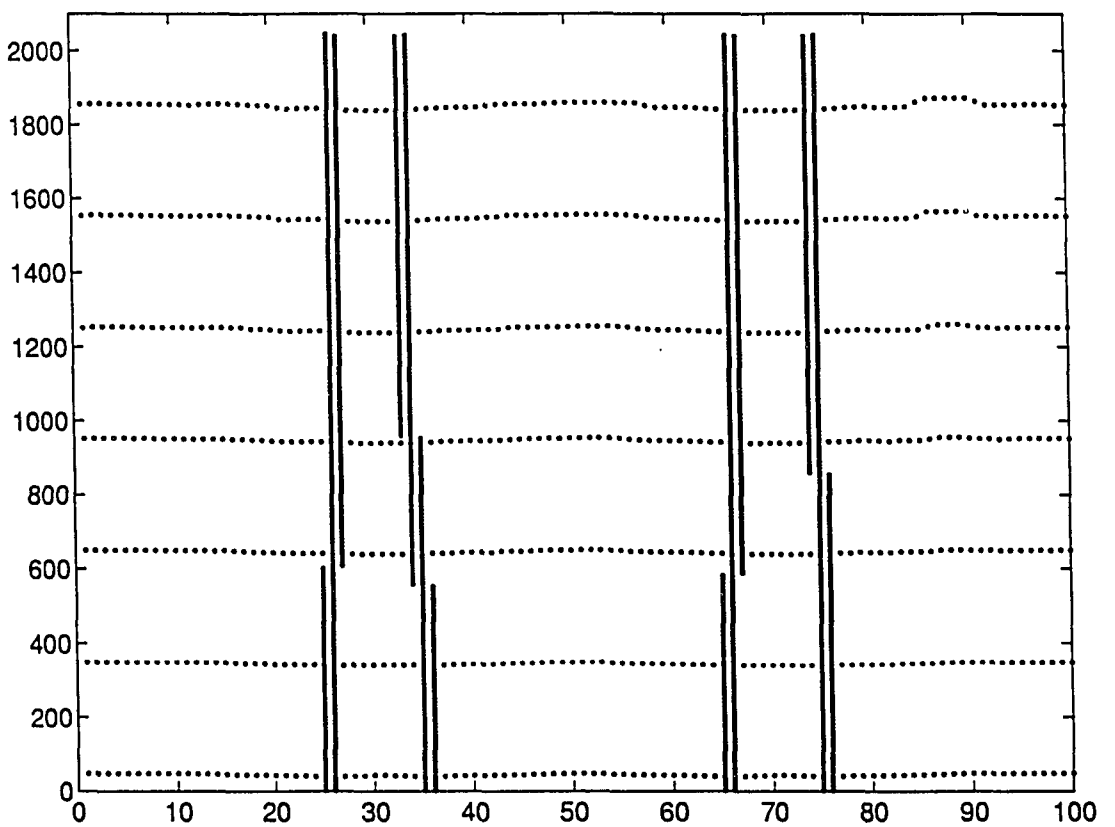

Figure 6.6: Simulation run for the Al-Al_2Cu system with $W = 100$, $H = 500$, $P = 0.0067$, countA $= 13$, countB $= -10$ and $2\eta = 0.8015$ with an initial perturbation corresponding to $N = 2$. Increments are taken 5 units every 500 sweeps and the interface is plotted every 15,000 sweeps.

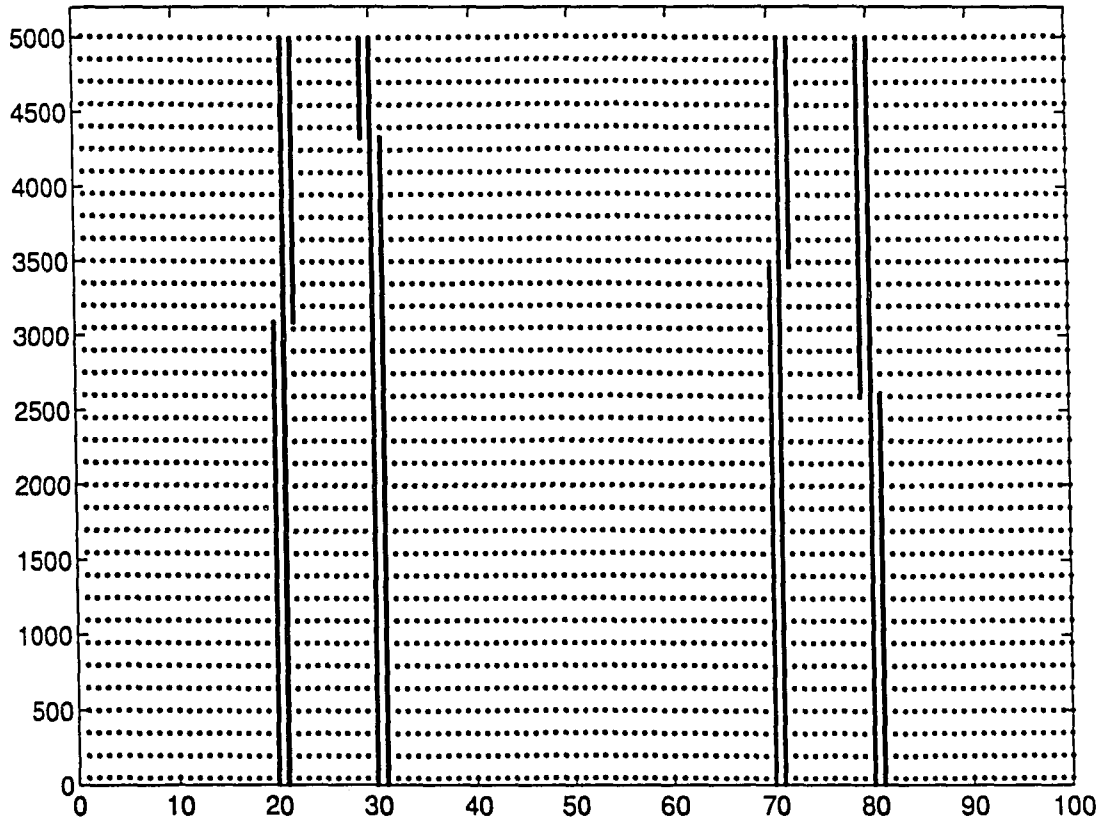

Figure 6.7: Simulation runs for the Al-Al_2Cu system with $W = 100$, $H = 500$, $P = 0.0095$, countA $= 18$, countB $= -13$ and $2\eta = 0.9285$ with an initial perturbation corresponding to $N = 1$. Increments are taken 5 units every 50 sweeps and the interface is plotted every 1500 sweeps.

CHAPTER 7. GENERAL CONCLUSIONS

By nature, the study of mathematics is a school of thought requiring regimented procedures, theoretical concepts and computational techniques. The subject of mathematical modeling takes these features and links them together with the common thread of the phenomenon of interest. In the present case, the common thread is the study of thin-film directional solidification of a binary eutectic.

Two-dimensional eutectic growth during thin-film directional solidification has been identified as a Stefan-type problem and a mathematical representation has been presented in the form of a diffusion equation with drift, a far-field condition, a conservation of mass boundary condition and a thermal boundary condition based on the Jackson and Hunt [7] model. The linear stability analysis presented in Chap. 3 captured two oscillatory modes using Fourier analysis and a perturbation tangential to the interface. The oscillations of interest are the experimentally observed acoustic oscillations and optical oscillations. Note that as long as the conservation condition holds (i.e., $U_\infty = 2\eta U_{\alpha E} + \rho U_{\beta E}$) the linear stability analysis applied to the Jackson and Hunt [7] model, the Datye and Langer [8] model and the Donaghey and Tiller [9] model agree to at least order P^2 (see Chap. 3, the Appendix of the included paper in Chap. 3 and Appendix B of this thesis). Although Caroli, Caroli and Roulet [20] have done some analytical work on the optical modes and Datye and Langer [8] have analytically found the acoustic modes, the material presented in Chap. 3 is noteable due to the simpler analysis, in the respect that the perturbation is in the x-direction only, and due to the single analysis, in the respect that one method is used to capture both modes.

The asymptotic analysis of Chap. 4, applied to the small Péclet number version of the nonlinear equations derived from the linear stability analysis, simplified the formidable task of finding the conditions under which the acoustic oscillations occur.

In particular, the relationship between the Péclet number, P, and the α phase volume fraction, 2η, was simplified. Unfortunately, the asymptotics presented were not valid for the nonlinear equation associated with the optical oscillations.

The revised mathematical representation of Chap. 5 extended the study of eutectic growth to a moderately high Péclet number, subject to growth occuring near the eutectic concentration. The nonlinear equations derived from the linear stability analysis applied to the revised model contained an additional factor involving P-dependent partition coefficients and slopes (i.e., the Péclet factor). For the systems tested and for various values of the parameter $P_D = (\lambda V_D)/(2D)$, the relationship between the concentration and the velocity (i.e., the volume fractions and the Péclet number) deviated from the initially derived relationship. The acoustic oscillations of the CBr_4-C_2Cl_6 system moved closer to the eutectic concentration and the optical oscillations of the Al-Al_2Cu system moved further from the eutectic concentration. The optical oscillations of the CBr_4-C_2Cl_6 system also deviated from the original relationship, moving away from or toward the eutectic concentration, depending on the inital position. Note that the acoustic oscillations of the Al-Al_2Cu system were not affected by this analysis.

Finally, the random walk simulations demonstrated the movement of the triple points under perturbation conditions. As stated at the end of Chap. 6, discrepencies between the analytic model and the simulation results exist. Additional considerations may be needed in the simulation model to capture the oscillatory behaviors. For example, it may be nessecary to incorporate local variations in the volume fractions to capture the optical oscillations or it may be nessecary to write the curvature term of the thermal boundary condition at the interface in a different manner.

The work presented in this thesis uncovers certain aspects of mathematically modeling the Stefan-type problem describing thin-film directional solidification of a binary alloy during eutectic growth. Further analysis would be necessary to determine whether or not the methods of this thesis could be applied to analyze other dynamical states such as tilt waves, growing and decaying oscillations, banding or chaotic behavior. Initial exploration in using the linear stability analysis to find tilt waves indicated that eutectic tilt waves exist at low velocities and that these tilt waves cease to exist with an increase in velocity. This is contradictory to numerical

findings by Kassner and Misbah [41], experiments by Faivre and Mergy [42] and the simulations of Xiao *et al.* [24]. Possible explanations for this discrepancy may be a lack of a perturbation in the z-direction, a restriction that the interface maintains an average z value of $\bar{\zeta}$, simplifications in the conservation of mass boundary condition or the averaging of the curvature. In earlier findings by Kassner and Misbah [43], they initially found, using a boundary-integral formulation and a numerical scheme, a collapse of the tilt angle to zero as the velocity was increased. However, after finding that their extrapolation formula overestimated the magnitude of curvature at the triple points and that this error became pronounced at large curvatures, which appear in tilted solutions, they reversed their initial findings. That is, they found that parity breaking was a standard supercritical bifurcation occuring at a critical velocity. Thus, the analysis presented in this dissertation, with the curvature assumptions as stated in Chap. 3, does not apply to the tilt wave case.

BIBLIOGRAPHY

[1] Seung Hoon Han, *Primary spacing selection in directionally solidified alloys*, Master's Thesis, (Iowa State University, 1991).

[2] M. Zimmermann, M. Carrard and W. Kurz, *Rapid solidification of Al-Cu eutectic alloy by laser remelting*, Acta Metall., **37** (12) (1989), pp. 3305–3313.

[3] Martin Zimmermann, Alain Karma and Michael Carrard, *Oscillatory lamellar microstructure on off-eutectic Al-Cu alloys*, Phys. Rev. B, **42** (1) (1990), pp. 833–837.

[4] G. J. Merchant and S. H. Davis, *Morphological instability in rapid directional solidification*, Acta metall. mater., **38** (12) (1990), pp. 2683–2693.

[5] Alain Karma and Armand Sarkissian, *Dynamics of banded structure formation in rapid solidification*, Phys. Rev. Lett., **68** (17) (1992), pp. 2616–2619.

[6] S. C. Gill and W. Kurz, *Rapidly solidified Al-Cu alloys–I. Experimental determination of the microstructure selection map*, Acta metall. mater., **41** (12) (1993), pp. 3563–3573

[7] K. A. Jackson and J. D. Hunt, *Lamellar and rod eutectic growth*, Trans. Metall. Soc. AIME, **236** (1966), pp. 1129–1142.

[8] V. Datye and J. S. Langer, *Stability of thin lamellar eutectic growth*, Phys. Rev. B, **24** (8) (1981), pp. 4155–4169.

[9] L. F. Donaghey and W. A. Tiller, *On the diffusion of solute during the eutectoid and eutectic transformations, Part I*, Mater. Sci. Eng., **3** (1968/69), pp. 231–239.

[10] W. W. Mullins and R. F. Sekerka, *Stability of a planar interface during solidification of a dilute binary alloy*, J. Appl. Phys., **35** (2) (1964), pp. 444–451.

[11] D. J. Wollkind and L. A. Segel, *A nonlinear stability analysis of the freezing of a dilute binary alloy*, Phil. Trans. Roy. Soc. London, **268** (1970), pp. 351–380.

[12] J. S. Langer, *Instabilities and pattern formation in crystal growth*, Rev. Mod. Phys., **52** (1980), pp. 1-28.

[13] John D. Weeks, Wim van Saarloos and Martin Grant, *Stability of cellular profiles in directional solidification: Expansion and matching methods*, J. Cryst. Growth, **112** (1991), pp. 244–282.

[14] B. Caroli, C. Caroli and B. Roulet, *On the emergence of one-dimensional front instabilities in directional solidification and diffusion of binary mixtures*, J. Physique, **43** (1982), pp. 1767–1780.

[15] H. E. Cline, *Theory of the lamellar dendritic transition in eutectic alloys*, Trans. Metall. Soc. AIME, **242** (1968), pp. 1613–1618.

[16] D. T. J. Hurle and E. Jakeman,*Morphological stability of lamellar eutectics*, J. Crystallogr. Growth, **3** (4) (1968), pp. 574–582.

[17] S. Strässler and W. R. Schneider, *Stability of lamellar eutectics*, Phys. Cond. Matter, **17** (1973), pp. 153–178.

[18] H. E. Cline, *Stabiltiy of lamellar eutectics*, J. Appl. Phys., **50** (7) (1979), pp. 4780–4785.

[19] Alain Karma, *Beyond steady-state lamellar eutectic growth*, Phys. Rev. Lett., **59** (1) (1987), pp. 71–74.

[20] B. Caroli, C. Caroli and B. Roulet, *Lamellar eutectic growth at large thermal gradient. II. Linear stabiliy*, J. Phys. (Paris) **51** (1990), pp. 1865–1876.

[21] K. Kassner and C. Misbah, *Growth of lamellar eutectic structures: the axisymmetric state*, Phys. Rev. A, **44** (10) (1991), pp. 6513–6532.

[22] P. Magnin and R. Trivedi, *Eutectic growth: a modification of the Jackson and Hunt theory*, Acta Metall. Matter, **39** (4) (1991), pp. 453–467.

[23] G. Faivre, C. Guthmann and J. Mergy, *Dynamical instability in the solidification front of lamellar eutectics*, Appl. Mech. Rev., **43** (no. 5, part 2) (1990), pp. S89–S90.

[24] Rong-Fu Xiao, J. Iwan D. Alexander and Franz Rosenberger, *Eutectic and off-eutectic growth patterns*, Mater. Sci. Eng., **A178** (1994), pp. 233–238.

[25] L. V. Kantorovich and V. I. Krylov, *Approximate Methods of Higher Analysis*, P. Noordhoff, Groningen (1958), Chap. 1, Section 5.

[26] Watson Fulks, *Advanced Calculus*, John Wiley & Sons, Inc., New York (1969), Chap. 19.

[27] Michael J. Aziz and Theodore Kaplan, *Continuous growth model for interface motion during alloy solidification*, Acta Metall., **36** (8) (1988), pp. 2335–2347.

[28] W. Kurz and R. Trivedi, *Eutectic growth under rapid solidification conditions*, Metall. Trans. A, **22A** (1991), pp. 3051–3057.

[29] W. J. Boettinger and S. R. Coriell, *Microstructure Formation in Rapidly Solidified Alloys* in Science and Technology of Undercooled Melt, P. R. Sahm, H. Jones, and C. M. Adam, eds., Martinus Nijhoff Publishers, Dordrecht, The Netherlands (1986), pp. 81–108.

[30] Rong-Fu Xiao, J. Iwan D. Alexander and Franz Rosenberg, *Microscopic-growth morphologies in binary systems*, Phys. Rev. A, **45** (2) (1991), pp. R571–R574.

[31] J. Iwan D. Alexander and Franz Rosenberger, personal communications.

[32] T. A. Witten, Jr. and L. M. Sander, *Diffusion-limited aggregation, a kinetic critical phenomenon*, Phys. Rev. Lett., **47** (19) (1981), pp. 1400–1403.

[33] Per Arne Rikvold, *Simulations of a stochastic model for cluster growth on a square lattice*, Phys. Rev. A, **26** (1) (1982), pp. 647–650.

[34] Tamás Vicsek, *Formation of solidification patterns in aggregation models*, Phys. Rev. A, **32** (5) (1985), pp. 3084–3089.

[35] Leo P. Kadanoff, *Simulating hydrodynamics: a pedestrian model*, J. Stat. Phys., **39** (3/4) (1985), pp. 267–283.

[36] Chao Tang, *Diffusion-limited aggregation and the Saffman-Tayler problem*, Phys. Rev. A, **31** (3) (1985), pp. 1977–1979.

[37] Shoudan Liang, *Random-walk simulations of flow in Hele Shaw cells*, Phys. Rev. A, **33** (4) (1986), pp. 2663–2674.

[38] A. P. Roberts and M. A. Knackstedt, *Growth in non-Laplacian fields*, Phys. Rev. E, **47** (4) (1993), pp. 2724–2728.

[39] Erich Zauderer, *Partial Differential Equations of Applied Mathematics*, John Wiley & Sons, New York, (1989), Chapter 1.

[40] Eitan Sadeh and Mark A. Franklin, *Monte Carlo solution of partial differential equations by special purpose digital computer*, IEEE Transactions on Computers, **c-23** (4) (1974), pp. 389–397.

[41] K. Kassner and C. Misbah, *Spontaneous parity-breaking transition in directional growth of lamellar eutectic structures*, Phys. Rev. A, **44** (10) (1991), pp. 6533–6543.

[42] G. Faivre and J. Mergy, *Tilt bifurcation and dynamical selection of tilt domains in thin-film lamellar eutectic growth: Experimental evidence of a tilt bifurcation*, Phys. Rev. A, **45** (10) (1992), pp. 7320–7329.

[43] K. Kassner and C. Misbah, *Parity breaking in eutectic growth*, American Physical Society, **65** (12) (1990), pp. 1458–1461

[44] Ronald B. Guenther and John W. Lee, *Partial Differential Equations of Mathematical Physics and Integral Equations*, Prentice-Hall, New Jersey (1988), Chap. 3.

[45] Charles Sparks Rees, S. M. Shah and C. V. Stanojević, *Theory and Applications of Fourier Analysis*, Marcel Dekker, Inc., New York (1981), Chaps. 3 and 5.

APPENDIX A: THE REAL AND IMAGINARY EQUATIONS AND THE CORRESPONDING FORTRAN PROGRAMS

The following Fortran programs are used to solve Eqs. (3.10) and (3.11) found in the paper contained in Chap. 3 and Eqs. (5.10) and (5.11) derived from the high Péclet number model, by using a Nag subroutine, C05AGF, which finds the roots of an equation given an initial guess. The subroutine requires a complex equation to be rewritten into its real and imaginary components so that the subroutine can be applied to each equation seperately.

The real and imaginary equations

The real and imaginary equations from Eqs. (3.10) and (3.11) with $\omega = bi$ are as follows. For $N = 1$ the real equation is written as

$$\frac{S(\eta)}{(2\eta)^2} - \frac{R(\eta)}{2\eta} + \frac{\Omega \sin(\phi_\alpha)}{(2\eta)^2} = \frac{T_1(P,b,0)}{\left[T_1(P,b,0)\right]^2 + \left[K_1(P,b,0)\right]^2}$$
$$+ \frac{1}{2\eta} \sum_{n=1}^{\infty} \frac{\sin(4n\pi\eta)}{n\pi} \left\{ \frac{T_1(P,b,n)}{\left[T_1(P,b,n)\right]^2 + \left[K_1(P,b,n)\right]^2} \right\}$$

and the imaginary equation is written as

$$b\frac{\Omega \cos(\phi_\alpha)}{(2\eta)\sqrt{P}} = \frac{K_1(P,b,0)}{\left[T_1(P,b,0)\right]^2 + \left[K_1(P,b,0)\right]^2}$$
$$+ \frac{1}{2\eta} \sum_{n=1}^{\infty} \frac{\sin(4n\pi\eta)}{n\pi} \left\{ \frac{K_1(P,b,n)}{\left[T_1(P,b,n)\right]^2 + \left[K_1(P,b,n)\right]^2} \right\}$$

where

$$T_N(P,b,n) = \frac{P}{2} + \frac{1}{\sqrt{2}}\left[M_N(P,b,n) + L_N(P,n)\right]^{1/2},$$

$$K_N(P,b,n) = \frac{1}{\sqrt{2}}\left[M_N(P,b,n) - L_N(P,n)\right]^{1/2},$$

$$M_N(P,b,n) = \left\{\left[\left(\frac{P}{2}\right)^2 + \left(\frac{n\pi}{N}\right)^2\right]^2 + b^2\right\}^{1/2}$$

and

$$L_N(P,n) = \left(\frac{P}{2}\right)^2 + \left(\frac{n\pi}{N}\right)^2.$$

Likewise for $N = 2$ we may write the real equation as

$$\frac{S(\eta)}{(2\eta)} - R(\eta) + \frac{\Omega \sin(\phi_\alpha)}{(2\eta)}$$

$$= \sum_{\text{odd } n=1}^{\infty} \frac{\sin(2n\pi\eta)}{(n\pi)/2}\left\{\frac{T_2(P,b,n)}{\left[T_2(P,b,n)\right]^2 + \left[K_2(P,b,n)\right]^2}\right\}$$

and the imaginary equation as

$$b\frac{\Omega\cos(\phi_\alpha)}{\sqrt{P}} = \sum_{\text{odd } n=1}^{\infty} \frac{\sin(2n\pi\eta)}{(n\pi)/2}\left\{\frac{K_1(P,b,n)}{\left[T_2(P,b,n)\right]^2 + \left[K_1(P,b,n)\right]^2}\right\}$$

Note that all series involved in the previous stated equations are uniformly convergent for $0 \leq 2\eta \leq 1$. Similiar equations may be written for Eqs. (5.10) and (5.11).

For a given system the following values must be set inside the Fortran programs: $\Omega = (2\Gamma_\alpha)/(m_\alpha \Delta C \lambda P)$, θ_α, $C_{\alpha E}$, $C_{\beta E}$, C_E and the Péclet number P (see the previous equations and Chap. 3). In addition, a value for $1/P_D$ must be set to incorporate the Péclet factor into the calculations (with $1/P_D = 0$ otherwise). For the values above, an initial guess for the α phase volume fraction, 2η, must also be entered.

To calculate the far-field concentration and the velocity as shown in Figs. 3.8 and 3.9 and Figs. 5.3 and 5.4 from the Péclet number and the alpha phase volume fraction (from the Fortran programs found in this appendix) the following equations are used:

$$V = \frac{(2D)^2}{\lambda^2 V} P^2$$

$$C_\infty = \frac{\rho_\alpha C_{\alpha E} 2\eta + \rho_\beta C_{\beta E}(1-2\eta)}{\rho_\alpha 2\eta + \rho_\beta (1-2\eta)}$$

where $\lambda^2 V$ is taken as a constant. ρ_α is the density for the alpha phase and ρ_β is the density for the beta phase. Note that in the above equation C_∞, $C_{\alpha E}$ and C_β are weight percents, not volume percents.

Fortran program for the optical oscillations

Calculations were run on a DECStation 5000 using ULTRIX 4.3 at Iowa State University. With the previous values set as indicated in 'PROGRAM N12eta', the command 'f77 N12eta.f -lnag' is entered at the cursor (%) and the following sample output is contained in 'a.out':

```
2eta for the real equation = 0.7991985355664054
ifail = 0
2eta for the imaginary equation = 0.7989852154998429
ifail=0
```

where ifail = 0 indicates that the subroutine ran with no difficulties. From this output the volume fractions are recorded for a fixed Péclet number. Then the Péclet number is changed and the program is rerun until the volume fractions agree to four decimal places. Note that this program and the Fortran program for the acoustic oscillations may be easily altered to solve for the Péclet number, P, given a fixed α phase volume fraction, 2η.

The Fortran program for the optical oscillations is as follows:

```
      PROGRAM N12eta

*     Brenda Diesslin
*     Revised: October 1, 1994
*     This program is used to solve for the alpha phase
*     concentration, 2eta, given the Peclet number, P, for the
*     real and imaginary equations for the N=1 case using the Nag
*     subroutine C05AGF.

************************************************************************
*     N, M : eta                                                       *
*     Y : parametric value=(2*gamma)/(slope*deltaC*lambda*P)           *
*     THETA : angle from the horizontal                                *
*     Q : Pi                                                           *
*     F, E, G, HH, P, T, K, PP : functions                             *
*     KALPHA, KBETA, SIGMA, SLOPE : high velocity functions            *
*     Z, ZZ, SUM, AA, BB, C, S, R, L, V, U, TEMP : temp. quantities    *
*     H : stepsize                                                     *
*     EPS, ETA, IFAIL, A, B : quantities used by the Nag subroutine    *
*     I : counter                                                      *
*     W : b where omega = bi                                           *
*     X : Peclet number P                                              *
*     DELTAC : miscibility gap                                         *
*     CEUT : eutectic concentration                                    *
*     CAE : eutectic solid concentration for the alpha phase           *
*     CBE : eutectic solid concentration for the beta phase            *
*     GAMMA : parameter used for high velocity terms                   *
*     CRYSTAL : 0 for CBr4-C2Cl6; 1 for Al-Al2Cu                       *
************************************************************************

*************************** begin program ****************************

      REAL*8 N, M, X, W, H, EPS, ETA, A, B
      REAL*8 F, E, G, HH, P, T, K, PP, X02AJF
      REAL*8 Y, Q, THETA, Z, ZZ
      REAL*8 KALPHA, KBETA, SIGMA, SLOPE
      INTEGER  I, IFAIL
      EXTERNAL F, E, G, HH, P, T, K, PP, C05AGF, X02AJF
```

```
      EXTERNAL KALPHA, KBETA, SIGMA, SLOPE
      INTRINSIC SQRT
*     N is the initial guess for eta in the real equation
      N=.5/2
*     H is the step size used by C05AGF
      H=.01
      EPS=SQRT(X02AJF())
      ETA=0.0
      IFAIL=0
      A=0.0
      B=1.0
      CALL C05AGF(N,H,EPS,ETA,F,A,B,IFAIL)
      PRINT*,'2eta for the real equation =',2*N
      PRINT*,'ifail =',IFAIL
*     M is the initial guess for eta in the imaginary equation
      M=.5/2
      IFAIL=0
      CALL C05AGF(M,H,EPS,ETA,T,A,B,IFAIL)
      PRINT*,'2eta for the imaginary equation =',2*M
      PRINT*,'ifail =',IFAIL
      STOP
      END

**************** main function for the real equation ****************

      REAL*8 FUNCTION F(N)
      REAL*8 N, X, W, E, G, HH, P, Y, Q, THETA, Z, ZZ
      REAL*8 GAMMA, CEUT, DELTAC, CAE, CBE, SIGMA, SLOPE
      INTEGER CRYSTAL
      EXTERNAL SIGMA, SLOPE
*     X is the Peclet number
      X=2.001
*     W is the given b value and 2eta value
      W=3
*     GAMMA=0 corresponds to no high velocity terms
      GAMMA=1./25.
*     -CBr: CRYSTAL=0, Al: CRYSTAL=1
      CRYSTAL=1
      IF (CRYSTAL .EQ. 0) THEN
         Y=0.0447
```

```
         Q=3.1415927
         THETA=Q*60/180
         CAE=0.0508
         CBE=0.1618
         CEUT=0.084
      ELSE
         Y=0.1045
         Q=3.1415927
         THETA=Q*65/180
         CAE=0.0565
         CBE=0.525
         CEUT=0.327
      END IF
      DELTAC=CBE-CAE
      Z=(TAN(THETA))**2 + (SQRT(X))**2
      ZZ=(Y*TAN(THETA)/SQRT(Z))/SLOPE(X,CEUT,CAE,GAMMA)
      ZZ=ZZ/SIGMA(X,CEUT,CAE,CBE,GAMMA,DELTAC)
      F=2*E(X,N,Q)-2*N*G(X,N,Q)-2*N*HH(X,N,Q,W)-((2*N)**2)*P(X,W)+ZZ
      RETURN
      END

************* main function for the imaginary equation **************

      REAL*8 FUNCTION T(M)
      REAL*8 M, X, W, K, PP, Y, Q, THETA, Z, ZZ
      REAL*8 GAMMA, CEUT, DELTAC, CAE, CBE, SIGMA, SLOPE
      INTEGER CRYSTAL
      EXTERNAL SIGMA, SLOPE
*     X is the Peclet number
      X=2.001
*     W is the given b value and 2eta value
      W=3
*     GAMMA=0 corresponds to no high velocity terms
      GAMMA=1./25.
*     -CBr: CRYSTAL=0, Al: CRYSTAL=1
      CRYSTAL=1
      IF (CRYSTAL .EQ. 0) THEN
         Y=0.0447
         Q=3.1415927
         THETA=Q*60/180
```

```
         CAE=0.0508
         CBE=0.1618
         CEUT=0.084
      ELSE
         Y=0.1045
         Q=3.1415927
         THETA=Q*65/180
         CAE=0.0565
         CBE=0.525
         CEUT=0.327
      END IF
      DELTAC=CBE-CAE
      Z=(TAN(THETA))**2 +(SQRT(X))**2
      ZZ=(Y/SQRT(Z))/SLOPE(X,CEUT,CAE,GAMMA)
      ZZ=ZZ/SIGMA(X,CEUT,CAE,CBE,GAMMA,DELTAC)
      T=K(W,X,M,Q)-2*M*PP(X,W)+W*ZZ
      RETURN
      END

************ secondary functions for the real equation *************

      REAL*8 FUNCTION E(X,N,Q)
      REAL*8 N, X, Q, SUM, AA
      INTEGER I
      SUM=0.0
      DO 20 I=1,200
         AA=(X/2)**2+(I*Q)**2
         SUM=SUM+(SIN(2*I*Q*N))**2/((X/2+SQRT(AA))*((I*Q)**2))
20    CONTINUE
      E=SUM
      RETURN
      END

      REAL*8 FUNCTION G(X,N,Q)
      REAL*8 N, X, Q, SUM, BB
      INTEGER I
      SUM=0.0
      DO 30 I=1,200
         BB=(X/2)**2+(I*Q)**2
         SUM=SUM+SIN(4*I*Q*N)/((X/2+SQRT(BB))*(I*Q))
```

```
30    CONTINUE
      G=SUM
      RETURN
      END

      REAL*8 FUNCTION HH(X,N,Q,W)
      REAL*8 N, X, W, Q, SUM, C, S, R, L
      INTEGER I
      SUM=0.0
      DO 40 I=1,200
         C=(X/2)**2+(I*Q)**2
         S=SQRT(C**2+W**2)
         R=SQRT((S+C)/2.0)
         L=(X/2+R)**2+(S-C)/2
         SUM=SUM+(X/2+R)*SIN(4*I*Q*N)/(L*(I*Q))
40    CONTINUE
      HH=SUM
      RETURN
      END

      REAL*8 FUNCTION P(X,W)
      REAL*8 X, W, V, U, R
      V=(X/2)**2
      U=SQRT(V**2+W**2)
      R=SQRT((U+V)/2.0)
      P=(X/2+R)/((X/2+R)**2+(U-V)/2.0)
      RETURN
      END

********** secondary functions for the imaginary equation *********

      REAL*8 FUNCTION K(W,X,M,Q)
      REAL*8 M, X, W, Q, SUM, D, V, R, L, S
      INTEGER I
      SUM=0.
      DO 50 I=1,200
         D=(X/2)**2+(I*Q)**2
         V=SQRT(D**2+W**2)
         S=SQRT((V-D)/2.0)
         R=SQRT((V+D)/2.0)
```

```
         L=(X/2+R)**2+(V-D)/2
         SUM=SUM-S*SIN(4*I*Q*M)/(L*(I*Q))
50     CONTINUE
       K=SUM
       RETURN
       END

       REAL*8 FUNCTION PP(X,W)
       REAL*8 X, W, V, U, R, C
       V=(X/2)**2
       U=SQRT(V**2+W**2)
       R=SQRT((U+V)/2.0)
       C=SQRT((U-V)/2.0)
       PP=C/((X/2+R)**2+(U-V)/2.0)
       RETURN
       END

********************* high velocity functions **********************

       REAL*8 FUNCTION KALPHA(X,CEUT,CAE,GAMMA)
       REAL*8 X, GAMMA, CEUT, CAE, TEMP
       TEMP=GAMMA*X+CAE*(1-CEUT)/CEUT
       KALPHA=TEMP/(GAMMA*X+(1-CEUT))
       RETURN
       END

       REAL*8 FUNCTION KBETA(X,CEUT,CBE,GAMMA)
       REAL*8 X, GAMMA, CEUT, CBE, TEMP
       TEMP=GAMMA*X+(1-CBE)*CEUT/(1-CEUT)
       KBETA=TEMP/(GAMMA*X+CEUT)
       RETURN
       END

       REAL*8 FUNCTION SIGMA(X,CEUT,CAE,CBE,GAMMA,DELTAC)
       REAL*8 X, GAMMA, CEUT, DELTAC, CAE, CBE
       REAL*8 KALPHA, KBETA, TEMP
       EXTERNAL   KALPHA, KBETA
       TEMP=CEUT*(1-KALPHA(X,CEUT,CAE,GAMMA))
       TEMP=TEMP-(CEUT-1)*(1-KBETA(X,CEUT,CBE,GAMMA))
       SIGMA=TEMP/DELTAC
```

```
      RETURN
      END

      REAL*8 FUNCTION SLOPE(X,CEUT, CAE,GAMMA)
      REAL*8 X, GAMMA, CEUT, CAE, KALPHA, TEMP
      EXTERNAL   KALPHA
      TEMP=KALPHA(X,CEUT,CAE,GAMMA)*(1-CAE)
      TEMP=TEMP/(CAE/CEUT*(1-KALPHA(X,CEUT,CAE,GAMMA)*CEUT))
      TEMP=(1-CEUT)*KALPHA(X,CEUT,CAE,GAMMA)*LOG(TEMP)
      TEMP=TEMP+1-KALPHA(X,CEUT,CAE,GAMMA)
      TEMP=TEMP*(1-CAE)
      SLOPE=TEMP/((1-KALPHA(X,CEUT,CAE,GAMMA)*CEUT)*(1-CAE/CEUT))
      RETURN
      END

************************** end of program **************************
```

Fortran program for the acoustic oscillations

With the input values set as indicated in 'PROGRAM N22eta' (see the discussion at the beginning of this appendix), the command 'f77 N22eta.f -lnag' is entered at the cursor (%) and the following sample output is contained in 'a.out':

```
2eta for the real equation = 0.5136263596942877
ifail = 0
2eta for the imaginary equation = 0.5137755951787052
ifail=0
```

where ifail = 0 indicates that the subroutine ran with no difficulties. As in the disussion of the output from 'PROGRAM N12eta', the volume fractions are recorded, the Péclet number is changed and the program is rerun until the volume fractions agree to four decimal places.

The Fortran program for the acoustic oscillations is as follows:

```
      PROGRAM N22eta

*     Brenda Diesslin
*     Revised: October 1, 1994
*     This program is used to solve for the alpha phase
*     concentration, 2eta, given the Peclet number, P, for the
*     real and imaginary equations for the N=2 case using the Nag
*     subroutine C05AGF.

************************************************************************
*     N, M : eta                                                       *
*     Y : parametric value=(2*gamma)/(slope*deltaC*lambda*P)           *
*     THETA : angle from the horizontal                                *
*     Q : Pi                                                           *
*     F, E, G, HH, T, K : functions                                    *
*     KALPHA, KBETA, SIGMA, SLOPE : high velocity functions            *
*     Z, ZZ, SUM, AA, BB, C, P, R, L, TEMP : temporary quantities      *
*     H : stepsize                                                     *
*     EPS, ETA, IFAIL, A, B : quantities used by the Nag subroutine    *
*     I : counter                                                      *
*     W : b where omega = bi                                           *
*     X : Peclet number P                                              *
*     DELTAC : miscibility gap                                         *
*     CEUT : eutectic concentration                                    *
*     CAE : eutectic solid concentration for the alpha phase           *
*     CBE : eutectic solid concentration for the beta phase            *
*     GAMMA : parameter used for high velocity terms                   *
*     CRYSTAL : 0 for CBr4-C2Cl6; 1 for Al-Al2Cu                       *
************************************************************************

*************************** begin program ****************************

      REAL*8 N, M, X, W, H, EPS, ETA, A, B
      REAL*8 F, E, G, HH, T, K, X02AJF
      REAL*8 Y, Q, THETA, Z, ZZ
      REAL*8 KALPHA, KBETA, SIGMA, SLOPE
      INTEGER  I, IFAIL
      EXTERNAL F, E, G, HH, T, K, C05AGF, X02AJF
```

```
      EXTERNAL KALPHA, KBETA, SIGMA, SLOPE
      INTRINSIC SQRT
*     N is the initial guess for eta in the real equation
      N=.45/2
*     H is the step size used by C05AGF
      H=.01
      EPS=SQRT(X02AJF())
      ETA=0.0
      IFAIL=0
      A=0.0
      B=1.0
      CALL C05AGF(N,H,EPS,ETA,F,A,B,IFAIL)
      PRINT*,'2eta for the real equation=',2*N
      PRINT*,'ifail=',IFAIL
*     M is the initial guess for eta in the imaginary equation
      M=.5/2
      IFAIL=0
      CALL C05AGF(M,H,EPS,ETA,T,A,B,IFAIL)
      PRINT*,'2eta for the imaginary equation=',2*M
      PRINT*,'ifail=',IFAIL
      STOP
      END

**************** main function for the real equation ****************

      REAL*8 FUNCTION F(N)
      REAL*8 N, X, W, E, G, HH, Y, Q, THETA, Z, ZZ
      REAL*8 GAMMA, CEUT, DELTAC, CAE, CBE, SIGMA, SLOPE
      INTEGER CRYSTAL
      EXTERNAL SIGMA, SLOPE
*     X is the Peclet number
      X=.9303
*     W is the given b value and 2eta value
      W=3
*     GAMMA=0 corresponds to no high velocity terms
      GAMMA=1./25.
*     -CBr: CRYSTAL=0, Al: CRYSTAL=1
      CRYSTAL=0
      IF (CRYSTAL .EQ. 0) THEN
         Y=0.0447
```

```
         Q=3.1415927
         THETA=Q*60/180
         CAE=0.0508
         CBE=0.1618
         CEUT=0.084
      ELSE
         Y=0.1045
         Q=3.1415927
         THETA=Q*65/180
         CAE=0.0565
         CBE=0.525
         CEUT=0.327
      END IF
      DELTAC=CBE-CAE
      Z=(TAN(THETA))**2 + (SQRT(X))**2
      ZZ=(Y*TAN(THETA)/SQRT(Z))/SLOPE(X,CEUT,CAE,GAMMA)
      ZZ=ZZ/SIGMA(X,CEUT,CAE,CBE,GAMMA,DELTAC)
      F=2*E(X,N,Q)-2*N*G(X,N,Q)-2*N*HH(X,N,Q,w)+ZZ
      RETURN
      END

************** main function for the imaginary equation **************

      REAL*8 FUNCTION T(M)
      REAL*8 M, X, W, K, Y, Q, THETA, Z, ZZ
      REAL*8 GAMMA, CEUT, DELTAC, CAE, CBE, SIGMA, SLOPE
      INTEGER CRYSTAL
      EXTERNAL SIGMA, SLOPE
*     X is the Peclet number
      X=.9303
*     W is the given b value and 2eta value
      W=3
*     GAMMA=0 corresponds to no high velocity terms
      GAMMA=1./25.
*     -CBr: CRYSTAL=0, Al: CRYSTAL=1
      CRYSTAL=0
      IF (CRYSTAL .EQ. 0) THEN
         Y=0.0447
         Q=3.1415927
         THETA=Q*60/180
```

```
         CAE=0.0508
         CBE=0.1618
         CEUT=0.084
      ELSE
         Y=0.1045
         Q=3.1415927
         THETA=Q*65/180
         CAE=0.0565
         CBE=0.525
         CEUT=0.327
      END IF
      DELTAC=CBE-CAE
      Z=(TAN(THETA))**2 +(SQRT(X))**2
      ZZ=(Y/SQRT(Z))/SLOPE(X,CEUT,CAE,GAMMA)
      ZZ=ZZ/SIGMA(X,CEUT,CAE,CBE,GAMMA,DELTAC)
      T=K(W,X,M,Q)+W*ZZ
      RETURN
      END

********** secondary functions for the real equation **********

      REAL*8 FUNCTION E(X,N,Q)
      REAL*8 N, X, Q, SUM, AA
      INTEGER I
      SUM=0.0
      DO 20 I=1,200
         AA=(X/2)**2+(I*Q)**2
         SUM=SUM+(SIN(2*I*Q*N))**2/((X/2+SQRT(AA))*((I*Q)**2))
20    CONTINUE
      E=SUM
      RETURN
      END

      REAL*8 FUNCTION G(X,N,Q)
      REAL*8 N, X, Q, SUM, BB
      INTEGER I
      SUM=0.0
      DO 30 I=1,200
         BB=(X/2)**2+(I*Q)**2
         SUM=SUM+SIN(4*I*Q*N)/((X/2+SQRT(BB))*(I*Q))
```

```
30    CONTINUE
      G=SUM
      RETURN
      END

      REAL*8 FUNCTION HH(X,N,Q,W)
      REAL*8 N, X, W, Q, SUM, C, S, R, L
      INTEGER I
      SUM=0.0
      DO 40 I=0,200
         C=(X/2)**2+((2*I+1)*Q/2)**2
         S=SQRT(C**2+W**2)
         R=SQRT((S+C)/2.0)
         L=(X/2+R)**2+(S-C)/2
         SUM=SUM+(X/2+R)*SIN(2*(2*I+1)*Q*N)/(L*((2*I+1)*Q/2))
40    CONTINUE
      HH=SUM
      RETURN
      END

********** secondary function for the imaginary equation **********

      REAL*8 FUNCTION K(W,X,M,Q)
      REAL*8 M, X, W, Q, SUM, D, P, R, L, S
      INTEGER I
      SUM=0.
      DO 50 I=0,200
         D=(X/2)**2+((2*I+1)*Q/2)**2
         P=SQRT(D**2+W**2)
         S=SQRT((P-D)/2.0)
         R=SQRT((P+D)/2.0)
         L=(X/2+R)**2+(P-D)/2
         SUM=SUM-S*SIN(2*(2*I+1)*Q*M)/(L*((2*I+1)*Q/2))
50    CONTINUE
      K=SUM
      RETURN
      END

********** high velocity functions **********
```

```
      REAL*8 FUNCTION KALPHA(X,CEUT,CAE,GAMMA)
      REAL*8 X, GAMMA, CEUT, CAE, TEMP
      TEMP=GAMMA*X+CAE*(1-CEUT)/CEUT
      KALPHA=TEMP/(GAMMA*X+(1-CEUT))
      RETURN
      END

      REAL*8 FUNCTION KBETA(X,CEUT,CBE,GAMMA)
      REAL*8 X, GAMMA, CEUT, CBE, TEMP
      TEMP=GAMMA*X+(1-CBE)*CEUT/(1-CEUT)
      KBETA=TEMP/(GAMMA*X+CEUT)
      RETURN
      END

      REAL*8 FUNCTION SIGMA(X,CEUT,CAE,CBE,GAMMA,DELTAC)
      REAL*8 X, GAMMA, CEUT, DELTAC, CAE,CBE
      REAL*8 KALPHA, KBETA, TEMP
      EXTERNAL   KALPHA, KBETA
      TEMP=CEUT*(1-KALPHA(X,CEUT,CAE,GAMMA))
      TEMP=TEMP-(CEUT-1)*(1-KBETA(X,CEUT,CBE,GAMMA))
      SIGMA=TEMP/DELTAC
      RETURN
      END

      REAL*8 FUNCTION SLOPE(X,CEUT,CAE,GAMMA)
      REAL*8 X, GAMMA, CEUT, CAE, KALPHA, TEMP
      EXTERNAL   KALPHA
      TEMP=KALPHA(X,CEUT,CAE,GAMMA)*(1-CAE)
      TEMP=TEMP/(CAE/CEUT*(1-KALPHA(X,CEUT,CAE,GAMMA)*CEUT))
      TEMP=(1-CEUT)*KALPHA(X,CEUT,CAE,GAMMA)*LOG(TEMP)
      TEMP=TEMP+1-KALPHA(X,CEUT,CAE,GAMMA)
      TEMP=TEMP*(1-CAE)
      SLOPE=TEMP/((1-KALPHA(X,CEUT,CAE,GAMMA)*CEUT)*(1-CAE/CEUT))
      RETURN
      END
```

********** end of program **********

APPENDIX B: ADDITIONAL INFORMATION PERTAINING TO CHAPTER 3 (THE OSCILLATORY PAPER)

Equations (3.1)-(3.4) are based on the model presented in Chap. 2 summarized by Eqs. (2.1)-(2.4). Note that in the equations of Chap. 3, D_L is written as D, C_L is written as C and the interface normal is taken as parallel to the direction of the growth velocity (due to the locally planar interface assumption).

Note 1: Finding the Fourier coefficients, E_n, for the JH model

To calculate Eq. (3.6) and Eq. (3.7) we let

$$f(x) = \sum_{n=-\infty}^{\infty} b_n e^{iqnx} = \begin{cases} U_E - U_{\alpha E} & \text{in the } \alpha \text{ phase} \\ U_E - U_{\beta E} & \text{in the } \beta \text{ phase} \end{cases}$$

where

$$b_0 = \frac{1}{2}\left[\int_{2j}^{2(j+\eta)} (U_E - U_{\alpha E})\,dx + \int_{2(j+\eta)}^{2(j+\eta+\rho)} (U_E - U_{\beta E})\,dx \right.$$

$$\left. + \int_{2(j+\eta+\rho)}^{2(j+1)} (U_E - U_{\alpha E})\,dx\right] = -2\eta\, U_{\alpha E} - \rho\, U_{\beta E} \equiv \tau$$

and

$$b_{n\neq 0} = \frac{1}{2}\left[\int_{2j}^{2(j+\eta)} (U_E - U_{\alpha E}) e^{-iqnx}\,dx \right.$$

$$\left. + \int_{2(j+\eta)}^{2(j+\eta+\rho)} (U_E - U_{\beta E}) e^{-iqnx}\,dx + \int_{2(j+\eta+\rho)}^{2(j+1)} (U_E - U_{\alpha E}) e^{-iqnx}\,dx\right]$$

$$= \frac{\sin(2n\pi\eta)}{n\pi}.$$

After substituting Eq. (3.4) into Eq. (3.2) and setting $z = \bar{\zeta}$, we obtain the relationship

$$E_n = P^{3/2}\,\frac{b_n}{F_n}.$$

From this relationship we find the Fourier coefficients E_n as stated in Eq. (3.6) and Eq. (3.7). Note that the Fourier series involved in the computations of this appendix, Chap. 3 and Chap. 5 are uniformly convergent series for $z \geq \bar{\zeta}$ and for all closed subintervals of the x-axis with no points of discontinuity and that conditions for term-wise integration and differentiation hold (uniform convergence can be shown by considering a sequence of partial sums or by writing the series as a Fourier cosine series and using an extension of Dirichlet's Theorem assuming piecewise smoothness [44. 45]).

Note 2: Finding the Fourier coefficients, $\hat{E}_n$, for the JH model

As intermediate steps to finding $\hat{E}_n$ from Eq. (3.9) in the linear stability analysis section of Chap. 3 . we write the following equations for $N = 1$ (with $\hat{q}_m = m\pi$):

$$\frac{1}{2}\int_{2j}^{2(j+1)}\left[\sum_{n=-\infty}^{\infty} E_n F_n\, e^{i q_n x}\, e^{-i\hat{q}_m x} + \sum_{n=-\infty}^{\infty} \hat{E}_n \hat{F}_n\, e^{i\hat{q}_n x}\, e^{-i\hat{q}_m x}\right] dx$$

$$+\frac{P^{3/2}}{2}\left\{\int_{2j}^{2(j+\hat{\eta})}(U_E - U_{\alpha E})e^{-i\hat{q}_m x}\,dx + \int_{2(j+\hat{\eta})}^{2(j+\hat{\eta}+\hat{\rho})}(U_E - U_{\beta E})e^{-i\hat{q}_m x}\,dx\ \&\right.$$

$$\left. + \int_{2(j+1-\hat{\delta})}^{2(j+1)}(U_E - U_{\alpha E})e^{-i\hat{q}_m x}\,dx\right\} = 0.$$

Note that after integration the only nonzero terms from the first integral are $E_m F_m$ and $\hat{E}_m \hat{F}_m$. For $m = 0$ we find that

$$-E_0 F_0 - \hat{E}_0(t)\,\hat{F}_0 + P^{3/2}\left[-(\hat{\eta}+\hat{\delta})\,U_{\alpha E} + \hat{\rho}\,U_{\beta E}\right] = 0$$

and for $m \neq 0$ we find that

$$-E_m F_m - \hat{E}_m(t)\,\hat{F}_m + P^{3/2}\left[\frac{\left(e^{-i\hat{q}_m 2\hat{\eta}} - e^{i\hat{q}_m 2\hat{\delta}}\right)}{-2i\hat{q}_m}\right] = 0.$$

After making the appropriate substitutions for $\hat{\eta}$, $\hat{\rho}$ and $\hat{\delta}$ in the previous equations and using expansions where necessary, we may write the Fourier coefficients, $\hat{E}_n$, for $N = 1$, as shown in Chap. 3. In addition, this method allows us to double check the Fourier coefficients, E_n.

Likewise for $N = 2$ [with $\hat{q}_m = (m\pi)/2$]: we write

$$\frac{1}{4}\int_{2j}^{2(j+2)}\left[\sum_{n=-\infty}^{\infty} E_n F_n\, e^{iqnx}\, e^{-i\hat{q}mx} + \sum_{n=-\infty}^{\infty} \hat{E}_n \hat{F}_n\, e^{i\hat{q}nx}\, e^{-i\hat{q}mx}\right] dx$$

$$+\frac{P^{3/2}}{4}\left\{\int_{2j}^{2(j+\hat{\eta})}(U_E - U_{\alpha E})e^{-i\hat{q}mx}\,dx + \int_{2(j+\hat{\eta})}^{2(j+\hat{\eta}+\hat{\rho})}(U_E - U_{\beta E})e^{-i\hat{q}mx}\,dx\right.$$

$$+\int_{2(j+1-\hat{\delta})}^{2(j+1+\hat{\eta})}(U_E - U_{\alpha E})e^{-i\hat{q}mx}\,dx + \int_{2(j+1+\hat{\eta})}^{2(j+1+\hat{\eta}+\hat{\rho})}(U_E - U_{\beta E})e^{-i\hat{q}mx}\,dx$$

$$\left.+\int_{2(j+2-\hat{\delta})}^{2(j+2)}(U_E - U_{\alpha E})e^{-i\hat{q}mx}\,dx\right\} = 0.$$

The nonzero terms of the first integral are $\hat{E}_m\hat{F}_m$ if m is odd and $E_{m/2}F_{m/2}$ and $\hat{E}_m\hat{F}_m$ if m is even. For $m = 0$ we find that

$$-E_0F_0 - \hat{E}_0(t)\,\hat{F}_0 + P^{3/2}\left[-(\hat{\eta}+\hat{\delta})\,U_{\alpha E} + \hat{\rho}\,U_{\beta E}\right] = 0$$

and for $m \neq 0$ we find that

$$P^{3/2}\left[\frac{(U_{\beta E} - U_{\alpha E})}{2\hat{q}m}\right]\left[e^{-2i\hat{q}mj}\sin(2\hat{q}m\hat{\eta}) + e^{-2i\hat{q}m(j+1)}\sin(2\hat{q}m\hat{\delta})\right]$$

$$= \begin{cases} E_{m/2}F_{m/2} + \hat{E}_m\hat{F}_m & \text{for even } m \\ \hat{E}_m\hat{F}_m & \text{for even } m. \end{cases}$$

As in the $N = 1$ case, after making the appropriate substitutions for $\hat{\eta}$, $\hat{\rho}$ and $\hat{\delta}$ in the previous equations and using expansions where necessary, we may write the Fourier coefficients, $\hat{E}_n$, for $N = 2$, as shown in Chap. 3.

Note 3: Donaghey and Tiller model

Just as the Datye and Langer [8] (DL) model differs from the JH model [7] in the conservation of mass boundary condition, Eq. (3.2), the Donaghey and Tiller [9] (DT) model differs from the JH model and the DL model in the same boundary condition. They use the boundary condition as it is written in Eq. (3.2) so that

$$\Delta U_i = \begin{cases} U_i - U_{\alpha E} - k_\alpha U_i & \text{in the } \alpha \text{ phase} \\ U_i - U_{\beta E} - k_\beta U_i & \text{in the } \beta \text{ phase} \end{cases}$$

where $k_\alpha \equiv m_\alpha^{liq}/m_\alpha^{solid}$ and $k_\beta \equiv m_\beta^{liq}/m_\beta^{solid}$. Note that k_α and k_β are in general different from k_1 and k_2 where $C_{\alpha E} = k_1 C_E$ and $(1 - C_{\beta E}) = k_2 (1 - C_E)$ (see Fig. 3.2). To find the Fourier coefficients, E_n, for the DT model, we let

$$\Delta U_i = g(x) U_i + f(x)$$

where $f(x)$ is as in note 1 of this appendix and

$$g(x) = \sum_{n=-\infty}^{\infty} c_n e^{iq_n x} = \begin{cases} 1 - k_\alpha & \text{in the } \alpha \text{ phase} \\ 1 - k_\beta & \text{in the } \beta \text{ phase} \end{cases}$$

with

$$\begin{aligned} c_0 &= 1 - \bar{k}, \\ \bar{k} &= 2\eta k_\alpha + \rho k_\beta, \\ c_n &= \Delta k \frac{\sin 2n\pi\eta}{n\pi} \quad \text{for } n \neq 0 \end{aligned}$$

and

$$\Delta k = k_\beta - k_\alpha.$$

Because ΔU_i contains a term of the form $g(x) U_i$, a double sum results when we substitutes Eq. (3.4) into Eq. (3.2). Thus we write E_n as

$$E_n = A_n + \sum_{m=-\infty}^{\infty} B_{n,m}\, E_m$$

where

$$A_n = P^{3/2}\left(\frac{b_n + U_\infty\, c_n}{F_n}\right),$$

$$B_{n,m} = P^{3/2}\left(\frac{c_{n-m}}{F_n}\right)$$

and

$$F_n = P^{1/2}\,|n\pi| + O(P^{3/2}).$$

For $P << 1$, we find the Fourier coefficients, E_n, from the above equations such that

$$E_0 = \left[\frac{(\tau + U_\infty)}{\bar{k}} - U_\infty\right] + P\,\frac{\Delta k}{\bar{k}}\,Q(\eta) + O(P^2)$$

and

$$E_n = \frac{P\,\sin(2n\pi\eta)}{|n\pi|\,n\pi}\left[1 + (\tau + U_\infty)\frac{\Delta k}{\bar{k}}\right] + O(P^2) \quad \text{for } n \neq 0 \text{ and } |\bar{k}| < 1.$$

If the conservation condition is satisfied, i.e., $\tau + U_\infty = 0$, and $P << 1$ then the DT model [9] agrees, at least to order P^2, with the JH model [7] and the DL model [8] for $n \neq 0$; however, the expressions for E_0 differ.

Note 4: The Fourier coefficients $\hat{E}_n$ for the DL and DT models

The Fourier coefficients resulting from the DL [8] and DT [9] models can be found as before. For the DL model with $N = 1$,

$$\hat{E}_0(t) = -\left[\frac{P^{3/2}}{\hat{F}_0 - P^{3/2}}\right]\,\hat{x}\,e^{i\sigma 2(j+\eta)+\omega t}$$

and for $n \neq 0$,

$$\hat{E}_n(t) = -\left[\frac{P^{3/2}}{\hat{F}_n - P^{3/2}}\right]\cos(2n\pi\eta)\,\hat{x}\,e^{i\sigma 2(j+\eta)+\omega t}.$$

For the DL model with $N = 2$,

$$\hat{E}_n(t) = 0 \quad \text{when } n \text{ is even}$$

and

$$\hat{E}_n(t) = P^{3/2} \left[\frac{(-1)^{j+1}}{\hat{F}_n - P^{3/2}} \right] \cos(n\pi\eta)\, \hat{x}\, e^{i\sigma 2(j+\eta)+\omega t} \quad \text{when } n \text{ is odd.}$$

For the DT model with $N = 1$,

$$\hat{E}_0(t) = -P \left\{ \frac{\left[1 + (\tau + U_\infty)\Delta k\right]}{\sqrt{\omega}} \right\} \hat{x}\, e^{i\sigma 2(j+\eta)+\omega t} + O(P^2)$$

and for $n \neq 0$,

$$\hat{E}_n(t) = -P \left\{ \frac{\left[1 + (\tau + U_\infty)\Delta k\right]}{\sqrt{(n\pi)^2 + \omega}} \right\} \cos(2n\pi\eta)\, \hat{x}\, e^{i\sigma 2(j+\eta)+\omega t} + O(P^2).$$

Finally, for the DT model with $N = 2$,

$$\hat{E}_n(t) = 0, \quad \text{when } n \text{ is even}$$

and

$$\hat{E}_n(t) = (-1)^{j+1} P \left\{ \frac{\left[1 + (\tau + U_\infty)\Delta k\right]}{\sqrt{(n\pi/2)^2 + \omega}} \right\} \cos(n\pi\eta)\, \hat{x}\, e^{i\sigma 2(j+\eta)+\omega t} + O(P^2)$$

when n is odd. In the DT cases, here, it is has been assumed that $(n\pi/N)^2 + \omega \gg (P/2)^2$ for $N = 1, 2$; and for all n.

Note that if $\tau + U_\infty$ is taken to be zero and $P \ll 1$, the above Fourier coefficients agree, at least to order P^2, with those found by using the JH model [7]. Also note that the differences in E_0 have no effect on the Fourier coefficients for the perturbed system.

APPENDIX C: SAMPLE RUNS AND THE FORTRAN PROGRAM FOR THE RANDOM WALK SIMULATIONS

The Fortran program presented in this appendix is used to carry out the simulations of Chap. 6. The program can be run using a batchjob command (BAT=1) or it can be run interactively (BAT=0). Either way, 'PROGRAM simulation' needs the following data to run: P, 2η, the number of grid sites in the z-direction (H), the number of grid sites in the x-direction (W), the number of times to sweep the interface (N), and a decision of whether to use a new or recorded interface. In addition, one must set CRYSTAL to the appropriate value to select the desired eutectic system. Data for the different systems (CBR_4-C_2Cl_6 or Al-Al_2Cu) is contained in the program. The data includes information about the following: C_E, $C_{\alpha E}$, $C_{\beta E}$, density for the alpha and beta phases, m_α, m_β, ΔC, ΔT, D, $\lambda^2 V$, Γ_α, Γ_β, σ_α, σ_β and $\sigma_{\alpha\beta}$ (see Chap. 6 and 'PROGRAM simulation').

Example of an interactive run

The following is an example of an interactive run of the program using a DEC-Station 5000 and ULTRIX 4.3 at Iowa State University.

```
vincent% f77 -o sim simulation.f -lnag
vincent% sim

new interface (o=no, 1=yes)
1
enter number of times to repeat
40000
```

```
crystal= 1
(AL crystal=1, CBr crystal=0)
uinfinity = 0.128507747998513
volume fraction of alpha phase= 0.400000005960464
W = 100
H = 500
DLP = 2.6800000000000000E-04
P = 6.700000000000000E-03
a count = 12.3789114194237
b count = -9.06108858057631
K= 5000
K= 10000
K= 15000
K= 20000
K= 25000
K= 30000
K= 35000
K= 40000
```

When the run is complete, the following will appear on the screen:

```
# of repeats = 40000
more (o=no, 1=yes)
```

At this time the simulation may be continued (1) or stopped (0). Information concerning the grid, flux values and the random number generator is contained in the files grid1.dat and flux1.dat. These files are updated periodically while the program is running so that a run can be continued from this data at a later time. The information needed to plot the growth of the eutectic crystal is contained in the files crys1.m, edge1.m and trippoints1.m and the plots are done using the command 'plotpoints1' in MATLAB.

Example of a run using a batchjob

A batchjob is used to run the program for an extended period of time. This allows the simulation to run while one is logged out or while one is seeing to other

tasks. The CPU time and the maxticket life for the computer must be set at the appropriate values. To run a batchjob set the following in 'PROGRAM simulation':

```
BAT= 1
REPLY= 0 (if you want to start with a new interface) or 1 (if you
        want to continue with a stored interface)
N= 40000 (number of times to sweep across the interface)
```

The following is an example of a run of the program, using the batchjob command, using a DECStation 5000 and ULTRIX 4.3 at Iowa State University.

```
vincent% add nag
vincent% add public
vincent% f77 -o sim simulation.f -lnag
vincent% batchjob -m 'sim < crys1.m edge1.m trippoints1.m
grid1.dat flux1.dat'
batchjob:  group PID of batch processes is 1605
batchjob:  to kill this job, enter the command 'batchjob -k 1605'
batchjob:  batch process log file will be written to
batch_254174944.log
vincent%
```

When the job is complete, a mail message is sent and the needed information is contained in the log file and the data files mentioned previously. An example of a log file after completion of a run is as follows:

```
To kill this job, issue the command 'batchjob -k 1605' on
pv3401.vincent.iastate.edu
Batchjob (0.3) Command: batchjob sim < crys1.m edge1.m trippoints1.m
grid1.dat flux1.dat
Job start date: Sun Sep 11 17:49:49 CDT 1994

 crystal=         1
 (AL crystal=1, CBr crystal=0)
 uinfinity = 0.128507747998513
```

```
volume fraction of alpha phase =  0.400000005960464
W =          100
H =          500
DLP =  2.6800000000000000E-04
P =    6.700000000000000E-03
a count =   12.3789114194237
b count =  -9.06108858057631
K=         5000
K=        10000
K=        15000
K=        20000
K=        25000
K=        30000
K=        35000
K=        40000

 # of repeats =           40000
 more (0=no, 1=yes)
Batch Process Timing Info:
0.298u 0.630s 0:28.24 3.2% 0+0k 21+21io 0pf+0w
Job end date: Sun Sep 11 17:50:26 CDT 1994
Tickets destroyed.
```

The remainder of the appendix contains the Fortran program 'PROGRAM simulation' and the Matlab file plotpoints1.m.

PROGRAM simulation

```
      PROGRAM simulation

*     Brenda Diesslin
*     Revised: October, 1994
*     This program is used to simulate eutectic growth.

*************************************************************************
*     H : height of grid                                                *
*     W : width of grid                                                 *
*     BAT : integer used to run a batchjob                              *
*     REPLY : 0 for a previous interface; 1 for a new interface         *
*     RESPON : 0 for no more runs; 1 for continuing                     *
```

```
*     N : number of times across the interface for one run          *
*     DLP : x-direction grid size*Peclet number                     *
*     UINFIN : far-field concentration                              *
*     CRYSTAL : 0 for CBr-C2Cl6; 1 for Al-Al2Cu                     *
*     CEUT : eutectic concentration                                 *
*     CALPHAE : eutectic solid concentration for the alpha phase    *
*     CBETAE : eutectic solid concentration for the beta phase      *
*     DENSALPHA : density for the alpha phase                       *
*     DENSBETA : density for the beta phase                         *
*     DELTAC : miscibility gap                                      *
*     UALPHAE : nondimensional CALPHAE                              *
*     UBETAE : nondimensional CBETAE                                *
*     DENBAR : "average" density of the solid phases                *
*     ETA : 2*ETA is the volume fraction of the alpha phase         *
*     Z : two dimensional array for the grid; elements = 0 for      *
*         liquid, 1 for the alpha solid, and 2 for the beta solid   *
*     FL : two dimensional array containing the z position of the   *
*          solid and the flux value of the corresponding bond       *
*     U : one dimensional array containing interface concentrations *
*     I, J, K : counters                                            *
*     INCRE : amount to move interface up to form pattern           *
*     TEMPN : previous number of times across the interface         *
*     COUNTM, COUNTQM : functions for the values that the tallies   *
*             must reach to change solid to liquid and vice versa   *
*     SUM : temporary quantity                                      *
*     LAR : maximum of the absolute values of the concentrations    *
*     PPLUS : probability of an infinity walk occurring             *
*     TEMPU : temporary quantity                                    *
*     G05CBF, G05CAF : Nag subroutines to generate random numbers   *
*     R1 : random number                                            *
*     G05CFF, G05CGF : nag subroutines which store and retrieve     *
*                      data about the current random number         *
*     IA, XA : one dimemsional arrays for the Nag subroutines       *
*              G05CFF and G05CGF                                    *
*     IFAIL : integer for the Nag subroutines G05CFF and G05CGF     *
*********************************************************************

*************************** begin program ***************************

      REAL*8  DLP, UINFIN, CEUT, CALPHAE, CBETAE, DENSALPHA, P
```

```
      REAL*8  DENSBETA, DELTAC, UALPHAE, UBETAE, DENBAR, ETA
      REAL*8  U(200), INCRE, TEMPU
      REAL*8  COUNTM, COUNTQM, SUM,  LAR, PPLUS, G05CAF, R1, XA(4)
      INTEGER H, W, BAT, REPLY, RESPON, N, CRYSTAL
      INTEGER Z(200,700), FL(200,2), I, J, K
      INTEGER TEMPN, IA(9), IFAIL
      EXTERNAL COUNTM, COUNTQM, G05CAF, G05CBF, G05CFF, G05CGF

*     H and W are the number of grid sites in the x and z direction
      H=500
      W=100
*     ->BAT=1:running as a batchjob
      BAT=0
      IF (BAT .EQ. 0) THEN
         PRINT*
         PRINT*,'new interface (0=no, 1=yes)'
         READ*, REPLY
      ELSE
         REPLY=0
      END IF

      RESPON=0
10    N=0
      IF (BAT .EQ. 0) THEN
         WRITE(*,*) 'enter number of times to repeat'
         READ*, N
*         WRITE(*,*) 'enter P'
*         READ*, P
          P=0.0067
*         WRITE(*,*) 'enter eta'
*         READ*, ETA
          ETA=0.7/2
      ELSE
         N=90000
         P=0.0067
         ETA=0.8/2
      END IF
      DLP=4*P/W

*     ->to pick the CBr or the Al system
```

```
      CRYSTAL=1
*        ->CBr:CRYSTAL=0, Al:CRYSTAL=1
         IF (CRYSTAL .EQ. 0) THEN
            CEUT=0.084
            CALPHAE=0.0508
            CBETAE=0.1618
            DENSALPHA=3.09
            DENSBETA=2.75
         ELSE
            CEUT=0.327
            CALPHAE=0.0565
            CBETAE=0.525
            DENSALPHA=2.5
            DENSBETA=4
         END IF
         DELTAC=CBETAE-CALPHAE
         UALPHAE=(CALPHAE-CEUT)/DELTAC
         UBETAE=(CBETAE-CEUT)/DELTAC
         TEMPU=DENSALPHA*UALPHAE*2*ETA+DENSBETA*UBETAE*(1-2*ETA)
*        ->uinfin is the far-field concentration
         UINFIN=TEMPU/(DENSALPHA*2*ETA+DENSBETA*(1-2*ETA))

       IF (RESPON .EQ. 0) THEN
*        ->this is a new run
         CALL G05CBF(0)
         IF (REPLY .EQ. 1) THEN
*           ->initialize grid as a eutectic with volume fraction of
*            the alpha phase as 2*ETA
            CALL INITIALIZE (W,H,Z,FL,U,ETA)
*           ->record the new interface and open files
            CALL NEWINT(FL,W,Z)
            OPEN (UNIT=40, FILE='crys1.m', STATUS='OLD')
            OPEN (UNIT=30, FILE='edge1.m', STATUS='OLD')
            OPEN (UNIT=25, FILE='trippoints1.m', STATUS='OLD')
            OPEN (UNIT=20, FILE='flux1.dat', STATUS='OLD')
            CLOSE (UNIT=40, STATUS='DELETE')
            CLOSE (UNIT=30, STATUS='DELETE')
            CLOSE (UNIT=25, STATUS='DELETE')
            CLOSE (UNIT=20, STATUS='DELETE')
            OPEN (UNIT=40, FILE='crys1.m', STATUS='NEW')
```

```
            OPEN (UNIT=30, FILE='edge1.m', STATUS='NEW')
            OPEN (UNIT=25, FILE='trippoints1.m', STATUS='NEW')
            OPEN (UNIT=20, FILE='flux1.dat', STATUS='NEW')
            OPEN (UNIT=35, FILE='grid1.dat', STATUS='OLD')
            OPEN (UNIT=45, FILE='curve1.dat', STATUS='OLD')
            REWIND 35
            WRITE (35,95) ((Z(I,J), J=1,300), I=1,W)
95          FORMAT (300I2)
            INCRE=0
            TEMPN=0
            CALL EDGE (INCRE,FL,W)
            CALL BOUNDARY (W,Z)
         ELSE
            OPEN (UNIT=40, FILE='crys1.m', STATUS='OLD')
            OPEN (UNIT=30, FILE='edge1.m', STATUS='OLD')
            OPEN (UNIT=25, FILE='trippoints1.m', STATUS='OLD')
            OPEN (UNIT=20, FILE='flux1.dat', STATUS='OLD')
            OPEN (UNIT=35, FILE='grid1.dat', STATUS='OLD')
            OPEN (UNIT=45, FILE='curve1.dat', STATUS='OLD')
            READ (35,150) ((Z(I,J), J=1,300), I=1,W)
150         FORMAT (300I2)
            DO I=1,W
               DO J=301,H
                  Z(I,J)=0
               END DO
            END DO
*           ->obtaining information about the old interface and
*            the last random number used
            READ (20,35) INCRE,TEMPN,W,(IA(J), J=1,9),(XA(J), J=1,4)
35          FORMAT (1F8.2,2I15,9I8,4F30.13)
            IFAIL=0
            CALL G05CGF(IA,9,XA,4,IFAIL)
            READ (20,40) ((FL(I,J), J=1,2), I=1,W)
40          FORMAT(2I6)
*           ->find interface
            CALL NEWINT(FL,W,Z)
         END IF
      END IF

      PRINT*
```

```
      PRINT*,'crystal=', CRYSTAL
      PRINT*,'(Al crystal=1, CBr crystal=0)'
      PRINT*,'uinfinity=', UINFIN
      PRINT*,'volume fraction of alpha phase=', 2*ETA
      PRINT*,'W=', W
      PRINT*,'H=', H
      PRINT*,'DLP=', DLP
      PRINT*,'P=',P
      PRINT*,'a count=',COUNTM(DLP,CALPHAE,CEUT,DELTAC,KARMA)
      PRINT*,'b count=',COUNTQM(DLP,CBETAE,CEUT,DELTAC,KARMA)

*     ->repeat across the interface N times
      DO K=TEMPN+1,TEMPN+N
*        ->finding the concentration for each solid on the interface
         CALL CONCEN (Z,U,FL,W,CRYSTAL,P,K)
*        ->calculating the prob. of picking an infinity walk or an
*         interface walk
*        ->SUM is the average absolute value of U on the interface
*        ->LAR is the maximum of the absolute value of U
         SUM=0.0
         LAR=0.0
         DO I=1,W
            SUM=SUM+ABS(U(I))
            IF (ABS(U(I)) .GT. LAR) THEN
               LAR=ABS(U(I))
            END IF
         END DO
         SUM=SUM/W
*        ->SUM is compared with the absolute value of the far-field
*         concentration
         PPLUS=(ABS(UINFIN))/(ABS(UINFIN)+SUM)
*        ->for each solid on the interface generate a random number
*        and compare with PPLUS
         DO I=1,W
            R1=G05CAF()
            IF (PPLUS .GT. R1) THEN
*              -proceed with an infinity walk
               CALL INFINITY(W,H,DLP,FL,ETA)
            ELSE
*              -proceed with an interface walk
```

```
                CALL INTERFACE(I,U,H,DLP,W,FL,LAR,Z)
              END IF
            END DO
*           ->after the interface is swept over once, for each solid on
*            the interface, the fluxes are considered to determine if the
*            solid melts and for each liquid on the interface, the fluxes
*            are considered to determine if a solid forms
           CALL TALLY (FL,DLP,Z,CRYSTAL,W)
*           ->after changes are made to the interface according to TALLY
*            the new interface is recorded, smoothed out, and recorded
*            again
           CALL NEWINT (FL,W,Z)
           CALL CHECK(W,Z)
           CALL NEWINT (FL,W,Z)
*           ->after a given number of times the edge and triple points
*            are recorded and the increment in the z direction is
*            increased
           IF (MOD(K,300) .EQ. 0) THEN
              INCRE=INCRE+6
              CALL POINTS (INCRE,FL,Z,W)
           END IF
           IF (MOD(K,1000) .EQ. 0) THEN
*             ->record information about the last
*              random number used, record flux and Z information
              IFAIL=0
              CALL G05CFF(IA,9,XA,4,IFAIL)
              REWIND 20
              WRITE (20,125) INCRE,K,W,(IA(J), J=1,9),(XA(J), J=1,4)
125           FORMAT (1F8.2,2I15,9I8,4F30.13)
              WRITE (20,135) ((FL(I,J), J=1,2), I=1,W)
135           FORMAT(2I6)
              REWIND 35
              WRITE (35,145) ((Z(I,J), J=1,300), I=1,W)
145           FORMAT(300I2)
           END IF
           IF (MOD(K,5000) .EQ. 0) THEN
              PRINT*,'K=',K
              CALL EDGE (INCRE,FL,W)
           END IF
         END DO
```

```
*     ->add TEMPN to N, obtain and record information about the
*      last random number used, record flux and Z information
      TEMPN=TEMPN+N
      IFAIL=0
      CALL G05CFF(IA,9,XA,4,IFAIL)
      REWIND 20
      WRITE (20,75) INCRE,TEMPN,W,(IA(J), J=1,9),(XA(J), J=1,4)
75    FORMAT (1F8.2,2I15,9I8,4F30.13)
      WRITE (20,85) ((FL(I,J), J=1,2), I=1,W)
85    FORMAT(2I6)
      REWIND 35
      WRITE (35,105) ((Z(I,J), J=1,300), I=1,W)
105   FORMAT(300I2)
      PRINT*
      PRINT*,'# of repeats=', TEMPN
      PRINT*,'more (0=no, 1=yes)'
      IF (BAT .EQ. 0) THEN
         READ*, RESPON
         IF (RESPON .EQ. 1) GO TO 10
      END IF
      STOP
      END

************************ end of main program ************************

***************************** functions *****************************

*     ->COUNTM and COUNTQM are the values that the flux  must
*      reach to change solid to liquid and liquid to solid at
*      the interface

      FUNCTION COUNTM (DLP,CALPHAE,CEUT,DELTAC)
      REAL*8 COUNTM, DLP, CEUT, DELTAC, CALPHAE
      COUNTM=DLP*((CEUT-CALPHAE)/DELTAC)*80000
      RETURN
      END

      FUNCTION COUNTQM (DLP,CBETAE,CEUT,DELTAC)
      REAL*8 COUNTQM, DLP, CEUT, DELTAC, CBETAE
```

```
      COUNTQM=DLP*((CEUT-CBETAE)/DELTAC)*80000
      RETURN
      END

************* subroutine to initialize arrays and grid **************
*********************************************************************
*     M : number of grid sites = 2eta                               *
*     I, J, K : counters                                            *
*     T : number of grid sites = lambda                             *
*     PERT1, PERT2 : parameter used to perturbed the interface      *
*     L : parameter used to give the interface some initial         *
*         curvatue                                                  *
*********************************************************************

      SUBROUTINE INITIALIZE (W,H,Z,FL,U,ETA)
      REAL*8  U(200), ETA
      INTEGER  W, H, Z(200,700), FL(200,2)
      INTEGER  PERT1, PERT2, M, I, J, K, T, L

*     ->M is the number of grid sites across for 1/2 an alpha phase
      M=NINT(ETA*W/2)
*     ->to seed different from uinfin
*      M=NINT(.54/2*W/2)
*     ->T is the number of grid sites across = lambda
      T=INT(REAL(W)/2)
*     ->PERT1 AND PERT2 are additional perturbations added
*      (PERT1=PERT2 for the acoustic mode and PERT1=-PERT2 for
*       the optical mode)
      PERT1=0
      PERT2=0
*     ->initialize Z array: contains a picture of the crystal with
*      1 being alpha solid, 2 being beta solid and 0 being liquid
*     ->1/2 alpha, beta, alpha, beta and then another 1/2 alpha
*      with volume fraction based on 2eta
      DO J=1,40
         DO I=1,M+PERT1
            Z(I,J)=1
         END DO
         DO I=M+PERT1+1,T-M+PERT2
            Z(I,J)=2
```

```
            END DO
            DO I=T-M+PERT2+1,T+M-PERT2
               Z(I,J)=1
            END DO
            DO I=T+M-PERT2+1,W-M-PERT1
               Z(I,J)=2
            END DO
            DO I=W-M-PERT1+1,W
               Z(I,J)=1
            END DO
         END DO
         DO I=1,W
            DO J=41,H
               Z(I,J)=0
            END DO
*           ->initialize concentration and flux array
            U(I)=0.0
            DO J=1,2
               FL(I,J)=0
            END DO
         END DO
*        ->adding in some initial curvature to the phases
         L=NINT(REAL(M)/3)
         DO K=1,L
            J=40+K
            DO I=1,M+PERT1-2*K
               Z(I,J)=1
            END DO
            DO I=M+PERT1+1+2*K,T-M+PERT2-2*K
               Z(I,J)=2
            END DO
            DO I=T-M+PERT2+1+2*K,T+M-PERT2-2*K
               Z(I,J)=1
            END DO
            DO I=T+M-PERT2+1+2*K,W-M-PERT1-2*K
               Z(I,J)=2
            END DO
            DO I=W-M-PERT1+1+2*K,W
               Z(I,J)=1
            END DO
```

```
      END DO
      RETURN
      END

********** subroutine to find and record the interface **********
*************************************************************************
*     K, N : temporary quantities                                       *
*     OLDFL : temporary array                                           *
*     I, J : counters                                                   *
*     LOWER, UPPER : bounds                                             *
*************************************************************************

      SUBROUTINE NEWINT(FL,W,Z)
      INTEGER FL(200,2), W, Z(200,700)
      INTEGER OLDFL(200,2), K, N, I, J, LOWER, UPPER

      DO J=1,W
         DO I=1,2
            OLDFL(J,I)=FL(J,I)
         END DO
      END DO
*     ->going across the grid
      DO I=1,W
*        ->if statements are here to deal with the periodicity
         IF (I .EQ. 1) THEN
            K=W
         ELSE
            K=I-1
         END IF
         IF (I .EQ. W) THEN
            N=1
         ELSE
            N=I+1
         END IF
*        ->for a fixed x position, check the z positions to see if
*         the z value is not 0, indicating solid
*        ->set some lower and upper bounds for checking the z
*         array containing the picture of the crystal as 0's, 1's,
*         or 2's so that the region for checking is limited
         LOWER=2
```

```
          UPPER=300
          DO J=LOWER,UPPER
             IF (Z(I,J) .NE. 0 .AND. Z(I,J+1) .EQ. 0) then
*               ->Z(I,J) is solid with liquid above
                   FL(I,1)=J
                   J=UPPER
             END IF
          END DO
       END DO

       DO I=1,W
*         ->set the new flux values to 0
          FL(I,2)=0
       END DO
*         ->Go through the old bond positions and see if they match
*          the new bond positions. If yes, record old flux value as
*          new flux value so that the new bonds have a flux of 0
*          and the old bonds retain their flux values
          DO J=1,W
             IF (FL(J,1) .EQ. OLDFL(J,1)) THEN
                 FL(J,2)=OLDFL(J,2)
             END IF
          END DO
       RETURN
       END

***************** subroutine to store interface edge ****************
*     I : counter                                                     *
***********************************************************************

       SUBROUTINE EDGE (INCRE,FL,W)
       REAL*8 INCRE
       INTEGER FL(200,2), W, I

       DO I= 1,W
          WRITE (30,110) REAL(I), REAL(FL(I,1))+INCRE
110       FORMAT (2F8.2)
       END DO
       RETURN
       END
```

```
*************** subroutine to store initial crystal ***************
*     I, J : counters                                             *
*     T : temporary quantity                                      *
*****************************************************************

      SUBROUTINE BOUNDARY (W,Z)
      INTEGER W, Z(200,700), I, J, T

      DO I=1,W
         DO J=1,40
*           ->periodicity conditions
            IF (I .EQ. W) THEN
               T=1
            ELSE
               T=I+1
            END IF
            IF (Z(I,J) .NE. Z(T,J)) THEN
               WRITE (40,140) I,J,T,J
140            FORMAT (4I6)
            END IF
         END DO
      END DO
      RETURN
      END

******* subroutine to calulate concentration at the interface *******
*****************************************************************
*     SLALPHA, SLBETA : absolute value of the slopes of the       *
*               liquidus lines of the phase diagram               *
*     DELTAC : miscibility gap                                    *
*     DELTT : change in temperature                               *
*     GGA, GGB : gamma                                            *
*     L2V : lambda squared times velocity/100                     *
*     DIFF : diffusion coefficient                                *
*     AALPH, ABET, ALPHBET : surface tensions                     *
*     I : counter                                                 *
*     NL, NA, NB : number of liquid, solid alpha, and solid beta  *
*         sites inside a circle around an interface site          *
*     UALPHA, UBETA : temporary quantities                        *
```

```
*     OMEGALP, OMEGBET : parameters                                    *
**********************************************************************

      SUBROUTINE CONCEN(Z,U,FL,W,CRYSTAL,P,K)
      REAL*8  U(200), SLALPHA, SLBETA, DELTAC, TE, DELTT, GGA, P
      REAL*8  GGB, AALPH, ABET, ALPHBET, NL, NA, NB,  UALPHA, UBETA
      REAL*8  L2V, OMEGALPH, OMEGBET, DIFF
      INTEGER  Z(200,700), FL(200,2), W, CRYSTAL, I, K

*        ->CBr:CRYSTAL=0, Al:CRYSTAL=1
         IF (CRYSTAL .EQ. 0) THEN
            SLALPHA=1.48
            SLBETA=2.16
            DELTAC=11.1
            DELTT=37.*(SQRT(0.0105))*P
            GGA=(0.8)*(83./95.)
            GGB=(1.14)
            L2V=3.8
            DIFF=1.0
            AALPH=.6328715
            ABET=0.5516889
            ALPHBET=1
         ELSE
            SLALPHA=4.6
            SLBETA=3.8
            DELTAC=46.85
            DELTT=93.*(SQRT(0.3289))*P
            GGA=(2.4)*(548.2/660.32)
            GGB=(0.55)
            L2V=1.03
            DIFF=2.91
            AALPH=.662309
            ABET=0.4879975
            ALPHBET=1
          END IF
       OMEGALP=(4*GGA*DIFF)/(SLALPHA*DELTAC*L2V)
       OMEGBET=(4*GGB*DIFF)/(SLBETA*DELTAC*L2V)

*      ->for each solid on the interface, calculate U
       DO I=1,W
```

```
*        ->NL, NA, and NB  are the number of liquid, alpha solid
*         and beta solid "near" the interface particle being
*         considered.  These values are initialized to 0 and are
*         calculated in the NUMBERS subroutine and used to
*         calculate the curvature effects
         NL=0.0
         NA=0.0
         NB=0.0
         CALL NUMBERS(I,FL(I,1),W,Z,NL,NA,NB,FL)
        IF (MOD(K,10000) .EQ. 0) THEN
              WRITE (45,240) k,NA,NB,(NL-NA),(NL-NB)
240           FORMAT (1I6,4F10.4)
              end if
         IF (Z(I,FL(I,1)) .EQ. 1) THEN
*           ->calculate U for an alpha solid
            UALPHA=P*OMEGALP*(-(NL-NA)+NB*(ABET-ALPHBET)/AALPH)
            U(I)=(DELTT)/(DELTAC*SLALPHA)+UALPHA
         ELSE
*           ->calculate U for a beta solid
            UBETA=P*OMEGBET*(-(NL-NB)+NA*(AALPH-ALPHBET)/ABET)
            U(I)=-1*(DELTT/(DELTAC*SLBETA)+UBETA)
         END IF
      END DO
      RETURN
      END

**********************************************************************
************* subroutine to calculate curvature numbers *************
*     I, J, K : counters                                             *
*     V, L : temporary quantities                                    *
*     N : total number of sites in a circle (=NL+NA+NB)              *
**********************************************************************

      SUBROUTINE NUMBERS(X,Y,W,Z,NL,NA,NB,FL)
      REAL*8 NL, NA, NB, N, TEMP
      INTEGER X, Y, W, Z(200,700), I, D, V, L, K, FL(200,2)
      INTEGER TEMP1

*     ->each site in a circle of radius L is checked to see if it
*      is alpha solid (Z=1), beta solid (Z=2), or liquid (Z=0)
```

```
      L=NINT(W/24.)
      DO I=X-L,X+L
*        ->if statement is for periodicity conditions
            IF (I .LE. 0) THEN
               V=W+I
            ELSE IF (I .GT. W) THEN
               V=I-W
            ELSE
               V=I
            END IF

            TEMP1=0
               IF (Y .EQ. FL(V,1)) THEN
                  TEMP1=1
               END IF
            IF (TEMP1 .EQ. 0) THEN
*              ->if the site is not on the boundary, check to see
*               if it is a alpha solid, beta solid, or liquid site
                 IF (Z(V,Y) .EQ. 1) THEN
*                   ->if site is alpha solid, increase NA
                    NA=NA+1
                 ELSE IF (Z(V,Y) .EQ. 2) THEN
*                   ->if site is beta solid, increase NB
                    NB=NB+1
                 ELSE
*                   ->if site is liquid, increase NL
                    NL=NL+1
                 END IF
            END IF
      END DO
      DO I=Y-L,Y+L
         TEMP1=0
               IF (I .EQ. FL(X,1)) THEN
                  TEMP1=1
               END IF
            IF (TEMP1 .EQ. 0) THEN
*              ->if the site is not on the boundary, check to see
*               if it is a alpha solid, beta solid, or liquid site
                 IF (Z(X,I) .EQ. 1) THEN
*                   ->if site is alpha solid, increase NA
```

```
                  NA=NA+1
                ELSE IF (Z(X,I) .EQ. 2) THEN
*                  ->if site is beta solid, increase NB
                  NB=NB+1
                ELSE
*                  ->if site is liquid, increase NL
                  NL=NL+1
                END IF
            END IF
         END DO
         DO D=1,L
            TEMP=D/L
            DO I=1,NINT(L*COS(ATAN(TEMP)))
*           ->if statement is for periodicity conditions
               IF (X+I .GT. W) THEN
                  V=X+I-W
               ELSE
                  V=X+I
               END IF
               TEMP1=0
                  IF (Y+D .EQ. FL(V,1)) THEN
                     TEMP1=1
                  END IF
                  IF (TEMP1 .EQ. 0) THEN
*                 ->if the site is not on the boundary, check to see
*                  if it is a alpha solid, beta solid, or liquid site
                    IF (Z(V,Y+D) .EQ. 1) THEN
*                      ->if site is alpha solid, increase NA
                      NA=NA+1
                    ELSE IF (Z(V,Y+D) .EQ. 2) THEN
*                      ->if site is beta solid, increase NB
                      NB=NB+1
                    ELSE
*                      ->if site is liquid, increase NL
                      NL=NL+1
                    END IF
                  END IF
               TEMP1=0
                  IF (Y-D .EQ. FL(V,1)) THEN
                     TEMP1=1
```

```
                END IF
                IF (TEMP1 .EQ. 0) THEN
*               ->if the site is not on the boundary, check to see
*                if it is a alpha solid, beta solid, or liquid site
                  IF (Z(V,Y-D) .EQ. 1) THEN
*                    ->if site is alpha solid, increase NA
                     NA=NA+1
                  ELSE IF (Z(V,Y-D) .EQ. 2) THEN
*                    ->if site is beta solid, increase NB
                     NB=NB+1
                  ELSE
*                    ->if site is liquid, increase NL
                     NL=NL+1
                  END IF
               END IF
             IF (X-I .LE. 0) THEN
               V=X+W-I
             ELSE
               V=X-I
             END IF
             TEMP1=0
               IF (Y+D .EQ. FL(V,1)) THEN
                  TEMP1=1
               END IF
             IF (TEMP1 .EQ. 0) THEN
*               ->if the site is not on the boundary, check to see
*                if it is a alpha solid, beta solid, or liquid site
                  IF (Z(V,Y+D) .EQ. 1) THEN
*                    ->if site is alpha solid, increase NA
                     NA=NA+1
                  ELSE IF (Z(V,Y+D) .EQ. 2) THEN
*                    ->if site is beta solid, increase NB
                     NB=NB+1
                  ELSE
*                    ->if site is liquid, increase NL
                     NL=NL+1
                  END IF
             END IF
             TEMP1=0
               IF (Y-D .EQ. FL(V,1)) THEN
```

```
                  TEMP1=1
               END IF
            IF (TEMP1 .EQ. 0) THEN
                  IF (Z(V,Y-D) .EQ. 1) THEN
*                    ->if site is alpha solid, increase NA
                     NA=NA+1
                  ELSE IF (Z(V,Y-D) .EQ. 2) THEN
*                    ->if site is beta solid, increase NB
                     NB=NB+1
                  ELSE
*                    ->if site is liquid, increase NL
                     NL=NL+1
                  END IF
               END IF
            END DO
            END DO
*     ->normalize number of alpha solid, beta solid, and liquid
*      sites
       N=NL+NA+NB
       NL=NL/N
       NA=NA/N
       NB=NB/N
       RETURN
       END

****************** subroutine for infinity walk ********************
************************************************************************
*     R2 : random number                                               *
*     X, Y : coordinates of the walker                                 *
*     J : counter                                                      *
*     TEMP : temporay quantity; =1 if walker has hit the interface     *
************************************************************************

      SUBROUTINE INFINITY (W,H,DLP,FL,ETA)

      REAL*8  R2, G05CAF, DLP, ETA
      INTEGER W, H, FL(200,2)
      INTEGER X, Y, TEMP, J
      EXTERNAL G05CAF
```

```
*     ->randomly determining the x position of the infinity walker
      R2=G05CAF()
      X=INT(R2*W+1)
      Y=H
      CALL WALK (X,Y,DLP)
*     ->checking to see if the walker hit the interface
*     ->the array FL contains the placement of the solid interface
*      particles with FL(x,1)=the z value
      TEMP=0
100     IF (Y-1 .EQ. FL(X,1)) THEN
*           ->walker hit the interface and FLUX1 is called to
*            change the count for the bonds where the walker "hit"
            TEMP=1
            CALL FLUX1(X,FL,ETA,W)
          END IF
*     ->if walker has not hit the interface or gone out the top
*      then another walk occurs
      IF (TEMP .NE. 1 .AND. Y .NE. H+1) THEN
         CALL WALK(X,Y,DLP)
*        ->periodic conditions
         IF (X .EQ. W+1) X=1
         IF (X .EQ. 0) X=W
*        ->repeat by checking if the walker hit the interface,
*         went out the top, or should walk again
         GO TO 100
      END IF
      RETURN
      END

****************** subroutine to walk in the liquid *****************
*************************************************************************
*     R5 : random number                                                *
*     X, Y : coordinates of walkers position                            *
*************************************************************************

      SUBROUTINE WALK(X,Y,DLP)
      REAL*8  DLP, R5, G05CAF
      INTEGER  X, Y
      EXTERNAL G05CAF
```

```
      R5=G05CAF()
         IF (R5 .LE. 0.25) THEN
*           ->move right
            X=X+1
         ELSE IF (R5 .LE. 0.5) THEN
*           ->move left
            X=X-1
         ELSE IF (R5 .LE. 0.75) THEN
*          ->move up
           Y=Y+1
         ELSE
*          ->move down
           Y=Y-1
         END IF
      RETURN
      END

********** subroutine to add flux for an infinity walker **********
*************************************************************************
*     R : random number                                                 *
*************************************************************************

      SUBROUTINE FLUX1 (X,FL,ETA,W)
      REAL*8  ETA, R, G05CAF
      INTEGER  X, FL(200,2), W
      EXTERNAL G05CAF

*     ->the flux value (recorded in Fl(_,2)) where the walker hit
*      the interface is increased by one if the fraction of alpha
*      phase(2eta) is > a random number and decreased by one
*      otherwise
      R=G05CAF()
      IF (2*eta .GT. R) THEN
         FL(X,2)=FL(X,2)+1
      ELSE
         FL(X,2)=FL(X,2)-1
      END IF
      RETURN
      END
```

```
****************** subroutine for interface walk ******************
*************************************************************************
*     X, Y : position of the Ith interface particle                     *
*     Q : probability of an interface walker being released             *
*     R4 : random number                                                *
*     TEMP : temporary quantity; =1 if walker hits the interface        *
*************************************************************************

      SUBROUTINE INTERFACE (I,U,H,DLP,W,FL,LAR,Z)
      REAL*8  U(200), DLP, LAR, Q, R4, G05CAF
      INTEGER  I, H, W, FL(200,2)
      INTEGER  X, Y, TEMP, TEMP2, Z(200,700)
      EXTERNAL G05CAF

       TEMP2=0
*      ->(X,Y) is the position of the Ith solid interface particle
*       where I is sent from the main program
       X=I
       Y=FL(I,1)
*      ->Q is associated with the probability of actually walking
*       from the interface
       Q=ABS(U(I))/LAR
       R4=G05CAF()
       TEMP=0
*      ->if Q is large then a walker has a high probability of
*       being released from the interface, else the walker stays
*       put and the next interface particle is considered
       IF (Q .GT. R4) THEN
*         ->to initially walk from the interface
          IF (Z(X,Y+1) .EQ. 0) THEN
             X=X
             Y=Y+1
             CALL WALK (X,Y,DLP)
*            ->periodic conditions
             IF (X .EQ. W+1) X=1
             IF (X .EQ. 0) X=W
             IF (Y .EQ. FL(X,1)) TEMP2=1
           IF (TEMP2 .EQ. 0) THEN
*         ->If statement and do loop to see if the interface has
*          been hit after a walk.  If yes, the flux values where
```

```
*          the walker left the interface and hit the interface
*          are changed by the subroutine FLUX2.
200       IF (Y-1 .EQ. FL(X,1)) THEN
               TEMP=1
               CALL FLUX2 (I,FL,X,W,U)
             END IF
*         ->if no hit occurs then check if the walker has gone out
*         the top
            IF (TEMP .EQ. 0 .AND. Y .NE. H+1) THEN
*            ->if no hit nor out the top, continue walking
             CALL WALK (X,Y,DLP)
*            ->periodic conditions
             IF (X .EQ. W+1) X=1
             IF (X .EQ. 0) X=W
*            ->repeat by checking if the walker hit the interface,
*             went out the top, or should walk again
             GO TO 200
            END IF
           END IF
          END IF
        END IF
        RETURN
        END

************ subroutine to add flux for an interface walk ***********
*****************************************************************
*     T : temporary quantities                                  *
*****************************************************************

        SUBROUTINE FLUX2(I,FL,X,W,U)
        REAL*8  U(200)
        INTEGER  I, FL(200,2), X, W, T

        IF (U(I) .LT. 0) THEN
*       ->the walker is from the beta phase
           T=-1
        ELSE
*       ->the walker is from the alpha phase
           T=1
        END IF
```

```
*     ->change flux values where walker hit and left
*     ->hit
      FL(X,5)=FL(X,5)-T
*     ->leave
      FL(I,5)=FL(I,5)+T
      RETURN
      END

************************ subroutine to tally ************************
*********************************************************************
*     COUNTM, COUNTQM, CEUT, DELTAC, CALPHAE, CBETAE : (see main    *
*             program)                                              *
*     I : counter                                                   *
*     SUM1, SUM2, TEMP1, TEMP2, L, T : temporary quantities         *
*********************************************************************

      SUBROUTINE TALLY(FL,DLP,Z,CRYSTAL,W)
      REAL*8   DLP, COUNTM, COUNTQM, CEUT, DELTAC, CALPHAE, CBETAE
      INTEGER  FL(200,2), Z(200,700)
      INTEGER  CRYSTAL, W
      INTEGER  SUM1, SUM2, TEMP1, TEMP2, T, L, I
      EXTERNAL COUNTM, COUNTQM

*        ->CBr:CRYSTAL=0, Al:CRYSTAL=1
         IF (CRYSTAL .EQ. 0) THEN
            CALPHAE=5.08
            CBETAE=16.18
            CEUT=8.4
            DELTAC=11.1
         ELSE
            CALPHAE=5.65
            CBETAE=52.5
            CEUT=32.7
            DELTAC=46.85
         END IF

*     ->to solidify liquid on the interface, consider the flux
      DO I=1,W
         TEMP1=0
         TEMP2=0
```

```
*          ->periodicity conditions
           IF (I .EQ. 1) THEN
              L=W
           ELSE
              L=I-1
           END IF
           IF (I .EQ. W) THEN
              T=1
           ELSE
              T=I+1
           END IF
*          ->check for alpha bonded to liquid
           IF (Z(T,FL(I,1)+1) .EQ. 1 .OR. Z(I,FL(I,1)+2) .EQ. 1
     +        .OR. Z(L,FL(I,1)+1) .EQ. 1 .OR.
     +         Z(I,FL(I,1)) .EQ. 1) THEN
               TEMP1=1
           END IF
*          ->check for beta bonded to liquid
           IF (Z(T,FL(I,1)+1) .EQ. 2 .OR. Z(I,FL(I,1)+2) .EQ. 2
     +        .OR. Z(L,FL(I,1)+1) .EQ. 2 .OR.
     +        Z(I,FL(I,1)) .EQ. 2) THEN
              TEMP2=1
           END IF
*          ->to solidify as alpha the liquid interface particle
*           must already be bonded to an alpha solid (temp1=1) and
*           the flux must be at least COUNTM
           IF (TEMP1 .EQ. 1 .AND. FL(I,2) .GE.
     +        COUNTM(DLP,CALPHAE,CEUT,DELTAC,KARMA)) THEN
              Z(I,FL(I,1)+1)=1
           END IF
*          ->to solidify as beta the liquid interface particle
*           must already be bonded to an beta solid (temp2=1) and
*           the flux must be less than COUNTQM (a negative number)
           IF (TEMP2 .EQ. 1 .AND. FL(I,2) .LE.
     +        COUNTQM(DLP,CBETAE,CEUT,DELTAC,KARMA)) THEN
              Z(I,FL(I,1)+1)=2
           END IF
         END DO

*        ->to melt solid on the interface, consider the flux
```

```
      DO I=1,W
*         ->for melting, if the solid is alpha then the flux is
*          compared with -COUNTM and if the solid is beta then the
*          flux is compared with -COUNTQM
        IF (Z(I,FL(I,1)) .EQ. 1) THEN
        IF (FL(I,2) .LE. -COUNTM(DLP,CALPHAE,CEUT,DELTAC,KARMA)) THEN
               Z(I,FL(I,1))=0
        END IF
        ELSE
        IF (FL(I,2) .GE. -COUNTQM(DLP,CBETAE,CEUT,DELTAC,KARMA)) THEN
               Z(I,FL(I,1))=0
        END IF
        END IF
      END DO
      RETURN
      END

*** subroutine to smooth interface out- related to curvature calc.***
**********************************************************************
*     I, J : counters                                                *
*     L, T , M, N, TEMPR, TEMPL : temporary quantities               *
*     R1 : random number                                             *
**********************************************************************

      SUBROUTINE CHECK(W,Z)
      REAL*8  R1, G05CAF
      INTEGER  W, Z(200,700), I, J, L, T, M, N, TEMPR, TEMPL
      EXTERNAL G05CAF

      DO I=1,W
         DO J=5,299
*           ->periodicity conditions
            L=I-1
            M=I-2
            T=I+1
            N=I+2
            IF (I .EQ. 1) THEN
               L=W
               M=W-1
            END IF
```

```
            IF (I .EQ. 2) M=W

            IF (I .EQ. W) THEN
               T=1
               N=2
            END IF
            IF (I .EQ. W-1) N=1
*           ->to fill in holes
            IF (Z(I,J) .NE. 0 .AND. Z(I,J-1) .EQ. 0) THEN
               IF (Z(L,J-1) .EQ. Z(I,J) .OR. Z(I,J-2) .EQ.
     +         Z(I,J) .OR. Z(T,J-1) .EQ. Z(I,J)) THEN
                  Z(I,J-1)=Z(I,J)
                  Z(I,J)=0
               ELSE
                  Z(I,J)=0
               END IF
            END IF
*           ->for towers with two open sides
            IF (Z(I,J) .NE. 0 .AND. Z(I,J+1) .NE. 0 .AND.
     +         Z(T,J) .EQ. 0 .AND. Z(L,J) .EQ. 0 .AND.
     +         Z(T,J+1) .EQ. 0 .AND. Z(L,J+1) .EQ. 0) THEN
              TEMPR=0
              TEMPL=0
              IF (Z(I,J) .EQ. Z(I,J+1) .OR. Z(T,J-1) .EQ.
     +            Z(I,J+1) .OR. Z(N,J) .EQ. Z(I,J+1)) THEN
                 TEMPR=1
              END IF
              IF (Z(I,J) .EQ. Z(I,J+1) .OR. Z(L,J-1) .EQ.
     +            Z(I,J+1) .OR. Z(M,J) .EQ. Z(I,J+1)) THEN
                 TEMPL=1
              END IF
              IF (TEMPR .EQ. 1 .AND. TEMPL .EQ. 1) THEN
                 R1=G05CAF()
                 IF (R1 .LE. 0.5) THEN
                    Z(T,J)=Z(I,J+1)
                    Z(I,J+1)=0
                 ELSE
                    Z(L,J)=Z(I,J+1)
                    Z(I,J+1)=0
                 END IF
```

```
                ELSE IF (TEMPR .EQ. 1 .AND. TEMPL .EQ. 0) THEN
                   Z(T,J)=Z(I,J+1)
                   Z(I,J+1)=0
                ELSE IF (TEMPR .EQ. 0 .AND. TEMPL .EQ. 1) THEN
                   Z(L,J)=Z(I,J+1)
                   Z(I,J+1)=0
                ELSE
                   Z(I,J+1)=0
                END IF
             END IF
*            ->for a tower open to the left
             IF (Z(I,J) .NE. 0 .AND. Z(I,J+1) .NE. 0 .AND.
     +         Z(T,J) .NE. 0 .AND. Z(L,J) .EQ. 0 .AND.
     +         Z(T,J+1) .EQ. 0 .AND. Z(L,J+1) .EQ. 0) THEN
                IF (Z(I,J) .EQ. Z(I,J+1) .OR. Z(L,J-1) .EQ.
     +          Z(I,J+1) .OR. Z(M,J) .EQ. Z(I,J+1)) THEN
                     Z(L,J)=Z(I,J+1)
                     Z(I,J+1)=0
                ELSE
                     Z(I,J+1)=0
                END IF
             END IF
*            ->for a tower open to the right
             IF (Z(I,J) .NE. 0 .AND. Z(I,J+1) .NE. 0 .AND.
     +         Z(T,J) .EQ. 0 .AND. Z(L,J) .NE. 0 .AND.
     +         Z(T,J+1) .EQ. 0 .AND. Z(L,J+1) .EQ. 0) THEN
                IF (Z(I,J) .EQ. Z(I,J+1) .OR. Z(T,J-1) .EQ.
     +          Z(I,J+1) .OR. Z(N,J) .EQ. Z(I,J+1)) THEN
                     Z(T,J)=Z(I,J+1)
                     Z(I,J+1)=0
                ELSE
                     Z(I,J+1)=0
                END IF
             END IF
          END DO
       END DO
       RETURN
       END
```

```
**************** subroutine to store triple points ****************
*************************************************************************
*     I : counter                                                       *
*************************************************************************

      SUBROUTINE POINTS (INCRE,FL,Z,W)
      REAL*8  INCRE
      INTEGER  FL(200,2), Z(200,700), W, I

*     ->to plot the triple points in time, check to see if the
*      interface changes from alpha to beta or beta to alpha
      DO I=1,W-1
         IF (Z(I,FL(I,1)) .NE. Z(I+1,FL(I+1,1))) THEN
            WRITE (25,100) REAL(I), REAL(FL(I,1))+INCRE,
     +      REAL(I+1), REAL(FL(I+1,1))+INCRE
100         FORMAT (4F8.2)
         END IF
      END DO
      RETURN
      END

************************** end of program **************************
```

Matlab file used for plotting

```
%M-file
hold off
load crys1.m
plot(crys1(:,1),crys1(:,2),'.',crys1(:,3),crys1(:,4),'.')
axis([0 100 0 2000])
hold on
load edge1.m
plot(edge1(:,1),edge1(:,2),'.')
load trippoints1.m
plot(trippoints1(:,1),trippoints1(:,2),'.',trippoints1(:,3),
trippoints1(:,4),'.')
```